

Group structure estimation for panel data – a general approach ^{*}

Lu Yu[†] Jiaying Gu[‡] Stanislav Volgushev[§]

January 7, 2022

Abstract

Consider a panel data setting where repeated observations on individuals are available. Often it is reasonable to assume that there exist groups of individuals that share similar effects of observed characteristics, but the grouping is typically unknown in advance. We propose a novel approach to estimate such unobserved groupings for general panel data models. Our method explicitly accounts for the uncertainty in individual parameter estimates and remains computationally feasible with a large number of individuals and/or repeated measurements on each individual. The developed ideas can be applied even when individual-level data are not available and only parameter estimates together with some quantification of uncertainty are given to the researcher.

Keywords: group structure estimation, spectral clustering, panel data models

^{*}We are grateful to professors H.J. Wang and Y. Zhang for sending us the code for their simulations in Zhang et al. (2019a) . We further thank Professor D. Millimet for kindly sharing this data with us. The data we use here is the same as in Millimet et al. (2003)

[†]Department of Statistical Sciences, University of Toronto. E-mail: stat.yu@mail.utoronto.ca

[‡]Department of Economics, University of Toronto. E-mail: jiaying.gu@utoronto.ca

[§]Department of Statistical Sciences, University of Toronto. E-mail: stanislav.volgushev@utoronto.ca

1 Introduction

Panel data models are a standard empirical tool in statistics, economics, marketing, and financial research. The conventional modeling approach is to assume that all individual heterogeneity can be summarized by an individual specific intercept, often known as the fixed effects, while assuming all covariates have a common effect among all the individuals, such that information can be pooled across individuals to gain efficiency of these common parameters. However, heterogeneous responses towards observed control variables are often better supported by empirical evidence, especially as detailed individual level data becomes more available.

An increasingly popular approach to model unobserved heterogeneity in the effects of covariates on individual responses is to assume the existence of a finite number of homogeneous groups. Here, parameters in a potentially non-linear model¹ are assumed to take common values within groups but differ across groups. The main challenge is to learn the unobserved group structure from observed data. An alternative way to model unobserved heterogeneity is through latent factors (e.g., Bai (2009)). This approach also has discrete heterogeneity in the sense that a small number of unobserved factors drive the co-movement of a large number of time series. Both group pattern and factor structure are useful empirical tools, but they have different interpretations. In this paper, we focus on group patterns.

The existing literature can be roughly categorized into three categories. Methods from the first category rely on minimizing a loss function that incorporates different coefficients for all individuals combined with a penalty which encourages the coefficient estimates to be similar. Su et al. (2016) propose the C-LASSO approach, which is applicable to both linear and nonlinear models. Differences among individual parameters are penalized through a LASSO type penalty, and consistent grouping can be achieved if the penalty parameter is chosen properly. Wang et al. (2018) propose a Panel-CARDS penalty which extends the idea of homogeneity pursuit Ke et al. (2015) from cross-sectional models to panel data models. Gu and Volgushev (2019) propose to use the convex clustering penalty of Hocking et al. (2011) in panel data quantile regression models with grouped individual intercepts and common slope parameters.

An alternative approach is to view the group structure estimation problem closely related to a clustering problem; here clusters in the coefficient vectors would correspond to latent groups of individuals. Estimating clusters has a long history in statistics and economics. Among the many clustering algorithms, the k -mean algorithm by MacQueen et al. (1967) is one of the most popular and commonly used methods. However, instead of directly applying k -mean methods on the estimated individual parameters, Lin and Ng (2012) and Bonhomme and Manresa (2015) propose to incorporate the regression loss function and

¹Examples include quantile regression and discrete outcome models.

re-estimate the group-specific coefficients in an iterative fashion. Originally proposed for linear regression models, this approach has also been extended to quantile regression models by Zhang et al. (2019a) and Leng et al. (2021). Further advancement of this literature has considered time varying group membership, for example Miao et al. (2020), Okui and Wang (2021) and Lumsdaine et al. (2021).

Both the penalization-based and clustering-based approaches described above require the repeated fitting of large regression models which involve all individuals and all individual-specific parameters in a large-scale minimization problem. This can be computationally costly especially for large scale datasets, which become more and more common in practice. In addition, the extensions of the k -means approach discussed above require repeated application with many different starting points. Motivated by those computational challenges, Chetverikov and Manresa (2021) propose an estimator for linear panel data models with grouped intercepts and common slope. Their approach is shown to guarantee the same theoretical properties as Bonhomme and Manresa (2015) but is computationally much faster. It should be pointed out however that their approach seems to be difficult to extend to non-linear panels. Wang and Su (2021) propose to use ordered individual-specific regression estimators to convert the grouping problem into a change-point detection setting and apply binary segmentation to learn the underlying group structure. This approach can be applied to both linear and nonlinear panel data models. It is computationally efficient because the individual-specific regressions only need to be estimated once rather than in an iterative fashion. They further show that by considering the spectral decomposition of an outer product of the individual parameter estimates and then applying binary segmentation on the leading eigenvectors can lead to improved group estimation.

In the present paper, we propose a novel approach that retains the computational advantages of working with individual-specific regressions but explicitly takes into account the uncertainty in the corresponding estimates. This information is particularly important in settings where different entries of a coefficient vector are estimated with different degrees of precision and hence carry varying amounts of information about group membership. In a nutshell, we propose to weigh the differences between coefficient estimates of different individuals by an estimated variance-covariance matrix. The resulting weighted differences can not be interpreted as a Euclidean distance. This renders many classical clustering approaches such as the vanilla k -means algorithm or extensions of homogeneity pursuit and binary segmentation inapplicable. We handle this challenge by interpreting the weighted distances as a quantification of dissimilarity between individuals and applying spectral clustering on a properly defined dissimilarity matrix between individuals. It is further worth noting that, in contrast to most proposals in the existing literature, our method remains applicable even when raw individual-level data are not available due to privacy or other concerns and only estimated coefficients and their uncertainty estimates are given.

The remaining paper is organized as follows. In Section 2, we give a detailed descrip-

tion of the proposed estimation procedure and illustrate it on several specific models that were previously considered in the literature. Section 3.1 contains theoretical guarantees on correct group estimation under high-level conditions. Those conditions are verified for several examples in Section 3.2. A simulation study is presented in Section 4. An empirical illustration analyzing the heterogeneous relationship between income and pollution level among different states using data from the United States is given in Section 5. We also apply our approach to the commuting zone summary statistics provided by Chetty and Hendren (2018) to analyze group patterns of intergenerational income mobility. Section 6 concludes. All proofs, part of tables and plots are deferred to the supplementary material.

2 Proposed Methodology

Assume that we have repeated observations $(\mathbf{x}_{it}, Y_{it})_{t=1, \dots, T}$ from individuals $i = 1, \dots, n$. Our goal is to assign the individuals into G^* groups such that the effect of predictors (or a sub-vector thereof) is similar for all individuals within a group. For now, let G^* be given, a data-driven choice of G^* will be discussed at a later point. To find such a grouping, assume that we have access to estimators $(\hat{\beta}_i)_{i=1, \dots, n}$ (taking values in \mathbb{R}^p) of some characteristics of each individual and corresponding quantification of uncertainty in the estimators given by matrices $\hat{\Sigma}_{i,j}$ for any $i \neq j$. Here, the vectors $\hat{\beta}_i$ can be the full vector of coefficients in a non-linear model linking the response Y_{it} to the covariates \mathbf{x}_{it} , a sub-vector thereof, or simply the intercept terms in a regression model. The matrices $\hat{\Sigma}_{i,j}$ will typically estimate the (asymptotic) variance matrix of $\hat{\beta}_i - \hat{\beta}_j$. However, our results remain applicable even if $\hat{\Sigma}_{i,j}$ is not a consistent estimator of the full variance matrix; for instance, having only estimators of the diagonal entries of the matrix and fill zeros for the off-diagonal entries can also lead to valid procedures.

In the above setup, it is natural to attempt and group individuals that share similar estimated coefficients $\hat{\beta}_i$. However, some care must be taken when defining the notion of similarity. We argue that such a notion of similarity should take into account the fact that different entries of the vectors $\hat{\beta}_i$, and estimators $\hat{\beta}_i$ corresponding to different individuals can be subject to varying degrees of estimation uncertainty. This leads us to defining dissimilarity of two individuals i, j through some monotone transformation of

$$\hat{V}_{ij} := \|\hat{\Sigma}_{i,j}^{-1/2}(\hat{\beta}_i - \hat{\beta}_j)\|_\infty. \quad (1)$$

The above definition explicitly takes into account estimation uncertainty for $\hat{\beta}_i - \hat{\beta}_j$. This is especially important if different components of the vector β_i are estimated with different degrees of uncertainty. As we will demonstrate in simulations, ignoring this information can lead to considerable deterioration in grouping accuracy (for example, in the logistic regression model considered in Section 4.1, ignoring variance information can lead to a decrease in the probability of perfect group recovery from 70% to 2%).

Next, observe that the problem of assigning individuals to groups can be equivalently seen as the problem of clustering the corresponding coefficient vectors. However, it is important to note that, due to the weighting with $\hat{\Sigma}_{i,j}^{-1/2}$, the dissimilarity measure in (1) does not correspond to a Euclidean distance. This renders procedures that explicitly work with such distances, such as k -means method, inapplicable. Two popular clustering approaches in the literature that work with general measures of dissimilarity are *k -medoids* Schubert and Rousseeuw (2019) and *spectral clustering* Ng et al. (2002); Chung and Graham (1997); Von Luxburg (2007). Similarly to k -means clustering, the k -medoids problem is NP-hard to solve exactly. In practice, approximate solutions to this problem are obtained by employing the algorithm *Partitioning Around Medoids* (PAM) Reynolds et al. (2006); Schubert and Rousseeuw (2019); Kaufman and Rousseeuw (2009). We refer to (Kaufman and Rousseeuw, 2009, Section 4.1, Chapter 2) for more details about the PAM algorithm. This can be viewed as a viable strategy to incorporate uncertainty information into the vanilla k -means approach. However, extensive preliminary simulations showed that in all settings considered spectral clustering leads to more accurate group estimation than PAM, and hence we focus on spectral clustering in what follows.

Since there are many variations of spectral clustering that are available in the literature, a detailed description of the specific version we use is given in Algorithm 1.

Algorithm 1 Spectral Clustering

Input: Number of clusters G^* , dissimilarity matrix $\hat{V} := (\hat{V}_{ij})$ computed in (1).

Output: Clusters $\hat{I}_1, \dots, \hat{I}_{G^*}$.

- 1: Compute the empirical adjacency matrix $\hat{A} \in \mathbb{R}^{n \times n}$ with entries $\hat{A}_{ij} := e^{-\hat{V}_{ij}}$ for $i \neq j$ and $\hat{A}_{ij} = 1$ for $i = j$.
- 2: Compute the empirical degree matrix $\hat{D} := \text{diag}(\hat{D}_1, \dots, \hat{D}_n)$, where $\hat{D}_i := \sum_{j=1}^n \hat{A}_{ij}, i = 1, \dots, n$.
- 3: Calculate the normalized graph Laplacian $\hat{L} := \hat{D}^{-1/2}(\hat{D} - \hat{A})\hat{D}^{-1/2}$.
- 4: Find G^* orthonormal eigenvectors corresponding to the G^* smallest eigenvalues of \hat{L} , and form the matrix $\hat{Z} \in \mathbb{R}^{n \times G^*}$ by stacking those vectors in columns. Normalize the rows of \hat{Z} , to have ℓ^2 -norm 1 and denote the resulting matrix by \hat{U} .
- 5: Apply standard k -means clustering with G^* clusters taking the rows of \hat{U} as input vectors, and return the clusters $\hat{I}_1, \dots, \hat{I}_{G^*}$.

Remark 2.1. *To intuitively understand the motivation behind the above algorithm observe that the dissimilarities \hat{V}_{ij} can be expected to be large if individuals i, j are from different groups. In the limit $T \rightarrow \infty$ those distances will tend to infinity, and thus $\hat{A}_{ij} \approx 0$ whenever i, j are from different groups. Similarly, \hat{V}_{ij} can be expected to be bounded when i, j are in the group, and thus \hat{A}_{ij} will usually be bounded away from zero for such pairs. Thus after rearranging the order of individuals we see that \hat{V}_{ij} will be approximately block diagonal with non-zero entries in the blocks. It is now straightforward to see that \hat{L} will have exactly G^* zero eigenvalues if there are G^* such blocks and all other eigenvalues will be strictly positive.*

Moreover, the eigen-space corresponding to zero eigenvalues will have an orthogonal basis consisting of vectors that have non-zero entries in the exact components corresponding to different groups, see also the discussion surrounding equation (14) and Lemma 10.1 in the supplementary material. For a more detailed discussion of the intuition and alternative formulations of the spectral clustering algorithm see Von Luxburg (2007) and the literature cited therein. Although the last step of the algorithm uses the standard k -means algorithm, we note that it is applied on the rows of \hat{U} which is a standard clustering problem with n data points in Euclidean space. No refitting of models on individual level or large scale models as in Bonhomme and Manresa (2015) is required.

Remark 2.2. Wang and Su (2021) also observe that the spectral decomposition of a certain matrix that is derived from individual-specific estimators contains information on the latent group structure. However, there are several crucial differences between their and our approach. Most importantly, we explicitly take into account the uncertainty that is associated with individual-specific estimators while Wang and Su (2021) work directly with raw estimators. Moreover, Wang and Su (2021) do not apply spectral clustering directly but rather use certain eigenvectors as input to a binary segmentation algorithm.

Remark 2.3. The idea to use spectral clustering for grouping different entities also appeared in van Delft and Dette (2021). The setting in the latter paper is very different from ours since van Delft and Dette (2021) consider grouping locally stationary functional time series and do not take into account estimation uncertainty when constructing their dissimilarity measure between observations. Still, some parts of our theoretical analysis under high-level assumptions are related to theirs, additional comments on this can be found in Remark 3.1.

So far we discussed an algorithm for assigning individuals to G^* groups for any given G^* . In some settings, G^* will be chosen based on domain knowledge about the problem at hand. If no such knowledge is available, we propose to select the G^* that maximizes the relative eigen-gap Von Luxburg (2007) of a modified graph Laplacian \tilde{L} . More precisely, consider the scaled dissimilarity $\tilde{V}_{ij} := \frac{2}{\sqrt{\log n \log T}} \hat{V}_{ij}$. Use \tilde{V}_{ij} as input to Algorithm 1 and obtain \tilde{L} as output from step 3 of that algorithm. Consider the values $\tilde{\lambda}_i := 1 - \hat{\lambda}_i$, $i = 1, \dots, n$, with $\hat{\lambda}_1 \leq \dots \leq \hat{\lambda}_n$ denoting the ordered eigenvalues of \tilde{L} . The estimated number of groups is

$$\hat{G} = \arg \max_{g=1, \dots, n-1} \frac{|\tilde{\lambda}_{g+1} - \tilde{\lambda}_g|}{\tilde{\lambda}_{g+1}}, \quad (2)$$

The motivation for using the scaling in \tilde{V}_{ij} is that, under technical assumptions made later, this scaling ensures $\tilde{V}_{ij} \rightarrow 0$ for all i, j in the same group. Without this scaling, the heuristic tends to have a small probability of not selecting a correct number of groups as T increases.

Similar heuristic eigen-gap methods for estimating the number of groups can also be found in van Delft and Dette (2021); John et al. (2020); Little et al. (2017), among many others.

Remark 2.4. There are at least two other popular approaches to selecting the number of groups or equivalently the number of clusters. The first type of method combines cross-validation with the idea that “true” cluster assignment should be stable under small perturbations of the data. This idea was exploited in Wang (2010) for selecting the number of clusters in a general setting and adapted by Zhang et al. (2019a) to selecting the number of groups for panel data quantile regression. However, as pointed out in Ben-David et al. (2006), methods that select the number of clusters based on stability can fail for certain cluster configurations. One such example will be given in the simulation section. The second drawback of such methods is that they, by construction, are not able to select a single cluster which limits their applicability in practice.

The second method uses information criteria which select the number of clusters that maximize a sum of objective function plus penalty, see for instance Su et al. (2016); Gu and Volgushev (2019); Wang and Su (2021) among many others. The main drawback of such approaches is that information criteria need to be derived case by case as they differ depending on the specific form of the objective function making them difficult to use for applied researchers. We note that this is different from the classical setting involving AIC and BIC in a maximum likelihood framework where only the number of parameters in the model matters. Moreover, computation of such information criteria typically requires access to raw data which might not always be available as in our second application.

We also conduct an extensive simulation comparing different methods of selecting the number of groups in Section 4.3. Results show that our heuristic approach works reasonably well in all settings considered. Unsurprisingly, we also find that there is no universally dominating method.

The setting above is generic and so far we did not assume anything about the specific structure of the estimators. In the remainder of this section, we provide several illustrative examples of model specifications that were considered previously and show how those examples fit into the proposed framework.

Example 2.1 (*Logistic regression regression individual-specific intercepts and grouping on slopes*). Consider binary responses $Y_{it} \in \{0, 1\}$ and assume that

$$\mathbb{P}(Y_{it} = 1) = \frac{\exp(\alpha_i + \mathbf{x}_{it}^\top \boldsymbol{\beta}_i)}{1 + \exp(\alpha_i + \mathbf{x}_{it}^\top \boldsymbol{\beta}_i)} = \frac{\exp(\mathbf{z}_{it}^\top \boldsymbol{\gamma}_i)}{1 + \exp(\mathbf{z}_{it}^\top \boldsymbol{\gamma}_i)},$$

where $\mathbf{z}_{it}^\top = (1, \mathbf{x}_{it}^\top)$ and $\boldsymbol{\gamma}_i^\top = (\alpha_i, \boldsymbol{\beta}_i^\top)$. We leave the $\alpha_i \in \mathbb{R}$ unrestricted and assume that certain sub-vectors of $\boldsymbol{\beta}_i \in \mathbb{R}^p$ have a group structure. This model will be considered in our data illustration in Section 5 where coefficients in logistic regression models will be utilized to analyze heterogeneity in income as a function of the pollution level.

Su et al. (2016) considers a similar model; they assume a Gaussian link function for the binary response. Ando et al. (2021) also considers the logit model with individual

specific slope coefficients and a factor structure on the individual fixed effects. Their way of modeling unobserved heterogeneity is different from ours as we focus on group patterns.

Example 2.2 (*Quantile regression with joint slope and grouping on intercepts*). Assume that the conditional quantile function of response Y_{it} given covariates \mathbf{x}_{it} for individual i is

$$q_{i,\tau}(\mathbf{x}_{it}) = \alpha_i(\tau) + \mathbf{x}_{it}^\top \boldsymbol{\beta}(\tau),$$

where the vector of slope coefficients $\boldsymbol{\beta}(\tau) \in \mathbb{R}^p$ is assumed to be the same across individuals.

This model was first considered in Koenker (2004), who proposed to regularize the individual fixed effects via ℓ_1 penalization. Lamarche (2010) considers the optimal choice of the penalty parameters in this approach. There has been an active literature on panel data quantile regression, mainly focusing on estimation of the common parameters $\boldsymbol{\beta}(\tau)$ (e.g., Kato et al. (2012), Galvao and Kato (2016), Harding and Lamarche (2017) and Galvao et al. (2020)). Zhang et al. (2019b) and Gu and Volgushev (2019) consider group structure on $\alpha_i(\tau) \in \mathbb{R}$.

Example 2.3 (*Quantile regression individual-specific intercepts and grouping on slopes*). Given the observations are $(\mathbf{x}_{it}, Y_{it})$, assume that the conditional quantile function of the response Y_{it} given covariates \mathbf{x}_{it} for individual i satisfies

$$q_{i,\tau}(\mathbf{z}_{it}) = \alpha_i(\tau) + \mathbf{x}_{it}^\top \boldsymbol{\beta}_i(\tau) = \mathbf{z}_{it}^\top \boldsymbol{\gamma}_i(\tau),$$

where $\alpha_i(\tau) \in \mathbb{R}$ are unrestricted and we search for a group structure on $\boldsymbol{\beta}_i(\tau) \in \mathbb{R}^p$.

This setting was also considered in Zhang et al. (2019a), Leng et al. (2021). Zhang et al. (2019a) propose an iterative algorithm based on the k -mean algorithm in Bonhomme and Manresa (2015) to learn group structure. Leng et al. (2021) use a k -means type of iterative algorithm, but allow for time fixed effect while grouping both the individual fixed effects and the slope coefficients. This model will be considered in Section 5 where coefficients of the panel quantile regression model will be utilized to analyze heterogeneous relationship between income and pollution level among different states in the US.

3 Theoretical Analysis

3.1 Generic spectral clustering results

In this section, we provide high-level conditions on the estimators $\hat{\boldsymbol{\beta}}_i \in \mathbb{R}^p$ and $\hat{\Sigma}_{i,j} \in \mathbb{R}^{p \times p}$ which ensure that the correct group structure is recovered with probability tending to one as n, T tend to infinity. Formally, assume that the true coefficients $\boldsymbol{\beta}_1, \dots, \boldsymbol{\beta}_n$ take G^* different values, say $\boldsymbol{\beta}_1^*, \dots, \boldsymbol{\beta}_{G^*}^*$ and the true group membership is given by

$$\boldsymbol{\beta}_i = \boldsymbol{\beta}_k^* \Leftrightarrow i \in I_k^*, \quad k = 1, \dots, G^*,$$

where $I_k^* \subseteq \{1, \dots, n\}$ denote the true underlying groups.

Assumption 3.1. *The true groups are $I_1^*, \dots, I_{G^*}^*$, with $I_k^* \subset \{1, \dots, n\}$, $k = 1, \dots, G^*$ and $I_k^* \cap I_l^* = \emptyset$ for any $k \neq l$ and the group sizes satisfy*

$$\frac{|I_j^*|}{n} \rightarrow \mu_j \in (0, 1), j = 1, \dots, G^*.$$

Assumption 3.2. *The estimators $\hat{\beta}_i$ are uniformly consistent with rate $a_{n,T}$, i.e.*

$$\sup_{i \in \{1, \dots, n\}} \|\hat{\beta}_i - \beta_i\|_2 = \mathcal{O}_{\mathbb{P}}(a_{n,T}), \text{ where } a_{n,T} = o(1).$$

Assumption 3.3. *There exists a sequence $b_T \rightarrow \infty$ and matrices $\Sigma_{i,j}$ satisfy*

$$\sup_{i,j} \left\| b_T \hat{\Sigma}_{i,j} - \Sigma_{i,j} \right\|_2 = o_{\mathbb{P}}(1),$$

where $\|\cdot\|_2$ denotes the spectral norm. Moreover, assume

$$0 < m < \lambda_{\min}(\Sigma_{i,j}) \leq \lambda_{\max}(\Sigma_{i,j}) < M < \infty \quad \forall i \neq j \in \{1, \dots, n\} \quad (3)$$

with some fixed constants $0 < m \leq M < \infty$.

Assumption 3.4. *Assume that $\log n = o(b_T)$.*

We now provide a brief discussion of the assumptions above. Assumption 3.1 states that the size of each group is of roughly the same order. Since we assume that the number of groups and location of group centers is fixed, it implies that the true group centers are well separated. Assumptions 3.2 and 3.3 impose minimal restrictions on the quality of the initial estimates $\hat{\beta}_i$ and $\hat{\Sigma}_{i,j}$. We emphasize that the matrices $\Sigma_{i,j}$ in Assumption 3.3 are not required to be equal to the true asymptotic covariance matrices of $\hat{\beta}_i - \hat{\beta}_j$ for the theory to work. However, as we will see in simulations, using consistent estimators for the true asymptotic covariances can lead to substantial improvements in small samples.

In all examples we consider later the individuals will be assumed independent and the estimators $\hat{\beta}_i$ will satisfy $\sqrt{T}(\hat{\beta}_i - \beta_i) \xrightarrow{\mathcal{D}} \mathcal{N}_p(0, \Sigma_i)$, $i = 1, \dots, n$. By independence among individuals the weak convergence above holds jointly for any given pair of individuals and the corresponding limits will be independent.

In this case, we will set $b_T = T$, $\Sigma_{i,j} := \Sigma_i + \Sigma_j$, $\hat{\Sigma}_{i,j} := \hat{\Sigma}_i + \hat{\Sigma}_j$ where $\hat{\Sigma}_i$ will be consistent estimators of Σ_i . The uniform consistency rate $a_{n,T}$ will be uniform over a growing number i and typically be of the form $a_{n,T} = \sqrt{T^{-1} \log n}$ where the additional $\sqrt{\log n}$ factor is to ensure uniformity. In the setting described above Assumption 3.4 will simplify to $\log n = o(T)$, thus allowing for the number of individuals n grow very quickly relative to the number of repeated observation per individual T .

We conclude by noting that our main result would continue to be true if some of the assumptions are relaxed and others are strengthened in return. For instance, it would be possible to relax the assumption that all groups are of the same size if the conditions on the relative orders of $b_T, n, a_{n,T}$ are strengthened. Similarly, we could allow the minimal separation between the true values of β_k^* to go to zero at certain rates which would need to be linked with the estimation quality $a_{n,T}$. In order to keep our main result simple and transparent, we chose to not pursue this type of generalization in the present paper.

The main result of this section shows that under the conditions given above the proposed algorithm finds the true group structure with probability tending to one.

Theorem 3.1. *Under Assumptions 3.1 - 3.4, the true group structure is recovered with probability tending to one as $T \rightarrow \infty$.*

Remark 3.1. *The proof relies on the type of arguments that appeared in earlier work on spectral clustering, in particular Ng et al. (2002), Von Luxburg (2007) and van Delft and Dette (2021). However, the setting we consider is different from any of the works mentioned above and the arguments need to be modified accordingly. The work of van Delft and Dette (2021) is closest in spirit, but our analysis is complicated by the fact that we allow the number of individuals n to diverge while the number of entities to be clustered was fixed in van Delft and Dette (2021). In order to deal with this complication, we leverage the fact that our construction of the similarity matrix gives rise to the different order for the diagonal blocks and off-diagonal blocks of the empirical Laplacian matrix. Taking advantage of this difference in order together with spectral information contained in the diagonal blocks of the empirical Laplacian matrix allows us to handle a diverging number of individuals.*

3.2 Verification of high level conditions for specific examples

In this section, we provide specific conditions in Example 2.1–Example 2.3 which guarantee that the high-level conditions 3.2 and 3.3 are satisfied. The set of examples that we consider is by no means exhaustive for the possible applications of our methodology. Rather, it is intended as a demonstration that our high-level conditions can be verified in several different settings including the presence of individual-specific and joint parameters, binary outcomes, and non-smooth objective functions.

3.2.1 Logistic regression with individual-specific intercepts and grouping on the slopes (Example 2.1)

The coefficient vector $\gamma_i^\top := (\alpha_i, \beta_i^\top)$ is estimated via maximum likelihood, i.e.

$$\hat{\gamma}_i := \arg \max_{\gamma \in \mathbb{R}^{p+1}} \frac{1}{T} \sum_{t=1}^T \left[Y_{it} \mathbf{z}_{it}^\top \gamma - \log(1 + \exp(\mathbf{z}_{it}^\top \gamma)) \right], \quad i = 1, \dots, n.$$

Recall that under standard assumptions this estimator is asymptotically normal with asymptotic variance given by

$$\tilde{\Sigma}_i = \left(\mathbb{E} \left[\frac{e^{\mathbf{z}_{it}^\top \boldsymbol{\gamma}_i^*}}{(1 + e^{\mathbf{z}_{it}^\top \boldsymbol{\gamma}_i^*})^2} \mathbf{z}_{it} \mathbf{z}_{it}^\top \right] \right)^{-1}.$$

The canonical plug-in estimator of $\tilde{\Sigma}_i$ takes the form

$$\hat{\tilde{\Sigma}}_i = \left(\frac{1}{T} \sum_{t=1}^T \frac{e^{\mathbf{z}_{it}^\top \hat{\boldsymbol{\gamma}}_i}}{(1 + e^{\mathbf{z}_{it}^\top \hat{\boldsymbol{\gamma}}_i})^2} \mathbf{z}_{it} \mathbf{z}_{it}^\top \right)^{-1}.$$

Denote by $\hat{\Sigma}_i$ the lower $p \times p$ sub-matrix of $\hat{\tilde{\Sigma}}_i$. Then we set

$$\hat{\Sigma}_{i,j} := T^{-1}(\hat{\Sigma}_i + \hat{\Sigma}_j). \quad (4)$$

Consider the following assumptions.

Assumption 3.5. *Assume $0 < \inf_i \left\{ \lambda_{\min}(\mathbb{E}[\mathbf{z}_{it} \mathbf{z}_{it}^\top]) \right\} < \sup_i \left\{ \lambda_{\max}(\mathbb{E}[\mathbf{z}_{it} \mathbf{z}_{it}^\top]) \right\} < \infty$.*

Assumption 3.6. *Assume $\sup_{i,t} \{\|\mathbf{z}_{it}\|_2\} < \kappa < \infty$ a.s. .*

Assumption 3.5 places mild restrictions on the design matrix. The boundedness condition in 3.6 is made for the sake of simplicity; it can be relaxed to designs with bounded moments at the cost of additional technicalities in the proofs.

Theorem 3.2. *Assume Assumptions 3.5 and 3.6 hold, and $T \rightarrow \infty, \log n/T \rightarrow 0$. Then*

$$\sup_{i \in \{1, \dots, n\}} \|\hat{\boldsymbol{\gamma}}_i - \boldsymbol{\gamma}_i^*\|_2 = \mathcal{O}_{\mathbb{P}} \left(\sqrt{\frac{\log n}{T}} \right). \quad (5)$$

Under the same assumptions the estimators $\hat{\Sigma}_{i,j}$ in (4) satisfy

$$\sup_{i \neq j} \left\| \left\| T \hat{\Sigma}_{i,j} - \Sigma_{i,j} \right\| \right\|_2 = o_{\mathbb{P}}(1), \quad (6)$$

where $\Sigma_{i,j}$ denotes the lower $p \times p$ submatrix of $\tilde{\Sigma}_i + \tilde{\Sigma}_j$. Furthermore $\Sigma_{i,j}$ satisfy (3) .

Theorem 3.2 implies that Assumptions 3.2 and 3.3 hold with $a_{n,T} = \sqrt{T^{-1} \log n}$, $b_T = T$ and $\Sigma_{i,j}$ corresponding to the scaled asymptotic variance matrix of $\hat{\boldsymbol{\beta}}_i - \hat{\boldsymbol{\beta}}_j$. In particular, Assumption 3.4 is satisfied provided that $\log n = o(T)$ which is a very mild assumption.

Note that the results directly imply that Assumptions 3.2 and 3.3 continue to hold for any sub-vectors of $\hat{\boldsymbol{\gamma}}_i$. This covers settings where we want to leave some coefficients individual-specific and only perform grouping on a part of the full coefficient vector.

At the cost of additional technicalities, it is possible to derive similar results data that exhibit temporal dependence across t . This would require different estimates of the vari-

ances $\Sigma_{i,j}$ and the assumption on the relative growth of T would become stricter. To keep things simple we do not pursue such extensions here.

3.2.2 Quantile regression with individual-specific intercepts and grouping on the slopes (Example 2.3)

Consider the quantile regression panel data model

$$q_{i,\tau}(\mathbf{z}_{it}) = \mathbf{z}_{it}^\top \boldsymbol{\gamma}_i^*(\tau), \quad t = 1, \dots, T, i = 1, \dots, n,$$

where $q_{i,\tau}(\mathbf{z}_{it}) := \inf\{y : \mathbb{P}(Y_{it} < y | \mathbf{z}_{it}) \geq \tau\}$ is the conditional τ -quantile of Y_{it} given \mathbf{z}_{it} .

We will assume that $(\mathbf{z}_{it}, Y_{it})$ are i.i.d. across t for each i and independent across i . Generalizations to temporal dependence across t can be derived along the lines of Galvao et al. (2020).

Consider the quantile regression estimator $\hat{\boldsymbol{\gamma}}_i^\top = (\hat{\alpha}_i, \hat{\boldsymbol{\beta}}_i^\top)$:

$$\hat{\boldsymbol{\gamma}}_i := \arg \min_{\boldsymbol{\gamma} \in \mathbb{R}^{p+1}} \frac{1}{T} \sum_{t=1}^T \rho_\tau(Y_{it} - \mathbf{z}_{it}^\top \boldsymbol{\gamma}),$$

where $\rho_\tau(u) := \{\tau - \mathbb{1}(u \leq 0)\}u$ denotes the check function.

Under mild regularity assumptions (in particular, this is true under assumption (A1)–(A3) given below) this estimator is asymptotically normal with asymptotic covariance matrix of the form $\tilde{\Sigma}_i = B_i^{-1} H_i B_i^{-1}$ where

$$H_i := \tau(1 - \tau) \mathbb{E}[\mathbf{z}_{i1} \mathbf{z}_{i1}^\top], \quad B_i = \mathbb{E}[f_{Y_{i1} | \mathbf{z}_{i1}}(q_{i,\tau}(\mathbf{z}_{i1}) | \mathbf{z}_{i1}) \mathbf{z}_{i1} \mathbf{z}_{i1}^\top], \quad (7)$$

with $f_{Y_{i1} | \mathbf{z}_{i1}}(y | \mathbf{z})$ as the density function of the conditional distribution $F_{Y_{i1} | \mathbf{z}_{i1}}(y | \mathbf{z})$.

A common way to estimate $\tilde{\Sigma}_i$ uses the Hendricks-Koenker sandwich covariance matrix estimator Hendricks and Koenker (1992) which takes the following form

$$\hat{\tilde{\Sigma}}_{iT} := \hat{B}_{iT}^{-1} \hat{H}_{iT} \hat{B}_{iT}^{-1}, \quad \text{with} \quad (8)$$

$$\hat{B}_{iT} := \frac{1}{T} \sum_{t=1}^T \hat{f}_{it} \mathbf{z}_{it} \mathbf{z}_{it}^\top, \quad \hat{H}_{iT} := \tau(1 - \tau) \frac{1}{T} \sum_{t=1}^T \mathbf{z}_{it} \mathbf{z}_{it}^\top, \quad \hat{f}_{it} := \frac{2d_T}{\mathbf{z}_{it}^\top (\hat{\boldsymbol{\gamma}}_i(\tau + d_T) - \hat{\boldsymbol{\gamma}}_i(\tau - d_T))}.$$

Here d_T denotes a smoothing parameter that should converge to zero at an appropriate rate. Let $\hat{\Sigma}_{iT}$ denote the lower $p \times p$ submatrix of $\hat{\tilde{\Sigma}}_{iT}$ and set

$$\hat{\Sigma}_{i,j} := T^{-1} (\hat{\Sigma}_{iT} + \hat{\Sigma}_{jT}). \quad (9)$$

We now verify Assumptions 3.2 3.3, under the following conditions.

(A1) Assume that $\|\mathbf{z}_{it}\|_2 \leq \kappa < \infty$, and that $c_\lambda \leq \lambda_{\min}(\mathbb{E}[\mathbf{z}_{it}\mathbf{z}_{it}^\top]) \leq \lambda_{\max}(\mathbb{E}[\mathbf{z}_{it}\mathbf{z}_{it}^\top]) \leq C_\lambda$ holds uniformly in i for some fixed constants $c_\lambda > 0$ and $\kappa, C_\lambda < \infty$.

(A2) Define $\mathcal{Z} := [-\kappa, \kappa]^{p+1}$. The conditional distribution $F_{Y_{i1}|\mathbf{z}_{i1}}(y|\mathbf{z})$ is twice differentiable w.r.t. y , with the corresponding derivatives $f_{Y_{i1}|\mathbf{z}_{i1}}(y|\mathbf{z})$ and $f'_{Y_{i1}|\mathbf{z}_{i1}}(y|\mathbf{z})$. Assume that

$$f_{\max} := \sup_i \sup_{y \in \mathbb{R}, \mathbf{z} \in \mathcal{Z}} |f_{Y_{i1}|\mathbf{z}_{i1}}(y|\mathbf{z})| < \infty, \quad \bar{f}' := \sup_i \sup_{y \in \mathbb{R}, \mathbf{z} \in \mathcal{Z}} |f'_{Y_{i1}|\mathbf{z}_{i1}}(y|\mathbf{z})| < \infty.$$

(A3) Denote by \mathcal{T} an open neighborhood of τ . Assume that uniformly across i , there exists a constant $f_{\min} < f_{\max}$ such that

$$0 < f_{\min} \leq \inf_i \inf_{\eta \in \mathcal{T}} \inf_{\mathbf{z} \in \mathcal{Z}} f_{Y_{i1}|\mathbf{z}_{i1}}(q_{i,\eta}(\mathbf{z})|\mathbf{z}).$$

(A4) Assume that $d_T = o(1)$, as $T \rightarrow \infty$ and

$$\frac{\log n}{Td_T} = o(1).$$

Assumptions (A1)–(A4) are fairly standard in the quantile regression literature and have been imposed in Kato et al. (2012) and Galvao et al. (2020) among many others.

Theorem 3.3. *Let Assumption 3.1, $\log n = o(T)$, $\min(n, T) \rightarrow \infty$, and Assumptions (A1)–(A3) hold. Then, it holds that*

$$\sup_{i \in \{1, \dots, n\}} \|\hat{\boldsymbol{\gamma}}_i - \boldsymbol{\gamma}_i^*\|_2 = \mathcal{O}_{\mathbb{P}}\left(\sqrt{\frac{\log n}{T}}\right).$$

In particular, Assumption 3.2 holds with $a_{n,T} = \sqrt{\frac{\log n}{T}}$. If in addition to the above Assumption (A4) holds, then Assumption 3.3 and 3.4 is also satisfied with $b_T := T$, $\Sigma_{i,j}$ denoting the lower $p \times p$ sub-matrix of $\tilde{\Sigma}_i + \tilde{\Sigma}_j$, and $\hat{\Sigma}_{i,j}$ defined in (9).

Theorem 3.2 implies that Assumptions 3.2 and 3.3 hold with $a_{n,T} = \sqrt{T^{-1} \log n}$, $b_T = T$ and $\Sigma_{i,j}$ corresponding to the scaled asymptotic variance matrix of $\hat{\boldsymbol{\beta}}_i - \hat{\boldsymbol{\beta}}_j$.

Similarly to the discussion in Section 3.2.1, the results directly imply that Assumptions 3.2 and 3.3 continue to hold for any sub-vectors of $\hat{\boldsymbol{\gamma}}_i$.

3.2.3 Quantile regression with common slope and grouping on the intercepts (Example 2.2)

Consider the quantile regression panel data model

$$q_{i,\tau}(\mathbf{x}_{it}) = \alpha_i^*(\tau) + \mathbf{x}_{it}^\top \boldsymbol{\beta}^*(\tau), \quad t = 1, \dots, T, i = 1, \dots, n,$$

where $q_{i,\tau}(\mathbf{x}_{it}) := \inf\{y : \mathbb{P}(Y_{it} < y | \mathbf{x}_{it}) \geq \tau\}$ denotes the conditional τ -quantile of Y_{it} given \mathbf{x}_{it} . In contrast to the setting in Section 3.2.2, we assume that the slope coefficient $\boldsymbol{\beta}^*$ is common across individuals and are only interested in grouping the intercepts. This model was considered in Gu and Volgushev (2019), who used a lasso-type penalty to enforce grouping on the intercepts α_i^* . The latter paper also demonstrated that putting this kind of regularization on α_i^* can result in improved estimation of $\boldsymbol{\beta}^*$ compared to leaving α_i^* unrestricted.

Assume that $(\mathbf{x}_{it}, Y_{it})$ are i.i.d. across t for each i and independent across i . Since only intercepts contain the grouping information, we aim to use the estimates for α_i^* , and their variance estimates to construct the similarity matrix. At this point, there are two possibilities for estimating α_i^* : (1) run individual-specific quantile regressions ignoring the fact that $\boldsymbol{\beta}^*$ is common across individuals or (2) put all individuals into a single large model in order to borrow information across individuals to improve the efficiency in estimating the joint coefficient vector $\boldsymbol{\beta}^*$.

Approach (1) has computational advantages, especially if n is large, but can also result in a loss of efficiency. The theoretical treatment of (1) easily follows from minor modifications of the results in Section 3.2.2, and we hence focus on the second approach. Define

$$(\tilde{\alpha}_1(\tau), \dots, \tilde{\alpha}_n(\tau), \tilde{\boldsymbol{\beta}}(\tau)) := \arg \min_{\alpha_1, \dots, \alpha_n, \boldsymbol{\beta}} \frac{1}{nT} \sum_{i=1}^n \sum_{t=1}^T \rho_\tau(Y_{it} - \alpha_i - \mathbf{x}_{it}^\top \boldsymbol{\beta}). \quad (10)$$

In what follows, we assume that $n \rightarrow \infty$ which is the more relevant case for group structure detection. In this case, it is possible to obtain simplified estimators for the asymptotic variance of $\tilde{\alpha}_i$. Those estimators will be motivated next.

The main insight is that under $n \rightarrow \infty$ the estimation of $\boldsymbol{\beta}^*$ has a negligible effect of the asymptotic variance of $\tilde{\alpha}_i$ since $\boldsymbol{\beta}^*$ is estimated at a faster rate due to borrowing information across individuals. Further observe that, defining $\hat{e}_{it} = Y_{it} - \mathbf{x}_{it}^\top \tilde{\boldsymbol{\beta}}$, we have

$$\tilde{\alpha}_i = \arg \min_{\alpha} \frac{1}{T} \sum_{t=1}^T \rho_\tau(\hat{e}_{it} - \alpha), \quad i = 1, \dots, n. \quad (11)$$

Thus $\tilde{\alpha}_i$ is approximately the sample quantile of $\{\hat{e}_{it}, t = 1, \dots, T\}$, which should be close to the sample quantile of $\{e_{it}, t = 1, \dots, T\}$, where $e_{it} := Y_{it} - \mathbf{x}_{it}^\top \boldsymbol{\beta}^*$.

If $n \rightarrow \infty$ this idea can be formalized by applying a modification of Lemma 7 in

Galvao et al. (2020) (after noting that the proof of the latter result can be modified to weaken the assumption $n(\log T)^2/T \rightarrow 0$ made in there). Denoting the sample quantile of $\{e_{it}, t = 1, \dots, T\}$ by $\hat{\alpha}_i$, the latter result implies

$$\sup_{i=1, \dots, n} |\hat{\alpha}_i - \tilde{\alpha}_i| = \mathcal{O}_{\mathbb{P}}\left(\|\tilde{\beta} - \beta^*\|_2 + T^{-1} \log(n \vee T)\right).$$

Observing that by the proof of Theorem 3.2 in Kato et al. (2012) we have $\|\tilde{\beta} - \beta^*\|_2 = o_{\mathbb{P}}(T^{-1/2})$, when $n \rightarrow \infty$ (note that this part of their result does not require the restrictive growth assumption on n which is needed for unbiased asymptotic normality of $\tilde{\beta}$), this implies $|\hat{\alpha}_i - \tilde{\alpha}_i| = o_{\mathbb{P}}(T^{-1/2})$ uniformly over i and thus the asymptotic distributions of $\hat{\alpha}_i$ and $\tilde{\alpha}_i$ coincide. Now classical results on the distribution of sample quantiles imply that the asymptotic variance of $\hat{\alpha}_i$ is

$$\Sigma_i = \tau(1 - \tau)/f_{e_i}^2(q_{e_i}(\tau)), \quad (12)$$

where f_{e_i}, q_{e_i} denote the (unconditional) density and quantile function of e_{i1} , respectively.

This motivates the following version of $\hat{\Sigma}_{i,j}$: for a bandwidth parameter d_T define

$$\hat{\Sigma}_{iT} := \tau(1 - \tau) \left(\frac{\tilde{\alpha}_i(\tau + d_T) - \tilde{\alpha}_i(\tau - d_T)}{2d_T} \right)^2, \quad i = 1, \dots, n$$

and compute

$$\hat{\Sigma}_{i,j} := T^{-1} \left(\hat{\Sigma}_{iT} + \hat{\Sigma}_{jT} \right). \quad (13)$$

Theorem 3.4. *Let Assumption 3.1, and Assumptions (A1)-(A3) with $\mathbf{z}_{it} = \mathbf{x}_{it}$ hold. Assume $\log n = o(T)$, $\min(n, T) \rightarrow \infty$. Then, it holds that*

$$\sup_{i \in \{1, \dots, n\}} |\tilde{\alpha}_i - \alpha_i^*| = \mathcal{O}_{\mathbb{P}}\left(\sqrt{\frac{\log(n \vee T)}{T}}\right).$$

In particular, Assumption 3.2 holds with $a_{n,T} = \sqrt{\frac{\log(n \vee T)}{T}}$. If in addition to the above $\log(n \vee T)/(nd_T^2) = o(1)$, then Assumption 3.3 and 3.4 is also satisfied with $b_T := T$, $\Sigma_{i,j} = \Sigma_i + \Sigma_j$ where Σ_i, Σ_j are defined in (12), and $\hat{\Sigma}_{i,j}$ defined in (13).

4 Numerical experiments

In Section 4.1 and Section 4.2, we report the performance of different algorithms in terms of assigning individuals to groups when the true number of groups is specified. We consider two performance metrics: perfect matching, which corresponds to the proportion of times that the exact group assignment is found, and average matching. The latter is computed as follows. Define the true cluster assignment as a set $\omega^* := \{\omega_1^*, \dots, \omega_n^*\}$, where $\omega_i^* \in$

$\{1, \dots, G^*\}$ denotes the ω_i^* -th group to which the individual i belongs. Define the set of permutations of the labels $\Phi := \{\phi : \phi \text{ is a bijection from } \{1, \dots, G^*\} \text{ to } \{1, \dots, G^*\}\}$. Define the estimated membership as a set $\hat{\omega} := \{\hat{\omega}_1, \dots, \hat{\omega}_n\}$, where $\hat{\omega}_i \in \{1, \dots, G^*\}$ denotes the estimated group number of the i -th individual. We define the average percentage of correct classification of the estimated membership $\hat{\omega}$ as

$$\max_{\phi \in \Phi} \frac{1}{n} \sum_{i=1}^n \mathbb{1}\{\phi(\omega_i^*) = \hat{\omega}_i\}.$$

A similar approach was taken in Su et al. (2016); Gu and Volgushev (2019); Leng et al. (2021). The performance of the heuristic (2) for selecting the number of groups is considered in Section 4.3. Additional models and simulation settings are discussed in the supplement.

4.1 Logistic regression

We consider the model

$$Y_{it} = \mathbb{1}\{\alpha_i + \mathbf{x}_{it}^\top \boldsymbol{\beta}_{g_i} \geq \epsilon_{it}\},$$

where ϵ_{it} follows a logistic distribution, $\alpha_i = 1$ for all i and $g_i \in \{1, 2, 3\}$ with equal proportions, and $\mathbf{x}_{it}^\top := (x_{1it}, x_{2it})$ with

$$x_{1it} = 0.5\alpha_i + \eta_i + z_{1it} \text{ and } x_{2it} = 0.5\alpha_i + \eta_i + z_{2it},$$

where $\eta_i \sim N(0, 1)$ and $z_{1it} \sim N(0, 4)$ and $z_{2it} \sim N(0, 0.04)$. Moreover,

$$\boldsymbol{\beta}_1 = (-4, 1)^\top, \boldsymbol{\beta}_2 = (0, 1)^\top, \boldsymbol{\beta}_3 = (4, 1)^\top.$$

Here, the data generating process is constructed such that the coefficient of x_2 is not informative on the group structure while at the same time it is estimated less precisely. On the contrary, the coefficient of x_1 is informative on group structure and also precisely estimated. We compare our method with the C-LASSO proposed by Su et al. (2016) as well as the k -means approach applied on the raw individual-specific logistic regression estimates of $\boldsymbol{\beta}_i$.

The C-LASSO approach proposed in Su et al. (2016) considers minimizing the following objective:

$$\frac{1}{nT} \sum_i \sum_t \psi(Y_{it}, \mathbf{x}_{it}, \boldsymbol{\beta}_i, \hat{\alpha}_i(\boldsymbol{\beta}_i)) + \frac{\lambda}{n} \sum_i \prod_{k=1}^{K_0} \|\boldsymbol{\beta}_i - \eta_k\|.$$

This itself is not a convex optimization, but at each k , we can focus on only the k -th element in the product term in the penalty, resulting in a convex program. For details of the implementation, we refer to our supplement or Su et al. (2016).

Both spectral clustering and C-LASSO rely on the individual logistic regression estimates $\hat{\alpha}_i, \hat{\boldsymbol{\beta}}_i$ as initial input. In a finite sample, we encounter two issues with individual-

specific logistic regression. First, for individuals with Y_i all zeros or all ones estimation is impossible and, hence we exclude such individuals from the sample. Second, when there exists an estimate of β_i such that there is a perfect separation between zeros and ones the minimization problem in logistic regression does not have a solution with finite values. In such cases we sample a new individual to make sure we always have the desired n ; additional details are provided in the supplement.

		Perfect Match						Average Match											
n	T	Spectral			C-LASSO			k-means			Spectral			C-LASSO			k-means		
30	30	0.34	0.13	0.34	0.29	0.06	0.00	0.963	0.879	0.937	0.939	0.854	0.498						
30	60	0.70	0.32	0.67	0.78	0.40	0.01	0.985	0.948	0.979	0.988	0.959	0.653						
30	90	0.81	0.44	0.80	0.86	0.55	0.02	0.993	0.968	0.990	0.993	0.978	0.710						
30	150	0.97	0.77	0.93	0.98	0.93	0.42	0.999	0.987	0.997	0.999	0.998	0.871						
60	30	0.09	0.00	0.07	0.16	0.02	0.00	0.963	0.877	0.928	0.941	0.876	0.453						
60	60	0.53	0.14	0.47	0.55	0.21	0.00	0.989	0.948	0.976	0.981	0.967	0.652						
60	90	0.69	0.21	0.57	0.70	0.54	0.01	0.994	0.959	0.985	0.990	0.987	0.724						
60	150	0.90	0.62	0.88	0.91	0.85	0.50	0.998	0.989	0.998	0.998	0.996	0.892						

Table 1: Comparison of group membership estimation. For C-LASSO, the four columns of the results are based on tuning parameter constants $c = 0.05 \times \{1, \frac{1}{4}, \frac{1}{8}, \frac{1}{32}\}$.

Table 1 reports the performance of three different grouping methods for several combinations of n and T . We evaluate the performance by the proportion of perfect matches out of 100 simulation repetitions and the average matches described at the beginning of Section 4. The k -mean method is applied directly on the individual logistic regression estimates of β_i without taking into account its associated precision estimates. The performance of k -mean is clearly dominated by our approach, showing the value of accounting for the uncertainty in the estimation of group structure. For C-LASSO, the penalty tuning parameter λ is set at $cT^{-1/3}\text{Var}(Y_{it})$ as recommended by the authors with a few different values of c . We see that the C-LASSO can perform very well for a suitably chosen constant, and our method matches that. However, it can perform poorly if the tuning parameter constant is not chosen carefully. This imposes challenges for its practical usage. Table 9 in the online supplement reports the respective computation time for our method versus C-LASSO, which requires iteration with the whole sample. Our approach is clearly computationally less challenging while maintaining similar performance.

4.2 Quantile regression

In this section, we consider quantile regression with individual-specific intercepts and grouping on the slopes as in Example 2.3, and with joint slope and grouping of intercepts from Example 2.2. We focus on the clustering performance with a given (correctly specified) number of groups, the performance of the proposed heuristic, and several other methods for selecting the number of groups is considered in Section 4.3.

4.2.1 Quantile regression individual-specific intercepts and grouping on slopes

Recall the model specification in Example 2.3: $q_{it}(\tau) = \alpha_i(\tau) + \mathbf{x}_{it}^\top \boldsymbol{\beta}_i(\tau) = \mathbf{z}_{it}^\top \boldsymbol{\gamma}_i(\tau)$. This setting was also considered in Zhang et al. (2019a) and we will compare the performance of the proposed method with theirs. We also present results for the proposed spectral clustering scheme with identity sample variance (Spectral^o), as well as naive k -means clustering based only on the estimators of coefficients (k -means^o). The precise form of the dissimilarity matrix \hat{V} employed in spectral clustering is as described in Section 3.2.2.

We consider two models. Model 1 corresponds to Model 3 from Zhang et al. (2019a).

Model 1:

$$y_{it} = \alpha_i + \mathbf{x}_{it}^\top \boldsymbol{\beta}_{g_i} + 0.5x_{2it}e_{it},$$

where

$$\alpha_i \stackrel{iid}{\sim} U(0, 1), i = 1, \dots, n, \quad g_i \text{ are sampled randomly with equal probabilities from } \{1, 2, 3\}.$$

Set

$$\boldsymbol{\beta}_1 = \begin{pmatrix} 0.1 \\ 0.1 \end{pmatrix}, \boldsymbol{\beta}_2 = \begin{pmatrix} 0.2 \\ 0.2 \end{pmatrix}, \boldsymbol{\beta}_3 = \begin{pmatrix} 0.3 \\ 0.3 \end{pmatrix},$$

$e_{it} \stackrel{iid}{\sim} N(0, 1)$ or $e_{it} \stackrel{iid}{\sim} t(3)$, and

$$\mathbf{x}_{it}^\top = (x_{1it}, x_{2it}), \text{ with } x_{1it} = 0.3\alpha_i + z_{1it}, \text{ with } z_{1it} \stackrel{iid}{\sim} N(0, 1), \text{ and } x_{2it} \sim U(0, 1).$$

Results for $\tau = 0.5$ are reported in Table 2, corresponding results for $\tau = 0.7$ are deferred to Table 10 in the online supplement. The proposed method shows uniformly best performance in terms of average and perfect matching across all settings considered. The approach of Zhang et al. (2019a) comes close in terms of average matching and is better than both methods which ignore variance information when it comes to average matching. Surprisingly, Zhang et al. (2019a) shows worse performance in terms of perfect matching. A closer look at the results revealed that in this model the method of Zhang et al. (2019a) often assigns one individual to the wrong group, resulting in good average matching but inferior perfect matching performance. Despite our best efforts at varying various parameters of Zhang et al. (2019a) (e.g. criteria for termination and number of random starting points), we were not able to alleviate this issue.

The second model we consider has four groups, with pairs of group centres being close together. Both entries of the coefficient vector carry information about the group structure, but one of them is estimated more precisely than the other one.

Model 2:

$$y_{it} = \alpha_i + \mathbf{x}_{it}^\top \boldsymbol{\beta}_{g_i} + 0.5x_{2it}e_{it},$$

where

$\alpha_i = 1, i = 1, \dots, n$, g_i are sampled randomly with equal probabilities from $\{1, 2, 3, 4\}$.

Set

$$\boldsymbol{\beta}_1 = \begin{pmatrix} 0.1 \\ 0.1 \end{pmatrix}, \boldsymbol{\beta}_2 = \begin{pmatrix} 0.2 \\ 0.2 \end{pmatrix}, \boldsymbol{\beta}_3 = \begin{pmatrix} 3 \\ 3 \end{pmatrix}, \boldsymbol{\beta}_4 = \begin{pmatrix} 3.1 \\ 3.1 \end{pmatrix},$$

$e_{it} \stackrel{iid}{\sim} N(0, 1)$ or $t(3)$, and set

$$\mathbf{x}_{it}^\top = (x_{1it}, x_{2it}), \text{ with } x_{1it} = 0.3\alpha_i + z_{1it}, \text{ where } z_{1it} \stackrel{iid}{\sim} N(0, 1), \text{ and } x_{2it} \sim U(0, 1).$$

Results for $\tau = 0.5$ are reported in Table 3, corresponding results for $\tau = 0.7$ are deferred to Table 11 in the online supplement. Similar to Model 1, the proposed method has the best performance with respect to perfect and average match. The method of Zhang et al. (2019a) outperforms both methods that do not take into account variance information.

n	T	Perfect Match			Average Match				
		Spectral	ZWZ19	Spectral ^o	k -means ^o	Spectral	ZWZ19	Spectral ^o	k -means ^o
$t(3), \tau = 0.5$									
30	60	0.20	0.08	0.00	0.00	0.948	0.870	0.585	0.590
30	90	0.47	0.28	0.00	0.00	0.977	0.950	0.660	0.660
30	120	0.78	0.53	0.00	0.00	0.992	0.978	0.709	0.745
60	60	0.00	0.00	0.00	0.00	0.937	0.885	0.566	0.569
60	90	0.14	0.05	0.00	0.00	0.973	0.952	0.645	0.655
60	120	0.57	0.25	0.00	0.00	0.988	0.975	0.709	0.725
90	60	0.00	0.00	0.00	0.00	0.938	0.895	0.571	0.572
90	90	0.07	0.03	0.00	0.00	0.968	0.955	0.648	0.657
90	120	0.41	0.11	0.00	0.00	0.986	0.976	0.709	0.723
$N(0, 1), \tau = 0.5$									
30	60	0.38	0.24	0.00	0.00	0.969	0.928	0.615	0.622
30	90	0.73	0.39	0.00	0.00	0.989	0.970	0.676	0.684
30	120	0.92	0.75	0.00	0.00	0.997	0.989	0.698	0.746
60	60	0.10	0.01	0.00	0.00	0.964	0.920	0.593	0.589
60	90	0.46	0.12	0.00	0.00	0.987	0.967	0.683	0.689
60	120	0.68	0.46	0.00	0.00	0.994	0.986	0.724	0.745
90	60	0.02	0.01	0.00	0.00	0.962	0.926	0.611	0.608
90	90	0.34	0.05	0.00	0.00	0.988	0.970	0.689	0.699
90	120	0.57	0.26	0.00	0.00	0.994	0.984	0.738	0.767

Table 2: Membership estimation based on Spectral (the proposed method), ZWZ19 Zhang et al. (2019a), Spectral^o, and k -means^o for Model 1 with $\tau = 0.5$.

4.2.2 Quantile regression with joint slope and grouping on intercepts

In this section, we consider the setting in Example 2.2. The spectral clustering approach is based on the estimators for the slopes and variances described in Section 3.2.3. More precisely, recall the definition of $\tilde{\alpha}_1, \tilde{\beta}$ in (10) and $\hat{\Sigma}_{i,j}$ defined in (13). The variation

n	T	Perfect Match			Average Match				
		Spectral	ZWZ19	Spectral°	k -means°	Spectral	ZWZ19	Spectral°	k -means°
$t(3), \tau = 0.5$									
40	40	0.01	0.00	0.00	0.00	0.915	0.752	0.619	0.632
40	80	0.38	0.09	0.00	0.00	0.975	0.863	0.672	0.690
40	120	0.76	0.17	0.00	0.00	0.992	0.843	0.751	0.772
60	40	0.00	0.00	0.00	0.00	0.916	0.785	0.636	0.638
60	80	0.20	0.04	0.00	0.00	0.974	0.848	0.689	0.705
60	120	0.65	0.18	0.00	0.00	0.992	0.839	0.740	0.766
$N(0, 1), \tau = 0.5$									
40	40	0.06	0.01	0.00	0.00	0.942	0.824	0.643	0.650
40	80	0.59	0.23	0.00	0.00	0.987	0.919	0.701	0.719
40	120	0.86	0.43	0.00	0.00	0.997	0.899	0.787	0.813
60	40	0.01	0.00	0.00	0.00	0.929	0.827	0.634	0.644
60	80	0.39	0.07	0.00	0.00	0.985	0.897	0.719	0.738
60	120	0.81	0.32	0.00	0.00	0.997	0.869	0.782	0.805

Table 3: Membership estimation based on Spectral, ZWZ19, Spectral°, and k -means°. Data are generated from Model 2 with $\tau = 0.5$.

matrix \hat{V} which we use as input to the spectral clustering algorithm is given by $\hat{V}_{ij} := \hat{\Sigma}_{i,j}^{-1/2} |\tilde{\alpha}_i - \tilde{\alpha}_j|$. For comparison, we also consider spectral clustering setting all variance estimators set to be equal, the naive k -means approach on estimated $\tilde{\alpha}_i$ from (10), and the convex clustering procedure of Gu and Volgushev (2019). Tuning parameters for Gu and Volgushev (2019) were set as described in the latter paper. The following model corresponds to DGP1 location scale shift model in Gu and Volgushev (2019).

Model 3:

$$y_{it} = \alpha_i + x_{it}\beta + (1 + x_{it}\gamma)e_{it}.$$

where $e_{it} \stackrel{iid}{\sim} N(0, 1)$ or $e_{it} \stackrel{iid}{\sim} t(3)$, $\alpha_i \in \{1, 2, 3\}$ with the same proportions, and $\beta = 1, \gamma = 0.1, x_{it} = \gamma_i + v_{it}$, where γ_i and v_{it} are independent and identically distributed from standard normal distribution over i, t , respectively.

Tables 4 and 12 summarize the proportion of perfect classification and the average of the percentage of correct classification based on the proposed method (Spectral), spectral clustering ignoring variance information (Spectral°), k -means clustering on $\tilde{\alpha}_i$ (k -means°) and the procedure from Gu and Volgushev (2019) (GV) for $\tau = 0.5$ (Table 4) and $\tau = 0.7$ (Table 12, deferred to the supplement) respectively. Interestingly, including variance information is not helpful in this setting and all considered methods show comparable performance with GV falling behind in terms of average match and perfect classification in some of the settings. Results in other models from Gu and Volgushev (2019) are similar and omitted for the sake of brevity. A possible explanation for variance information not being useful in this model is that the α_i are one-dimensional and there are no directions of larger or smaller variation in their estimates.

n	T	Perfect Match				Average Match			
		Spectral	Spectral [°]	k -means [°]	GV	Spectral	Spectral [°]	k -means [°]	GV
$t(3), \tau = 0.5$									
30	15	0.01	0.01	0.01	0.01	0.870	0.861	0.871	0.638
30	30	0.26	0.26	0.31	0.23	0.953	0.952	0.957	0.836
30	60	0.82	0.84	0.83	0.80	0.993	0.994	0.994	0.975
60	15	0.00	0.00	0.00	0.00	0.881	0.876	0.882	0.595
60	30	0.10	0.11	0.11	0.08	0.960	0.960	0.963	0.850
60	60	0.83	0.83	0.85	0.71	0.996	0.996	0.997	0.983
90	15	0.00	0.00	0.00	0.00	0.883	0.886	0.888	0.550
90	30	0.04	0.04	0.04	0.03	0.964	0.965	0.968	0.851
90	60	0.66	0.68	0.68	0.63	0.996	0.996	0.996	0.984
$N(0, 1), \tau = 0.5$									
30	15	0.07	0.08	0.10	0.03	0.905	0.894	0.899	0.670
30	30	0.60	0.58	0.55	0.39	0.981	0.980	0.980	0.880
30	60	0.95	0.95	0.96	0.91	0.998	0.998	0.999	0.988
60	15	0.01	0.01	0.00	0.00	0.908	0.908	0.911	0.663
60	30	0.46	0.45	0.39	0.22	0.985	0.985	0.986	0.903
60	60	0.99	0.99	0.98	0.86	0.999	0.999	0.999	0.994
90	15	0.00	0.00	0.00	0.00	0.917	0.916	0.918	0.662
90	30	0.26	0.27	0.28	0.12	0.985	0.986	0.986	0.908
90	60	0.92	0.92	0.91	0.83	0.999	0.999	0.999	0.994

Table 4: Membership estimation based on Spectral, k -means, Spectral[°], and k -means[°] methods, and also the method proposed in Gu and Volgushev (2019) (GV) for Model 3 with $\tau = 0.5$.

4.3 Determining the Number of Groups

In this section, we compare the proposed heuristic in (2) for selecting the number of groups with other proposals from the literature. A general principle for determining the number of clusters using cross-validation in combination with the stability of cluster assignments was proposed by Wang (2010) and adapted to quantile regression with grouping on the slopes in Zhang et al. (2019a). The underlying idea is directly applicable to any clustering algorithm, and hence we consider two versions: CV-kmeans corresponding to the proposal of Zhang et al. (2019a), and CV-Spectral which uses spectral clustering as proposed in the present paper as the underlying clustering algorithm. The maximum numbers of clusters to consider, denoted by Gmax, is set to 10 throughout.

Results for Model 1 are presented in Table 5 ($\tau = 0.5$) and Table 14 ($\tau = 0.7$) respectively. Tables 6 and 15 summarize the results for Model 2 for $\tau = 0.5$ and $\tau = 0.7$, respectively. We defer the results corresponding to $\tau = 0.7$ to the online supplement.

For Model 1, the proposed heuristic has the best performance for all settings except for $t(3)$ errors with $\tau = 0.7$ and $n = 30, 60, T = 60$ where the two CV methods work better with CV-Spectral outperforming CV-kmeans. CV-Spectral shows better performance than CV-kmeans across the board. We note that Model 1 is perfectly symmetric with an odd number of groups, this corresponds to a setting that is favorable for stability-based methods. Breaking this symmetry while keeping the same number of groups leads to surprising results, additional details are provided in the online supplement.

Model 2 corresponds to an even number of groups, and both CV methods fail in this setting because they always pick 2 groups. In light of the findings in Ben-David et al. (2006), this is not surprising; see also Von Luxburg (2010). The issue is that a wrong grouping with two groups corresponding to coefficients $(0.1, 0.1), (0.2, 0.2)$ in one group and $(3, 3), (3.1, 3.1)$ in the other is very stable under variations of the data which leads to confusion of the stability-based methods. In the online supplement, we plot the paths of cross-validated stability scores for different n, T combinations and different realizations of the data (Figure 4). For larger T there is a local minimum at the true number of groups $G = 4$, but the global minima are always at $G = 2$. The proposed heuristic works reasonably well and is able to pick up the correct number of groups as T increases.

Model 3 corresponds to common slopes and group structure on the intercept (see also Example 2.2). Since this setting was also considered in Gu and Volgushev (2019), we consider the information criterion proposed in there. Results for $\tau = 0.5$ and $\tau = 0.7$ are presented in Table 7 and Table 16 (deferred to the online supplement). We also include cross-validation with spectral clustering, denoted by CV-spectral, for comparison. Note that CV-kmeans is not applicable in this setting.

For $\tau = 0.5, n = 30, T = 15$, the best performing method is Gu and Volgushev (2019) with about a 10% – 15% advantage over the other two methods which show comparable performance; the advantage of Gu and Volgushev (2019) is even clearer for $\tau = 0.7, n = 30, T = 15$. In all other settings, CV-Spectral is the best or close to best (within 5%) performer. The heuristic method performs better or is similar to Gu and Volgushev (2019) for most cases with $n = 90, T \geq 60$ while the results between those two are mixed in other settings.

In conclusion, there is no clear winner that performs best across all models and settings. This is not surprising because selecting the number of clusters is a very difficult problem in general. This also explains why there exists no unifying approach for selecting the number of groups. Our proposed eigenvalue heuristic is competitive in most cases considered, and clearly the best on some. Stability-based methods have two major limitations: they cannot select one group by construction, and they can fail for models with stable clusters for the wrong number of groups. The information criterion in Gu and Volgushev (2019) can select one group and performs well when n, T are smaller but falls behind when n is large. No information criterion is known for quantile regression models with unrestricted intercepts and grouping on the slopes. Such a criterion could potentially be derived, but it would only be valid in this specific setting and we refrained from taking this route since we aimed to propose a method that is applicable in more generality.

n	T	N(0, 1)					t(3)				
		1	2	3	4	≥ 5	1	2	3	4	≥ 5
CV-Spectral, $\tau = 0.5$											
30	60	—	0.14	0.78	0.06	0.02	—	0.30	0.56	0.08	0.06
30	90	—	0.00	0.98	0.02	0.00	—	0.02	0.92	0.04	0.02
30	120	—	0.04	0.96	0.00	0.00	—	0.16	0.84	0.00	0.00
60	60	—	0.00	1.00	0.00	0.00	—	0.00	0.96	0.00	0.04
60	90	—	0.00	1.00	0.00	0.00	—	0.00	1.00	0.00	0.00
60	120	—	0.00	1.00	0.00	0.00	—	0.00	1.00	0.00	0.00
CV-kmeans, $\tau = 0.5$											
30	60	—	0.22	0.60	0.06	0.12	—	0.22	0.42	0.14	0.22
30	90	—	0.12	0.72	0.16	0.00	—	0.22	0.58	0.16	0.04
30	120	—	0.10	0.86	0.04	0.00	—	0.08	0.84	0.06	0.02
60	60	—	0.06	0.36	0.22	0.36	—	0.02	0.26	0.24	0.48
60	90	—	0.06	0.74	0.12	0.08	—	0.10	0.52	0.18	0.20
60	120	—	0.06	0.90	0.04	0.00	—	0.04	0.78	0.14	0.04
Heuristic, $\tau = 0.5$											
30	60	0.01	0.12	0.85	0.01	0.01	0.02	0.36	0.59	0.03	0.00
30	90	0.00	0.00	0.96	0.04	0.00	0.00	0.07	0.93	0.00	0.00
30	120	0.00	0.00	0.98	0.02	0.00	0.00	0.00	1.00	0.00	0.00
60	60	0.01	0.00	0.99	0.00	0.00	0.16	0.01	0.83	0.00	0.00
60	90	0.00	0.00	1.00	0.00	0.00	0.00	0.00	1.00	0.00	0.00
60	120	0.00	0.00	1.00	0.00	0.00	0.00	0.00	1.00	0.00	0.00

Table 5: Percentage of estimated number of groups based on CV-Spectral, CV-kmeans, and Heuristic for Model 1 with $\tau = 0.5$.

5 Empirical Applications

5.1 Heterogeneity in environmental Kuznet curves

We first apply our methodology to a panel data quantile regression analysis on the environmental Kuznet curves (EKC). The concept first emerged in the influential study of Grossman and Krueger (1991). Various empirical studies have since then provided evidence in different countries that there exists an inverse-U relationship between economic development and the pollution level. As income per capita increases, we expect to see first deterioration of the environment, and then an improvement as income continues to rise. Understanding the relationship between pollution and per capita income is important for the design of the optimal environmental policy. Here we focus our analysis on using state-level panel data in the United States during the period of 1929 - 1994 and for brevity, we focus on the emission of SO_2 . The dataset is available from the National Air Pollutant Emission Trends, 1900 - 1994, published by the US Environmental Protection Agency. Most early empirical work on EKC uses least squares methods pooling all the states together and utilizes either a quadratic or cubic specification to estimate the relationship between the emission level and per capita income. Millimet et al. (2003) discusses in detail some of the model specification issues and explores semi-parametric methods that provide a set of more flexible modelling tools. Given concerns that different states may take a different

n	T	N(0, 1)					t(3)				
		1	2	3	4	≥5	1	2	3	4	≥5
CV-Spectral, $\tau = 0.5$											
40	40	0.00	1.00	0.00	0.00	0.00	0.00	1.00	0.00	0.00	0.00
40	80	0.00	1.00	0.00	0.00	0.00	0.00	1.00	0.00	0.00	0.00
40	160	0.00	1.00	0.00	0.00	0.00	0.00	1.00	0.00	0.00	0.00
60	40	0.00	1.00	0.00	0.00	0.00	0.00	1.00	0.00	0.00	0.00
60	80	0.00	1.00	0.00	0.00	0.00	0.00	1.00	0.00	0.00	0.00
60	160	0.00	1.00	0.00	0.00	0.00	0.00	1.00	0.00	0.00	0.00
CV-kmeans, $\tau = 0.5$											
40	40	0.00	1.00	0.00	0.00	0.00	0.00	1.00	0.00	0.00	0.00
40	80	0.00	1.00	0.00	0.00	0.00	0.00	1.00	0.00	0.00	0.00
40	160	0.00	1.00	0.00	0.00	0.00	0.00	1.00	0.00	0.00	0.00
60	40	0.00	1.00	0.00	0.00	0.00	0.00	1.00	0.00	0.00	0.00
60	80	0.00	1.00	0.00	0.00	0.00	0.00	1.00	0.00	0.00	0.00
60	160	0.00	1.00	0.00	0.00	0.00	0.00	1.00	0.00	0.00	0.00
Heuristic, $\tau = 0.5$											
40	40	0.00	0.72	0.00	0.28	0.00	0.00	0.94	0.00	0.06	0.00
40	80	0.00	0.01	0.00	0.98	0.01	0.00	0.01	0.00	0.99	0.00
40	160	0.00	0.00	0.00	1.00	0.00	0.00	0.00	0.00	1.00	0.00
60	40	0.00	0.49	0.00	0.50	0.01	0.00	0.90	0.00	0.10	0.00
60	80	0.00	0.00	0.00	1.00	0.00	0.00	0.00	0.00	1.00	0.00
60	160	0.00	0.00	0.00	1.00	0.00	0.00	0.00	0.00	1.00	0.00

Table 6: Percentage of estimated number of groups with CV-Spectral, CV-kmeans and Heuristic methods for Model 2 with $\tau = 0.5$.

environmental transition path as income level arises, List and Gallet (1999) estimates the EKC with both the quadratic and cubic specification state by state to account for potential state heterogeneity. They then group these states into three groups depending on whether the estimated peak of the state-specific EKC falls below, inside or above the 95% confidence interval implied by a pooled model. This provides an interesting piece of evidence for some form of group heterogeneity, yet how group membership is constructed is ad hoc and does not account for the statistical uncertainty of the state-specific least square estimates. On the other hand, Flores et al. (2014) has criticized the least square approach and advocates the use of quantile regression methods. They document that quantile regression offers a more complete picture of the relationship between pollution and income. However, for a given quantile, they estimate the panel data quantile regression with state fixed effect without allowing the EKC coefficients to be state-dependent. Combining the insights of List and Gallet (1999) and Flores et al. (2014), we apply our methodology in a panel data quantile regression model which allows individual fixed effects while estimating the group structure of the slope coefficients that determine the shape of the EKC curves across different states.

For a given quantile level τ , our model specification is:

$$q_{i,\tau}(Z_{it}) = \alpha_i(\tau) + \lambda_t(\tau) + Z_{it}\beta_{1,g_i}(\tau) + Z_{it}^2\beta_{2,g_i}(\tau),$$

n	T	N(0, 1)					t(3)				
		1	2	3	4	≥ 5	1	2	3	4	≥ 5
CV-Spectral, $\tau = 0.5$											
30	15	—	0.28	0.40	0.12	0.20	—	0.40	0.38	0.06	0.16
30	30	—	0.04	0.94	0.00	0.02	—	0.10	0.86	0.02	0.02
30	60	—	0.00	1.00	0.00	0.00	—	0.02	0.94	0.04	0.00
60	15	—	0.18	0.64	0.04	0.14	—	0.24	0.46	0.00	0.30
60	30	—	0.00	1.00	0.00	0.00	—	0.00	1.00	0.00	0.00
60	60	—	0.00	1.00	0.00	0.00	—	0.00	1.00	0.00	0.00
90	15	—	0.06	0.72	0.00	0.22	—	0.16	0.64	0.00	0.20
90	30	—	0.00	1.00	0.00	0.00	—	0.00	1.00	0.00	0.00
90	60	—	0.00	1.00	0.00	0.00	—	0.00	1.00	0.00	0.00
Heuristic, $\tau = 0.5$											
30	15	0.05	0.36	0.39	0.04	0.16	0.13	0.41	0.35	0.06	0.05
30	30	0.00	0.02	0.93	0.03	0.02	0.00	0.22	0.72	0.00	0.06
30	60	0.00	0.00	0.98	0.00	0.02	0.00	0.00	0.98	0.00	0.02
60	15	0.19	0.37	0.44	0.00	0.00	0.43	0.37	0.19	0.00	0.01
60	30	0.00	0.00	1.00	0.00	0.00	0.00	0.07	0.93	0.00	0.00
60	60	0.00	0.00	1.00	0.00	0.00	0.00	0.00	1.00	0.00	0.00
90	15	0.03	0.38	0.56	0.02	0.01	0.12	0.48	0.38	0.00	0.02
90	30	0.00	0.00	1.00	0.00	0.00	0.00	0.02	0.98	0.00	0.00
90	60	0.00	0.00	1.00	0.00	0.00	0.00	0.00	1.00	0.00	0.00
GV, $\tau = 0.5$											
30	15	0.00	0.06	0.51	0.34	0.09	0.00	0.16	0.50	0.27	0.08
30	30	0.00	0.00	0.81	0.16	0.03	0.00	0.01	0.76	0.20	0.04
30	60	0.00	0.00	0.98	0.02	0.00	0.00	0.00	0.96	0.03	0.00
60	15	0.00	0.04	0.52	0.32	0.12	0.00	0.11	0.44	0.33	0.12
60	30	0.00	0.00	0.86	0.13	0.02	0.00	0.00	0.78	0.18	0.04
60	60	0.00	0.00	0.99	0.01	0.00	0.00	0.00	0.98	0.02	0.00
90	15	0.00	0.03	0.51	0.32	0.14	0.00	0.11	0.37	0.33	0.19
90	30	0.00	0.00	0.88	0.11	0.01	0.00	0.00	0.79	0.17	0.03
90	60	0.00	0.00	0.99	0.01	0.00	0.00	0.00	0.98	0.02	0.00

Table 7: Percentage of estimated number of groups based on CV-Spectral, Heuristic, and Gu and Volgushev (2019) (GV) methods for Model 3 with $\tau = 0.5$.

where i corresponds to states, t it the time index and g_i records the group membership. We denote by $q_{i,\tau}(Z_{it})$ the conditional quantile function of Y_{it} given Z_{it} where the response Y_{it} is the state-year per capita emission level of SO_2 and Z_{it} is the per capita real income using 1987 dollar. We focus on the quadratic specification for better visualization of the estimation results. Cubic specification leads to similar grouping results. Other control variables can be added, for example, population density and the number of days with extreme temperature as considered in Flores et al. (2014). However, Flores et al. (2014) report that these additional control variables do not change the estimates for the quadratics of the EKC. We first obtain state-specific estimates $\hat{\beta}_{1,i}(\tau), \hat{\beta}_{2,i}(\tau)$ as well as their associated covariance matrix.

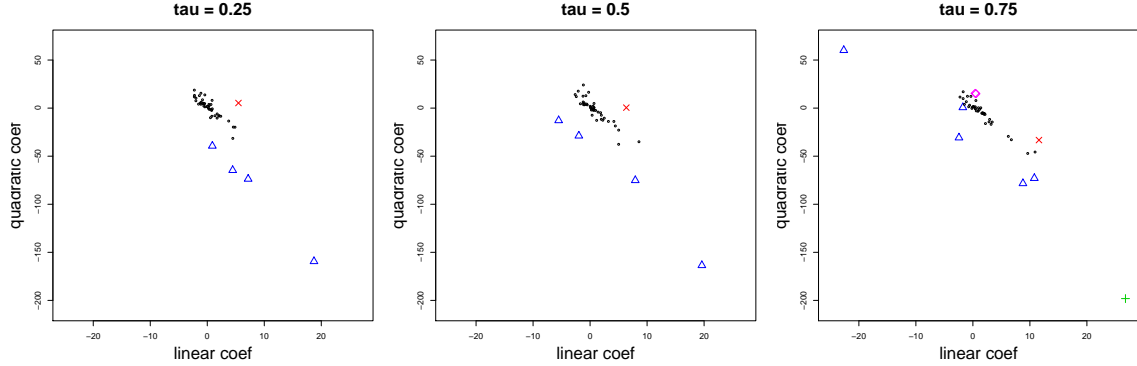


Figure 1: Raw state specific estimates for $\hat{\beta}_{1,i}(\tau), \hat{\beta}_{2,i}(\tau)$ and grouping of states for quantile levels $\tau = \{0.25, 0.5, 0.75\}$. Each symbol represents a different group.

To estimate the number of groups for different quantile levels $\tau = \{0.25, 0.5, 0.75\}$, we apply the heuristic in (2); see Figure 5 in the online supplement for corresponding plots. For both 25 and 50th quantile, we find three groups and for 75th quantile, we find 5 groups. Given these estimates, we then apply the spectral clustering method on these raw estimates, accounting for the statistical uncertainty. Figure 1 shows the estimated group membership for $(\hat{\beta}_{1,i}(\tau), \hat{\beta}_{2,i}(\tau))$. Noticeably, for both 25th and 50th quantile, the grouping of the states are the same. The red cross in Figure 1 corresponds to West Virginia, while the blue triangles correspond to Arizona, Montana, Nevada, and Utah. A close inspection of the data suggests that the EKC for West Virginia looks to be closer to a linear trend within the range of years under consideration, while Arizona, Montana, Nevada, and Utah are states that have relatively higher emission level and a much more positive linear coefficient and a much negative quadratic coefficient when compared to all other states. Interestingly, these four states are also noted as the “outlier” states in Flores et al. (2014) which documents that the residuals of these states are alarmingly high. Since their specification requires the EKC coefficients to be the same for all states, this provides some evidence that these states might have a different EKC. This is clearly confirmed by our analysis. For the 75th quantile, the State of Arizona has a more extreme estimate and now becomes a group by herself, as well as West Virginia. Two smaller groups consist of North Dakota and Wyoming as one group and Illinois, Montana, Nevada, New Mexico, and Utah as the other group.

5.2 Heterogeneity in intergenerational income mobility

The study on intergenerational income mobility across the United States by Chetty et al. (2014), Chetty et al. (2018) and Chetty and Hendren (2018) has been influential. Using tax records on the entire U.S. population, they document how children’s expected incomes conditional on their parents’ incomes differ across different geographical regions in the United States. Although the raw data used to obtain these estimates are not publicly available, they publish the region specific estimates at the commuting zone, county or census tract

level, together with their associated standard errors. These estimates are used for policy purposes to encourage welfare improvements for children resides in the areas that have low mobility rates as for instance considered in Bergman et al. (2019). The categorization of a region having low mobility is often solely based on the point estimates without accounting for the associated statistical uncertainty. Our analysis focuses on the plausible hypothesis that although different geographical locations are likely to have heterogeneous mobility ratings, they may be divided into a few distinct groups and we let the data determine the number of groups utilizing both point estimates and their levels of precision.

We focus on the 100 most populous commuting zones. Let the point estimates of the income mobility to be $\hat{\beta}_i$ and the associated standard error to be $\hat{\Sigma}_i$. To apply the heuristic for the estimation of the number of groups, we also know T_i which is the amount of data that leads to the estimates $(\hat{\beta}_i, \hat{\Sigma}_i)$.²

We first use our method to select the number of groups. The left plot in Figure 5.2 shows that the number of groups is estimated to be nine and the right plot illustrates the gap of the adjacent eigen values. We then apply our algorithm to estimate the group membership, which is illustrated in Figure 5.2. Further details on the grouping of the hundred most populous commuting zones is provided in Table 8. Fayetteville and Memphis have the lowest point estimates for their income mobility among all the hundred commuting zones considered and they are grouped together. There are ten commuting zones grouped together as the top tier. The grouping provides a parsimonious description of the mobility heterogeneity. It also suggests that citizens in the commuting zones that belong to the same group, although having different point estimates, are likely to have similar true mobility ratings.

²All these information are publicly available from <https://opportunityinsights.org/data>.

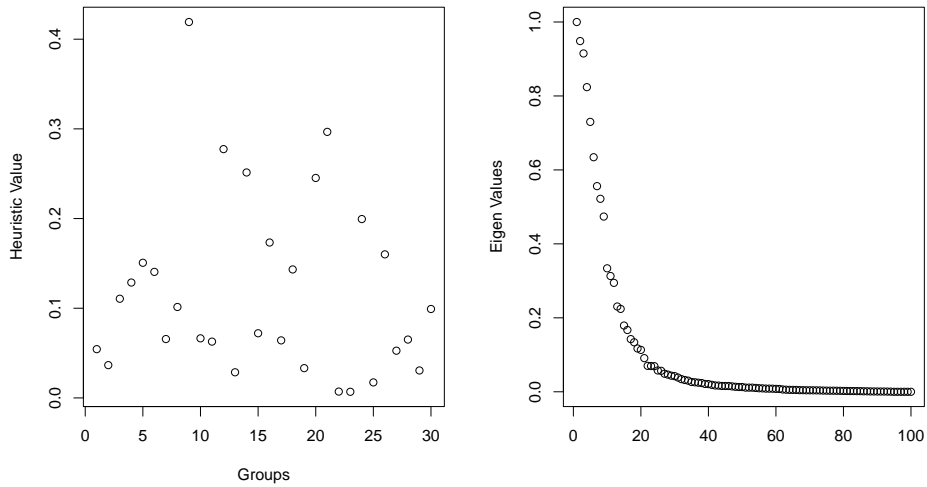


Figure 2: The heuristic value for group selection and the associated eigen values for the 100 most populous commuting zones using publicly data in Chetty and Hendren (2018).



Figure 3: Points in the figure are the sorted point estimates $\hat{\beta}_i$ for the 100 most populous commuting zones in the United States. The blue bars indicates the confidence set of each point estimates with ± 2 s.e. The dotted line are the division lines for the 9 groups based on the estimated group membership.

Grouped Commuting Zones	
1	Boston, Des Moines, Honolulu, Minneapolis, Newark, Toms River, Salt Lake City San Francisco, San Jose, Scranton
2	Albany, Allentown, Brownsville, Los Angeles, Madison, Manchester, New York Pittsburgh, Providence, Reading, Santa Barbara, Santa Rosa, Seattle, Spokane
3	Bakersfield, Buffalo, Bridgeport, Canton, Denver, El Paso, Erie Harrisburg, Houston, Modesto, Omaha, Portland, Poughkeepsie, Sacramento San Diego, Springfield, Syracuse, Washington DC
4	Austin, Eugene, Fort Worth, Miami, Oklahoma City, Philadelphia Rockford, San Antonio, Tulsa, Youngstown
5	Albuquerque, Baton Rouge, Cape Coral, Chicago, Cleveland, Dallas Fresno, Gary, Grand Rapids, Kansas City, Las Vegas, Milwaukee, Orlando Port St. Lucie, Phoenix, Sarasota, South Bend, Toledo, Tucson
6	Baltimore, Cincinnati, Columbus, Dayton, Detroit, Louisville Nashville, New Orleans, Pensacola, St. Louis, Tampa, Virginia Beach
7	Knoxville, Indianapolis, Lakeland, Little Rock, Mobile, Raleigh, Richmond
8	Atlanta, Birmingham, Charlotte, Columbia, Greensboro, Greenville, Jacksonville
9	Fayetteville, Memphis

Table 8: The 100 most populous commuting zones grouped using our method. First group are for those with the highest income mobility rating and the last group the lowest.

6 Conclusion

In this paper, we propose a general methodology for studying group heterogeneity of effects in panel data models. We provide high-level conditions for the proposed method to achieve correct group identification and verify these conditions for several leading non-linear models often applied in empirical studies. We demonstrate that incorporating uncertainty information in individual-level estimates is useful for estimating group patterns. Although we focus on non-linear models, our methodology is naturally applicable to linear models, as well to situations where micro-level data is not available and summary statistics are accessible to the researcher. Extending our approach to more complex models with time-varying group heterogeneity seems a natural next step which we plan to address in future research.

References

Ando, T., J. Bai, and K. Li (2021). Bayesian and maximum likelihood analysis of large-scale panel choice models with unobserved heterogeneity. *Journal of Econometrics*.

Bai, J. (2009). Panel data models with interactive fixed effects. *Econometrica* 77(4), 1229–1279.

Ben-David, S., U. Von Luxburg, and D. Pál (2006). A sober look at clustering stability. In *International Conference on Computational Learning Theory*, pp. 5–19. Springer.

Bergman, P., R. Chetty, S. DeLuca, N. Hendren, L. F. Katz, and C. Palmer (2019). Creating moves to opportunity: Experimental evidence on barriers to neighborhood choice. Technical report, National Bureau of Economic Research.

Bonhomme, S. and E. Manresa (2015). Grouped patterns of heterogeneity in panel data. *Econometrica* 83(3), 1147–1184.

Chao, S.-K., S. Volgushev, and G. Cheng (2017). Quantile processes for semi and nonparametric regression. *Electronic Journal of Statistics* 11(2), 3272–3331.

Chetty, R., J. N. Friedman, N. Hendren, M. R. Jones, and S. R. Porter (2018). The opportunity atlas: Mapping the childhood roots of social mobility. Technical report, National Bureau of Economic Research.

Chetty, R. and N. Hendren (2018). The impacts of neighborhoods on intergenerational mobility i: Childhood exposure effects. *The Quarterly Journal of Economics* 133(3), 1107–1162.

Chetty, R., N. Hendren, P. Kline, and E. Saez (2014). Where is the land of opportunity? the geography of intergenerational mobility in the united states. *The Quarterly Journal of Economics* 129(4), 1553–1623.

Chetverikov, D. and E. Manresa (2021). Spectral and post-spectral estimators for grouped panel data models. *working paper*.

Chung, F. and M. Radcliffe (2011). On the spectra of general random graphs. *the electronic journal of combinatorics*, P215–P215.

Chung, F. R. and F. C. Graham (1997). *Spectral graph theory*. Number 92. American Mathematical Soc.

Flores, C. A., A. Flores-Lagunes, and D. Kapetanakis (2014). Lessons from quantile panel estimation of the environmental kuznets curve. *Econometric Reviews* 33(8), 815–853.

Galvao, A. F., J. Gu, and S. Volgushev (2020). On the unbiased asymptotic normality of quantile regression with fixed effects. *Journal of Econometrics*.

Galvao, A. F. and K. Kato (2016). Smoothed quantile regression for panel data. *Journal of Econometrics* 193(1), 92–112.

Grossman, G. M. and A. B. Krueger (1991). Environmental impacts of a north american free trade agreement.

Gu, J. and S. Volgushev (2019). Panel data quantile regression with grouped fixed effects. *Journal of Econometrics* 213(1), 68–91.

Harding, M. and C. Lamarche (2017). Penalized quantile regression with semiparametric correlated effects: An application with heterogeneous preferences. *Journal of Applied Econometrics* 32(2), 342–358.

Hendricks, W. and R. Koenker (1992). Hierarchical spline models for conditional quantiles and the demand for electricity. *Journal of the American statistical Association* 87(417), 58–68.

Hocking, T. D., A. Joulin, F. Bach, and J.-P. Vert (2011). Clusterpath an algorithm for clustering using convex fusion penalties. In *28th international conference on machine learning*, pp. 1.

John, C. R., D. Watson, M. R. Barnes, C. Pitzalis, and M. J. Lewis (2020). Spectrum: Fast density-aware spectral clustering for single and multi-omic data. *Bioinformatics* 36(4), 1159–1166.

Kato, K., A. F. Galvao Jr, and G. V. Montes-Rojas (2012). Asymptotics for panel quantile regression models with individual effects. *Journal of Econometrics* 170(1), 76–91.

Kaufman, L. and P. J. Rousseeuw (2009). *Finding groups in data: an introduction to cluster analysis*, Volume 344. John Wiley & Sons.

Ke, Z. T., J. Fan, and Y. Wu (2015). Homogeneity pursuit. *Journal of the American Statistical Association* 110(509), 175–194.

Koenker, R. (2004). Quantile regression for longitudinal data. *Journal of Multivariate Analysis* 91(1), 74–89.

Lamarche, C. (2010). Robust penalized quantile regression estimation for panel data. *Journal of Econometrics* 157, 396–408.

Leng, X., W. Wang, and H. Chen (2021). Multi-dimensional latent group structures with heterogeneous distributions. *preprint*.

Lin, C.-C. and S. Ng (2012). Estimation of panel data models with parameter heterogeneity when group membership is unknown. *Journal of Econometric Methods* 1(1), 42–55.

List, J. A. and C. A. Gallet (1999). The environmental kuznets curve: does one size fit all? *Ecological economics* 31(3), 409–423.

Little, A., M. Maggioni, and J. M. Murphy (2017). Path-based spectral clustering: Guarantees, robustness to outliers, and fast algorithms. *arXiv preprint arXiv:1712.06206*.

Lumsdaine, R. L., R. Okui, and W. Wang (2021). Estimation of panel group structure models with structural breaks in group memberships and coefficients. *Available at SSRN 3617416*.

MacQueen, J. et al. (1967). Some methods for classification and analysis of multivariate observations. In *Proceedings of the fifth Berkeley symposium on mathematical statistics and probability*, Volume 1, pp. 281–297. Oakland, CA, USA.

Miao, K., L. Su, and W. Wang (2020). Panel threshold regressions with latent group structures. *Journal of Econometrics* 214(2), 451–481.

Millimet, D. L., J. A. List, and T. Stengos (2003). The environmental kuznets curve: real progress or misspecified models? *Review of Economics and Statistics* 85(4), 1038–1047.

Ng, A. Y., M. I. Jordan, and Y. Weiss (2002). On spectral clustering: Analysis and an algorithm. In *Advances in neural information processing systems*, pp. 849–856.

Okui, R. and W. Wang (2021). Heterogeneous structural breaks in panel data models. *Journal of Econometrics* 220(2), 447–473.

Reynolds, A. P., G. Richards, B. de la Iglesia, and V. J. Rayward-Smith (2006). Clustering rules: a comparison of partitioning and hierarchical clustering algorithms. *Journal of Mathematical Modelling and Algorithms* 5(4), 475–504.

Schubert, E. and P. J. Rousseeuw (2019). Faster k-medoids clustering: improving the pam, clara, and clarans algorithms. In *International conference on similarity search and applications*, pp. 171–187. Springer.

Su, L., Z. Shi, and P. C. Phillips (2016). Identifying latent structures in panel data. *Econometrica* 84(6), 2215–2264.

van Delft, A. and H. Dette (2021). A similarity measure for second order properties of non-stationary functional time series with applications to clustering and testing. *Bernoulli* 27(1), 469–501.

van der Vaart, A. and J. Wellner (1996). Weak convergence and empirical processes. Springer.

Von Luxburg, U. (2007). A tutorial on spectral clustering. *Statistics and computing* 17(4), 395–416.

Von Luxburg, U. (2010). *Clustering stability: an overview*. Now Publishers Inc.

Wang, J. (2010). Consistent selection of the number of clusters via crossvalidation. *Biometrika* 97(4), 893–904.

Wang, W., P. C. Phillips, and L. Su (2018). Homogeneity pursuit in panel data models: Theory and application. *Journal of Applied Econometrics* 33(6), 797–815.

Wang, W. and L. Su (2021). Identifying latent group structures in nonlinear panels. *Journal of Econometrics* 220(2), 272–295.

Yu, Y., T. Wang, and R. J. Samworth (2015). A useful variant of the davis–kahan theorem for statisticians. *Biometrika* 102(2), 315–323.

Zhang, Y., H. J. Wang, and Z. Zhu (2019a). Quantile-regression-based clustering for panel data. *Journal of Econometrics*.

Zhang, Y., H. J. Wang, and Z. Zhu (2019b). Robust subgroup identification. *Statistica Sinica* 29(1), 1873–1889.

SUPPLEMENTARY MATERIAL

In this supplementary material, we provide more simulation details, additional simulation results, and more plots for real data analysis, as well as proofs of the main results in Section 3.1 and Section 3.2.

7 Simulation Studies

We provide more details about the simulation studies in Section 4. All results reported in Section 4 are based on 100 simulation repetitions.

7.1 Simulations in Section 4.1

In the simulation of Su et al. (2016) published on <https://github.com/zhentaoshi/C-LASSO>, they also encounter the same finite sample issues as described above. They handle the first issue in the same fashion as we do. However, for the second issue, they replace the estimates for $\{\alpha_i, \beta_i\}$ by their true value whenever these estimates exceed 5 or when the mean outcome for the individual is outside of the range [0.2, 0.8]. This is not feasible in practice since we do not know the true values and we thus simply remove such individuals from our analysis.

We implement the CLASSO estimator using CVX in Matlab with the mosek solver with version Mosek 8. The algorithm is initiated with β_i being the individual logistic regression estimates and η_k being the origin for all K_0 groups. For instance when the objective function differs by a quantity less than 0.001 and when the ℓ_2 norm of the estimated group centre η_k changes by less than 0.1%.

7.2 Simulations in Section 4.2.1

Simulations are done in the **quantreg** package in R. Covariance estimates are computed using the function **summary.rq()** with option **se="nid"** and default bandwidth choice **hs=true**.

Besides the models we present in the main text, we consider the following model

$$\text{Model 4:} \quad y_{it} = \alpha_i + \mathbf{x}_{it}^\top \boldsymbol{\beta}_{g_i} + e_{it},$$

where $\alpha_i = 1, i = 1, \dots, n$, $g_i \in \{1, 2, 3\}$ with each occurring exactly $n/3$ times. Set

$$\boldsymbol{\beta}_1 = \begin{pmatrix} -5 \\ 1 \end{pmatrix}, \boldsymbol{\beta}_2 = \begin{pmatrix} 0 \\ 1 \end{pmatrix}, \boldsymbol{\beta}_3 = \begin{pmatrix} 3 \\ 1 \end{pmatrix},$$

$e_{it} \stackrel{iid}{\sim} N(0, 1)$ or $e_{it} \stackrel{iid}{\sim} t(3)$, and set $\mathbf{x}_{it}^\top = (x_{1it}, x_{2it})$ with $x_{1it} = 0.5\alpha_i + \eta_i + z_{1it}$ and $x_{2it} = 0.5\alpha_i + \eta_i + z_{2it}$, where $\eta_i \stackrel{iid}{\sim} N(0, 1)$ and $z_{1it} \stackrel{iid}{\sim} N(0, 1)$, $z_{2it} \stackrel{iid}{\sim} N(0, 0.05)$.

Membership estimation results based on the method proposed in this paper (Spectral), Zhang et al. (2019a)(ZWZ19), spectral clustering ignoring variance information (Spectral $^\circ$),

and naive k -means on estimated coefficients ignoring variance information (k -means $^\circ$) are reported in Table 13. Percentage of estimated number of groups based on CV-Spectral, CV-kmeans, and Heuristic methods are provided in Table 17. Model 4 still has an odd number of groups, but the coefficients are slightly asymmetric. The heuristic method performs best or close to best for all settings. The other two approaches show surprising patterns where an increase in T , which makes the problem easier because coefficients are estimated more precisely, does not always correspond to an improvement in selecting the number of groups (for instance $n = 30, \tau = 0.5, N(0, 1)$ errors and to some extent $t(3)$ errors). A possible explanation for this surprising behavior is the presence of a slight asymmetry in the values of coefficient vectors.

7.3 Simulations in Section 4.2.2

The bandwidth d_T used in (13) is based on the method implemented in the **quantreg** package in R (function `summary.rq()` with `se="nid"` and default choice `hs=true`).

7.4 Simulations in Section 4.3

The maximum numbers of clusters to consider G_{\max} is set to $G_{\max} = 5$ for $n \leq 30$ and $G_{\max} = 10$ for $n > 30$ cases for the CV methods, and we set $G_{\max} = 10$ across all settings for the heuristic method. For the cross-validation method, we use 100 (4:4:2) random splits of the dataset into training and validation data (see Wang (2010) for details on the meaning of this splitting).

8 Tables

8.1 Tables in Section 4.1

n	T	Spectral	C-LASSO
30	30	0.89	7.12
30	60	0.91	8.44
30	90	0.97	10.40
30	150	0.99	11.63
60	30	3.75	9.75
60	60	3.80	14.46
60	90	3.86	18.51
60	150	3.87	20.71

Table 9: Comparison of computation time in seconds: this includes the computation of individual-specific estimates and the algorithm used to estimate grouping for one data realization. For C-LASSO we set the maximum iteration to be 20.

8.2 Tables in Section 4.2

n	T	Perfect Match			Average Match				
		Spectral	ZWZ19	Spectral ^o	k-means ^o	Spectral	ZWZ19	Spectral ^o	k-means ^o
$t(3), \tau = 0.7$									
30	60	0.11	0.02	0.00	0.00	0.908	0.826	0.564	0.568
30	90	0.33	0.12	0.00	0.00	0.965	0.929	0.624	0.617
30	120	0.63	0.45	0.00	0.00	0.985	0.967	0.667	0.672
60	60	0.01	0.00	0.00	0.00	0.910	0.828	0.540	0.540
60	90	0.05	0.04	0.00	0.00	0.962	0.929	0.598	0.600
60	120	0.41	0.10	0.00	0.00	0.983	0.965	0.652	0.659
90	60	0.00	0.00	0.00	0.00	0.919	0.846	0.537	0.539
90	90	0.02	0.01	0.00	0.00	0.963	0.936	0.593	0.592
90	120	0.15	0.04	0.00	0.00	0.980	0.962	0.653	0.653
$N(0, 1), \tau = 0.7$									
30	60	0.28	0.12	0.00	0.00	0.957	0.917	0.605	0.614
30	90	0.60	0.34	0.00	0.00	0.985	0.971	0.658	0.675
30	120	0.81	0.67	0.00	0.00	0.993	0.986	0.673	0.697
60	60	0.06	0.00	0.00	0.00	0.950	0.903	0.571	0.573
60	90	0.35	0.12	0.00	0.00	0.983	0.966	0.657	0.667
60	120	0.62	0.39	0.00	0.00	0.993	0.985	0.695	0.709
90	60	0.01	0.00	0.00	0.00	0.950	0.912	0.591	0.596
90	90	0.23	0.07	0.00	0.00	0.983	0.968	0.668	0.679
90	120	0.58	0.26	0.00	0.00	0.994	0.985	0.705	0.735

Table 10: Membership estimation based on Spectral (the method proposed in this paper), ZWZ19 (Zhang et al. (2019a)), spectral clustering ignoring variance information Spectral^o, and naive k-means on estimated coefficients ignoring variance information k-means^o. Data are generated from Model 1 with $\tau = 0.7$.

n	T	Perfect Match			Average Match				
		Spectral	ZWZ19	Spectral ^o	k-means ^o	Spectral	ZWZ19	Spectral ^o	k-means ^o
$t(3), \tau = 0.7$									
40	40	0.01	0.00	0.00	0.00	0.886	0.674	0.608	0.619
40	80	0.21	0.04	0.00	0.00	0.957	0.741	0.664	0.675
40	120	0.52	0.03	0.00	0.00	0.984	0.749	0.686	0.712
60	40	0.00	0.00	0.00	0.00	0.897	0.690	0.619	0.626
60	80	0.09	0.00	0.00	0.00	0.963	0.716	0.651	0.667
60	120	0.51	0.02	0.00	0.00	0.989	0.735	0.702	0.717
$N(0, 1), \tau = 0.7$									
40	40	0.06	0.00	0.00	0.00	0.924	0.724	0.632	0.639
40	80	0.45	0.07	0.00	0.00	0.982	0.783	0.679	0.697
40	120	0.74	0.18	0.00	0.00	0.992	0.785	0.757	0.777
60	40	0.00	0.00	0.00	0.00	0.923	0.755	0.625	0.630
60	80	0.38	0.02	0.00	0.00	0.982	0.765	0.692	0.711
60	120	0.81	0.08	0.00	0.00	0.997	0.771	0.747	0.775

Table 11: Membership estimation based on Spectral (the method proposed in this paper), ZWZ19 (Zhang et al. (2019a)), spectral clustering ignoring variance information Spectral^o, and naive k-means on estimated coefficients ignoring variance information k-means^o. Data are generated from Model 2.

n	T	Perfect Match				Average Match			
		Spectral	Spectral ^o	k-means ^o	GV	Spectral	Spectral ^o	k-means ^o	GV
$t(3), \tau = 0.7$									
30	15	0.00	0.00	0.00	0.00	0.828	0.817	0.829	0.618
30	30	0.10	0.08	0.08	0.09	0.936	0.926	0.935	0.793
30	60	0.69	0.69	0.67	0.61	0.988	0.986	0.986	0.950
60	15	0.00	0.00	0.00	0.00	0.847	0.841	0.844	0.593
60	30	0.04	0.05	0.06	0.01	0.942	0.939	0.946	0.790
60	60	0.53	0.54	0.58	0.45	0.989	0.989	0.989	0.962
90	15	0.00	0.00	0.00	0.00	0.848	0.841	0.847	0.568
90	30	0.00	0.00	0.00	0.00	0.946	0.945	0.948	0.783
90	60	0.42	0.42	0.42	0.33	0.989	0.989	0.990	0.962
$N(0, 1), \tau = 0.7$									
30	15	0.03	0.05	0.05	0.02	0.880	0.887	0.892	0.682
30	30	0.47	0.44	0.47	0.29	0.973	0.974	0.975	0.863
30	60	0.95	0.94	0.96	0.87	0.998	0.998	0.999	0.986
60	15	0.00	0.00	0.00	0.00	0.899	0.896	0.901	0.673
60	30	0.24	0.25	0.28	0.14	0.976	0.977	0.978	0.890
60	60	0.91	0.91	0.90	0.80	0.998	0.998	0.999	0.989
90	15	0.00	0.00	0.00	0.00	0.896	0.896	0.901	0.650
90	30	0.12	0.12	0.17	0.06	0.975	0.976	0.977	0.895
90	60	0.78	0.78	0.81	0.74	0.997	0.997	0.998	0.989

Table 12: Membership estimation based on Spectral, k -means, Spectral^o, and k -means^o methods, and also the method proposed in Gu and Volgushev (2019) (GV) for Model 3 with $\tau = 0.7$.

n	T	Perfect Match				Average Match			
		Spectral	ZWZ19	Spectral [°]	k-means [°]	Spectral	ZWZ19	Spectral [°]	k-means [°]
$t(3), \tau = 0.5$									
30	15	0.94	0.20	0.19	0.49	0.998	0.942	0.733	0.881
30	30	1.00	0.46	0.93	1.00	1.000	0.977	0.976	1.000
30	60	1.00	0.83	1.00	1.00	1.000	0.994	1.000	1.000
60	15	0.91	0.01	0.11	0.29	0.999	0.911	0.716	0.858
60	30	1.00	0.21	0.88	1.00	1.000	0.975	0.960	1.000
60	60	1.00	0.65	1.00	1.00	1.000	0.994	1.000	1.000
90	15	0.90	0.00	0.15	0.35	0.999	0.923	0.728	0.856
90	30	1.00	0.08	0.78	1.00	1.000	0.972	0.928	1.000
90	60	1.00	0.47	1.00	1.00	1.000	0.992	1.000	1.000
$t(3), \tau = 0.7$									
30	15	0.87	0.12	0.07	0.16	0.995	0.919	0.686	0.787
30	30	1.00	0.52	0.66	0.90	1.000	0.972	0.895	0.986
30	60	1.00	0.87	0.97	1.00	1.000	0.995	0.990	1.000
60	15	0.80	0.00	0.01	0.11	0.997	0.895	0.675	0.772
60	30	1.00	0.12	0.66	0.96	1.000	0.963	0.896	0.996
60	60	1.00	0.54	0.99	1.00	1.000	0.990	0.997	1.000
90	15	0.68	0.00	0.06	0.03	0.993	0.904	0.689	0.742
90	30	1.00	0.06	0.62	0.96	1.000	0.966	0.882	0.999
90	60	1.00	0.31	0.98	1.00	1.000	0.987	0.993	1.000
$N(0, 1), \tau = 0.5$									
30	15	1.00	0.30	0.60	0.85	1.000	0.960	0.884	0.980
30	30	1.00	0.67	0.91	0.99	1.000	0.986	0.978	0.999
30	60	1.00	0.92	1.00	1.00	1.000	0.997	1.000	1.000
60	15	1.00	0.02	0.49	0.81	1.000	0.931	0.846	0.975
60	30	1.00	0.24	0.93	1.00	1.000	0.978	0.984	1.000
60	60	1.00	0.82	1.00	1.00	1.000	0.997	1.000	1.000
90	15	1.00	0.00	0.58	0.84	1.000	0.942	0.866	0.983
90	30	1.00	0.15	0.95	1.00	1.000	0.979	0.984	1.000
90	60	1.00	0.58	1.00	1.00	1.000	0.994	1.000	1.000
$N(0, 1), \tau = 0.7$									
30	15	1.00	0.25	0.37	0.63	1.000	0.953	0.822	0.931
30	30	1.00	0.66	0.93	1.00	1.000	0.986	0.976	1.000
30	60	1.00	0.86	1.00	1.00	1.000	0.995	1.000	1.000
60	15	1.00	0.01	0.45	0.58	1.000	0.927	0.828	0.936
60	30	1.00	0.21	0.93	1.00	1.000	0.977	0.977	1.000
60	60	1.00	0.75	0.99	1.00	1.000	0.995	0.997	1.000
90	15	1.00	0.01	0.31	0.76	1.000	0.939	0.797	0.960
90	30	1.00	0.14	0.93	0.99	1.000	0.978	0.980	0.999
90	60	1.00	0.54	1.00	1.00	1.000	0.994	1.000	1.000

Table 13: Membership estimation based on Spectral (the method proposed in this paper), ZWZ19 (Zhang et al. (2019a)), spectral clustering ignoring variance information Spectral[°], and naive k-means on estimated coefficients ignoring variance information k-means[°]. Data are generated from Model 4.

8.3 Tables in Section 4.3

n	T	N(0, 1)					t(3)				
		1	2	3	4	≥ 5	1	2	3	4	≥ 5
CV-Spectral, $\tau = 0.7$											
30	60	—	0.22	0.62	0.10	0.06	—	0.32	0.42	0.12	0.14
30	90	—	0.04	0.90	0.02	0.04	—	0.10	0.70	0.14	0.06
30	120	—	0.02	0.96	0.02	0.00	—	0.06	0.92	0.00	0.02
60	60	—	0.02	0.94	0.00	0.04	—	0.06	0.76	0.00	0.18
60	90	—	0.00	1.00	0.00	0.00	—	0.00	0.98	0.02	0.00
60	120	—	0.00	1.00	0.00	0.00	—	0.00	1.00	0.00	0.00
CV-kmeans, $\tau = 0.7$											
30	60	—	0.32	0.32	0.22	0.14	—	0.42	0.20	0.18	0.20
30	90	—	0.24	0.64	0.12	0.00	—	0.26	0.50	0.16	0.08
30	120	—	0.14	0.76	0.10	0.00	—	0.20	0.60	0.14	0.06
60	60	—	0.18	0.28	0.10	0.44	—	0.04	0.18	0.06	0.72
60	90	—	0.06	0.62	0.26	0.06	—	0.14	0.36	0.22	0.28
60	120	—	0.02	0.96	0.02	0.00	—	0.06	0.56	0.20	0.18
Heuristic, $\tau = 0.7$											
30	60	0.02	0.21	0.75	0.02	0.00	0.35	0.51	0.14	0.00	0.00
30	90	0.00	0.00	0.98	0.02	0.00	0.01	0.18	0.79	0.02	0.00
30	120	0.00	0.00	0.99	0.01	0.00	0.00	0.00	0.96	0.04	0.00
60	60	0.15	0.00	0.85	0.00	0.00	0.87	0.01	0.12	0.00	0.00
60	90	0.00	0.00	1.00	0.00	0.00	0.04	0.00	0.96	0.00	0.00
60	120	0.00	0.00	1.00	0.00	0.00	0.00	0.00	1.00	0.00	0.00

Table 14: Percentage of estimated number of groups based on CV-Spectral, CV-kmeans, and Heuristic methods for Model 1 with $\tau = 0.7$.

n	T	N(0, 1)					t(3)				
		1	2	3	4	≥ 5	1	2	3	4	≥ 5
CV-Spectral, $\tau = 0.7$											
40	40	0.00	1.00	0.00	0.00	0.00	0.00	1.00	0.00	0.00	0.00
40	80	0.00	1.00	0.00	0.00	0.00	0.00	1.00	0.00	0.00	0.00
40	160	0.00	1.00	0.00	0.00	0.00	0.00	1.00	0.00	0.00	0.00
60	40	0.00	1.00	0.00	0.00	0.00	0.00	1.00	0.00	0.00	0.00
60	80	0.00	1.00	0.00	0.00	0.00	0.00	1.00	0.00	0.00	0.00
60	160	0.00	1.00	0.00	0.00	0.00	0.00	1.00	0.00	0.00	0.00
CV-kmeans, $\tau = 0.7$											
40	40	0.00	1.00	0.00	0.00	0.00	0.00	1.00	0.00	0.00	0.00
40	80	0.00	1.00	0.00	0.00	0.00	0.00	1.00	0.00	0.00	0.00
40	160	0.00	1.00	0.00	0.00	0.00	0.00	1.00	0.00	0.00	0.00
60	40	0.00	1.00	0.00	0.00	0.00	0.00	1.00	0.00	0.00	0.00
60	80	0.00	1.00	0.00	0.00	0.00	0.00	1.00	0.00	0.00	0.00
60	160	0.00	1.00	0.00	0.00	0.00	0.00	1.00	0.00	0.00	0.00
Heuristic, $\tau = 0.7$											
40	40	0.00	0.83	0.00	0.17	0.00	0.00	1.00	0.00	0.00	0.00
40	80	0.00	0.02	0.00	0.98	0.00	0.00	0.22	0.00	0.77	0.01
40	160	0.00	0.00	0.00	0.99	0.01	0.00	0.00	0.00	1.00	0.00
60	40	0.00	0.00	0.00	0.85	0.15	0.00	1.00	0.00	0.00	0.00
60	80	0.00	0.00	0.00	1.00	0.00	0.00	0.12	0.00	0.88	0.00
60	160	0.00	0.00	0.00	1.00	0.00	0.00	0.00	1.00	0.00	0.00

Table 15: Percentage of estimated number of groups with CV-Spectral, CV-kmeans and Heuristic methods for Model 2 with $\tau = 0.7$.

n	T	N(0, 1)					t(3)				
		1	2	3	4	≥ 5	1	2	3	4	≥ 5
CV-Spectral, $\tau = 0.7$											
30	15	—	0.38	0.30	0.14	0.18	—	0.28	0.20	0.10	0.42
30	30	—	0.06	0.86	0.06	0.02	—	0.18	0.68	0.08	0.06
30	60	—	0.02	1.00	0.00	0.00	—	0.00	1.00	0.00	0.02
60	15	—	0.24	0.56	0.02	0.18	—	0.24	0.32	0.02	0.42
60	30	—	0.00	1.00	0.00	0.00	—	0.06	0.88	0.00	0.06
60	60	—	0.00	1.00	0.00	0.00	—	0.00	1.00	0.00	0.00
90	15	—	0.12	0.64	0.02	0.22	—	0.22	0.38	0.04	0.36
90	30	—	0.00	1.00	0.00	0.00	—	0.00	1.00	0.00	0.00
90	60	—	0.00	1.00	0.00	0.00	—	0.00	1.00	0.00	0.00
Heuristic, $\tau = 0.7$											
30	15	0.03	0.18	0.30	0.11	0.38	0.08	0.30	0.20	0.13	0.29
30	30	0.00	0.06	0.82	0.02	0.10	0.00	0.24	0.62	0.04	0.10
30	60	0.00	0.00	0.93	0.01	0.06	0.00	0.01	0.89	0.02	0.08
60	15	0.10	0.36	0.47	0.04	0.03	0.42	0.31	0.25	0.02	0.00
60	30	0.00	0.02	0.95	0.01	0.02	0.00	0.15	0.75	0.04	0.06
60	60	0.00	0.00	0.98	0.00	0.02	0.00	0.00	0.98	0.00	0.02
90	15	0.17	0.36	0.47	0.00	0.00	0.65	0.22	0.13	0.00	0.00
90	30	0.00	0.02	0.98	0.00	0.00	0.00	0.09	0.88	0.01	0.02
90	60	0.00	0.00	1.00	0.00	0.00	0.00	0.00	1.00	0.00	0.00
GV, $\tau = 0.7$											
30	15	0.00	0.12	0.50	0.30	0.08	0.00	0.27	0.44	0.23	0.06
30	30	0.00	0.00	0.77	0.20	0.03	0.00	0.08	0.65	0.24	0.04
30	60	0.00	0.00	0.98	0.02	0.00	0.00	0.00	0.91	0.08	0.01
60	15	0.00	0.08	0.46	0.32	0.14	0.00	0.17	0.36	0.32	0.15
60	30	0.00	0.00	0.80	0.17	0.03	0.00	0.03	0.59	0.31	0.08
60	60	0.00	0.00	0.98	0.02	0.00	0.00	0.00	0.93	0.07	0.00
90	15	0.00	0.07	0.41	0.35	0.17	0.00	0.15	0.31	0.32	0.22
90	30	0.00	0.00	0.80	0.18	0.02	0.00	0.02	0.56	0.31	0.10
90	60	0.00	0.00	0.98	0.02	0.00	0.00	0.00	0.92	0.08	0.01

Table 16: Percentage of estimated number of groups based on CV-Spectral, Heuristic, and Gu and Volgushev (2019) (GV) methods for Model 3 with $\tau = 0.7$.

n	T	N(0, 1)					t(3)				
		1	2	3	4	≥ 5	1	2	3	4	≥ 5
CV-Spectral, $\tau = 0.5$											
30	15	—	0.04	0.96	0.00	0.00	—	0.00	1.00	0.00	0.00
30	30	—	0.36	0.64	0.00	0.00	—	0.02	0.98	0.00	0.00
30	60	—	0.30	0.70	0.00	0.00	—	0.04	0.96	0.00	0.00
60	15	—	0.06	0.94	0.00	0.00	—	0.08	0.92	0.00	0.00
60	30	—	0.00	1.00	0.00	0.00	—	0.06	0.94	0.00	0.00
60	60	—	0.00	1.00	0.00	0.00	—	0.00	1.00	0.00	0.00
CV-kmeans, $\tau = 0.5$											
30	15	—	0.46	0.48	0.04	0.02	—	0.38	0.38	0.22	0.02
30	30	—	0.62	0.24	0.12	0.02	—	0.64	0.20	0.10	0.06
30	60	—	0.72	0.14	0.12	0.02	—	0.54	0.36	0.06	0.04
60	15	—	0.58	0.34	0.04	0.04	—	0.60	0.32	0.06	0.02
60	30	—	0.40	0.58	0.02	0.00	—	0.48	0.46	0.04	0.02
60	60	—	0.42	0.56	0.02	0.00	—	0.50	0.48	0.01	0.00
Heuristic, $\tau = 0.5$											
30	15	0.00	0.00	1.00	0.00	0.00	0.00	0.00	0.98	0.02	0.00
30	30	0.00	0.00	1.00	0.00	0.00	0.00	0.00	0.97	0.03	0.00
30	60	0.00	0.00	1.00	0.00	0.00	0.00	0.00	0.98	0.02	0.00
60	15	0.00	0.00	1.00	0.00	0.00	0.00	0.00	0.99	0.01	0.00
60	30	0.00	0.00	1.00	0.00	0.00	0.00	0.00	0.99	0.01	0.00
60	60	0.00	0.00	1.00	0.00	0.00	0.00	0.00	1.00	0.00	0.00
CV-Spectral, $\tau = 0.7$											
30	15	—	0.02	0.98	0.00	0.00	—	0.00	1.00	0.00	0.00
30	30	—	0.00	1.00	0.00	0.00	—	0.02	0.98	0.00	0.00
30	60	—	0.56	0.44	0.00	0.00	—	0.04	0.96	0.00	0.00
60	15	—	0.00	1.00	0.00	0.00	—	0.08	0.92	0.00	0.00
60	30	—	0.08	0.92	0.00	0.00	—	0.06	0.94	0.00	0.00
60	60	—	0.00	1.00	0.00	0.00	—	0.00	1.00	0.00	0.00
CV-kmeans, $\tau = 0.7$											
30	15	—	0.02	0.86	0.08	0.04	—	0.06	0.72	0.10	0.12
30	30	—	0.02	0.82	0.12	0.04	—	0.02	0.78	0.16	0.04
30	60	—	0.00	0.96	0.02	0.02	—	0.00	0.90	0.10	0.00
60	15	—	0.00	0.84	0.16	0.00	—	0.00	0.62	0.08	0.30
60	30	—	0.00	0.98	0.00	0.02	—	0.00	0.88	0.10	0.03
60	60	—	0.00	1.00	0.00	0.00	—	0.00	0.98	0.02	0.00
Heuristic, $\tau = 0.7$											
30	15	0.00	0.00	0.94	0.00	0.06	0.00	0.00	0.97	0.02	0.01
30	30	0.00	0.00	0.98	0.02	0.00	0.00	0.00	0.97	0.03	0.00
30	60	0.00	0.00	0.99	0.01	0.00	0.00	0.00	0.99	0.01	0.00
60	15	0.00	0.00	0.99	0.01	0.00	0.00	0.00	0.98	0.02	0.00
60	30	0.00	0.00	1.00	0.00	0.00	0.00	0.00	1.00	0.00	0.00
60	60	0.00	0.00	1.00	0.00	0.00	0.00	0.00	1.00	0.00	0.00

Table 17: Percentage of estimated number of groups based on CV-Spectral, CV-kmeans, and Heuristic methods for Model 4 with $\tau = 0.5$ and $\tau = 0.7$.

9 Plots

9.1 Plots in Section 4.3

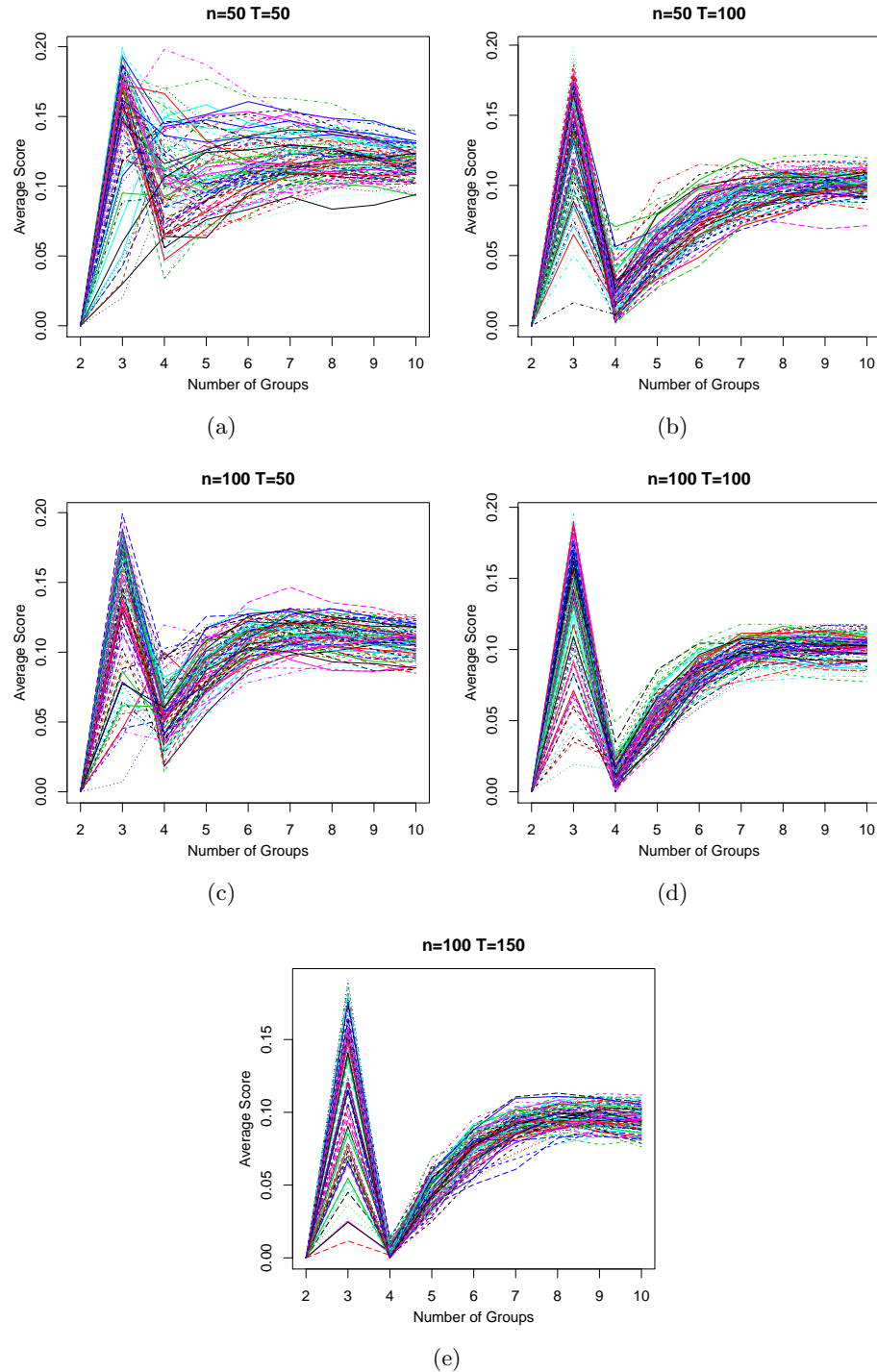


Figure 4: Stability score for Model 3 with $t(3)$ error and $\tau = 0.5$.

9.2 Plots in Section 5

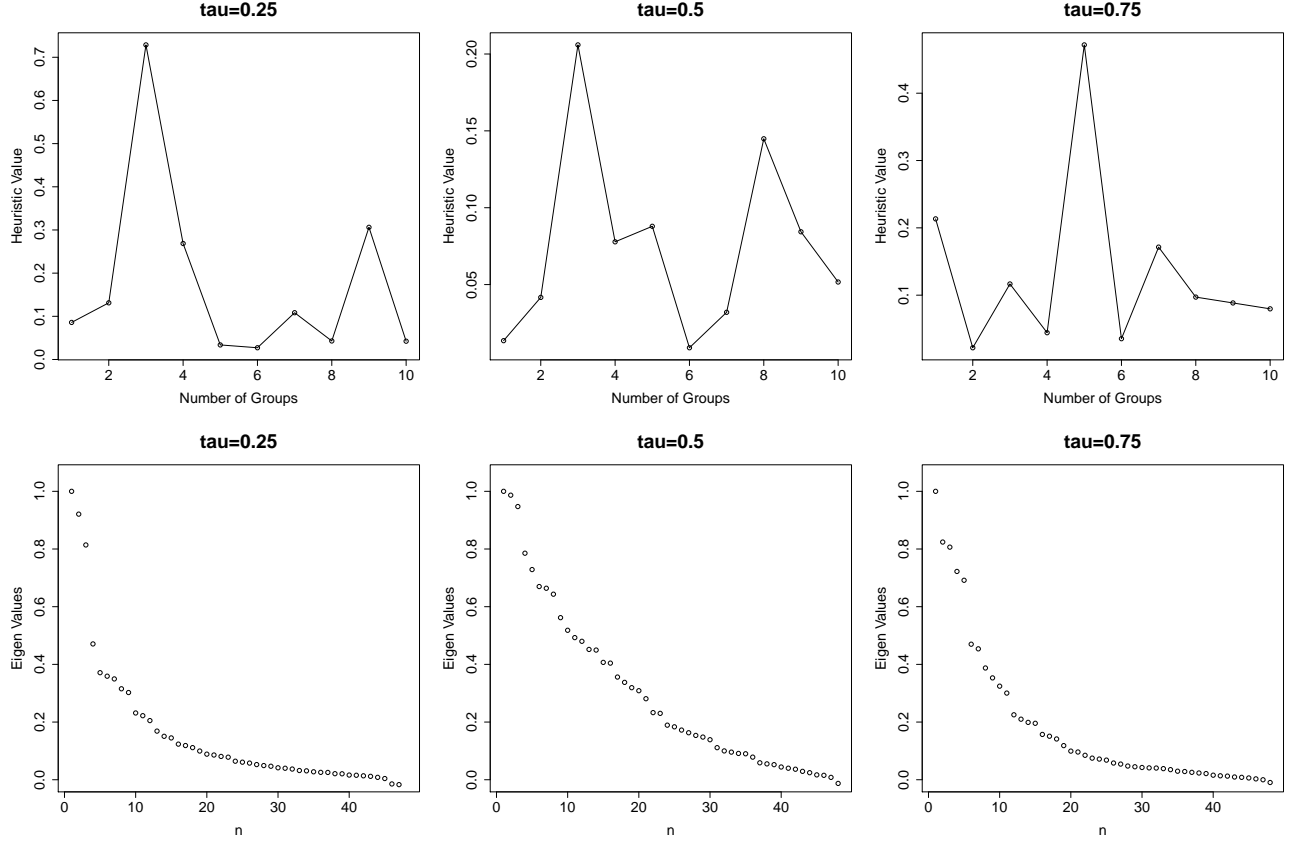


Figure 5: The heuristic values and the eigen-value plot for three different quantile levels $\tau = \{0.25, 0.5, 0.75\}$.

10 Proofs

10.1 Notation

Let $a_n \lesssim_p b_n$ denotes that there exists a non-random constant $C \in (0, \infty)$ that is independent of n, T , such that $\mathbb{P}(a_n \leq Cb_n) \rightarrow 1$. For a matrix $A \in \mathbb{R}^{n \times p}$, we define the operator norm of A as the maximum absolute column sum of the matrix $\|A\|_\infty := \max_{1 \leq i \leq n} \sum_{j=1}^p |A_{ij}|$, define the Frobenius norm of A as the square root of the sum of the absolute squares of all elements $\|A\|_F := \sqrt{\sum_{i=1}^n \sum_{j=1}^p |A_{ij}|^2}$, and define the spectral norm of A as its largest singular value $\|A\|_2 := \sigma_{\max}(A)$.

To lighten notation we abbreviate the true number of groups as G instead of G^* whenever there is no risk of confusion.

10.2 Proof of the generic spectral clustering result (Theorem 3.1)

To simplify notation, we will without loss of generality assume that the units are ordered according to their true grouping, i.e. unit $1, \dots, |I_1^*|$ belong to group 1, unit $|I_1^*| + 1, \dots, |I_2^*|$ belong to group 2, etc. This is to shorten notation only, all arguments will work with more complex notation if this assumption is dropped.

To proceed to the proof of Theorem 3.1, we first consider the decomposition $\hat{A} = \hat{A}_{\text{diag}} + \hat{A}_{\text{off-diag}}$, where

$$\hat{A}_{\text{diag}} := \begin{pmatrix} \hat{A}^{(11)} & \mathbf{0} & \dots & \mathbf{0} \\ \mathbf{0} & \hat{A}^{(22)} & \dots & \mathbf{0} \\ \dots & \dots & \dots & \dots \\ \mathbf{0} & \mathbf{0} & \dots & \hat{A}^{(GG)} \end{pmatrix}$$

and

$$\hat{A}_{\text{off-diag}} := \begin{pmatrix} \mathbf{0} & \hat{A}^{(12)} & \dots & \hat{A}^{(1G)} \\ \hat{A}^{(21)} & \mathbf{0} & \dots & \hat{A}^{(2G)} \\ \dots & \dots & \dots & \dots \\ \hat{A}^{(G1)} & \hat{A}^{(G2)} & \dots & \mathbf{0} \end{pmatrix},$$

with $\hat{A}^{(ij)} \in \mathbb{R}^{|I_i^*| \times |I_j^*|}$, $i, j = 1, \dots, G$. Define the degree matrix \hat{D}_{diag} corresponding to \hat{A}_{diag} as

$$\hat{D}_{\text{diag}} := \text{diag}((\hat{D}_{\text{diag}})_1, \dots, (\hat{D}_{\text{diag}})_n),$$

with the elements $(\hat{D}_{\text{diag}})_i := \sum_{j=1}^n (\hat{A}_{\text{diag}})_{ij}$. Define the corresponding graph Laplacian \hat{L}_{diag} as

$$\hat{L}_{\text{diag}} := I - \hat{D}_{\text{diag}}^{-1/2} \hat{A}_{\text{diag}} \hat{D}_{\text{diag}}^{-1/2}.$$

The remaining proof proceeds as follows: in step 1, we show that \hat{L}_{diag} has non-negative eigenvalues and that the eigenvalue zero has multiplicity G . Moreover, the eigenspace corresponding to that eigenvalue is spanned by the vectors $\hat{D}_{\text{diag}} \mathbf{1}_{I_j^*} \in \mathbb{R}^n$ with entries

$$(\mathbf{1}_{I_j^*})_k = \begin{cases} 1, & k \in I_j^* \\ 0, & k \notin I_j^* \end{cases}, \quad (14)$$

see Lemma 10.1. In step 2, we bound the distance in operator norm between \hat{L} and \hat{L}_{diag} (Lemma 10.3). In step 3, we quantify the gap between the G -th and $(G+1)$ -th smallest eigenvalues of \hat{L}_{diag} (Lemma 10.4). In step 4, we use the results from step 2 and step 3 to show that the matrix \hat{U} defined in step 4 of the spectral clustering algorithm is close to a rotation of the matrix $U \in \mathbb{R}^{n \times G}$ defined via

$$U := (\mathbf{1}_{I_1^*}, \dots, \mathbf{1}_{I_G^*})$$

in Frobenius norm (Lemma 10.5), i.e. the Frobenius norm of the difference between those matrices converges to zero. This convergence together with a simple analysis of the k -means algorithm yields our main result in step 5.

Step 1: *Eigenstructure of \hat{L}_{diag} .*

The following result is essentially a reformulation of Proposition 4 from Von Luxburg (2007) in our setting. The proof follows by exactly the same type of arguments as in the latter paper, for the sake of completeness and for the reader's convenience we provide a short proof in our specific setting.

Lemma 10.1. *The multiplicity of the eigenvalue 0 of \hat{L}_{diag} equals G . The eigenspace of the eigenvalue 0 of \hat{L}_{diag} is spanned by the vectors $\hat{D}_{\text{diag}}^{1/2} \mathbb{1}_{I_j^*}$ where $\mathbb{1}_{I_j^*}$ are defined in (14).*

Proof of Lemma 10.1. Begin by observing that \hat{L}_{diag} is block-diagonal with G blocks, say $\hat{L}^{(11)}, \dots, \hat{L}^{(GG)}$, of size $|I_1^*| \times |I_1^*|, \dots, |I_G^*| \times |I_G^*|$. It thus suffices to show that the eigenvalues of each block are non-negative and that the multiplicity of the eigenvalue 0 for each block equals 1. Since all blocks share a similar structure we will focus on the first block. Assume that $v = (v_1, \dots, v_{|I_1^*|})^\top$ is an eigenvector of $\hat{L}_{\text{diag}}^{(11)}$ with norm 1 corresponding to eigenvalue λ . Then, we have

$$\begin{aligned} \lambda &= v^\top \hat{L}_{\text{diag}}^{(11)} v \\ &= \sum_{i \in I_1} v_i^2 - \sum_{i,j \in I_1} v_i \frac{\hat{A}_{ij}}{\sqrt{(\hat{D}_{\text{diag}})_i} \sqrt{(\hat{D}_{\text{diag}})_j}} v_j \\ &= \frac{1}{2} \left(\sum_{i \in I_1} v_i^2 - 2 \sum_{i,j \in I_1} \hat{A}_{ij} \frac{v_i}{\sqrt{(\hat{D}_{\text{diag}})_i}} \frac{v_j}{\sqrt{(\hat{D}_{\text{diag}})_j}} + \sum_{j \in I_1} v_j^2 \right) \\ &= \frac{1}{2} \sum_{i,j \in I_1} \hat{A}_{ij} \left(\frac{v_i}{\sqrt{(\hat{D}_{\text{diag}})_i}} - \frac{v_j}{\sqrt{(\hat{D}_{\text{diag}})_j}} \right)^2 \\ &\geq 0, \end{aligned}$$

where $(\hat{D}_{\text{diag}})_i$ denotes the i -th diagonal elements of \hat{D}_{diag} , and the last line follows since by construction $\hat{A}_{ij} > 0$. The latter also implies that $\lambda = 0$ if and only if $v_i / \sqrt{(\hat{D}_{\text{diag}})_i} = v_j / \sqrt{(\hat{D}_{\text{diag}})_j}$ for all i, j , which is only possible if $v_i = C \sqrt{(\hat{D}_{\text{diag}})_i}$ for a constant C independent of i . This completes the proof. \square

Step 2: *Bound on operator norm distance between \hat{L} and \hat{L}_{diag} .*

To derive the bound for the distance in operator norm between \hat{L} and \hat{L}_{diag} , we first bound the element \hat{V}_{ij} . To this end we introduce the population version of the empirical variation

matrix \hat{V} . Define the entries of population variation matrix $V \in \mathbb{R}^{n \times n}$ through

$$V_{ij} := \|b_T^{1/2} \Sigma_{i,j}^{-1/2} (\beta_l^* - \beta_k^*)\|_\infty, \quad i \in I_l^*, j \in I_k^*.$$

Define

$$M_{n,T} := \max_{i,j \text{ in the same group}} |\hat{V}_{ij} - V_{ij}|, \quad m_{n,T} := \max_{i,j \text{ in different groups}} |\hat{V}_{ij} - V_{ij}|.$$

Here, $M_{n,T}$ and $m_{n,T}$ take the maximum over $i, j \in \{1, \dots, n\}$ with i, j in the same group or in different groups, respectively. The same notation is maintained in the following for ease of notation.

Lemma 10.2. *Under Assumption 3.2 and Assumption 3.3, it holds that*

$$\begin{aligned} \max_{i,j \text{ in the same group}} \hat{V}_{ij} &\leq M_{n,T} \\ \max_{i,j \text{ in different groups}} \hat{V}_{ij} &\leq C_1 \sqrt{b_T} + m_{n,T} \\ \min_{i,j \text{ in different groups}} \hat{V}_{ij} &\geq C_2 \sqrt{b_T} - m_{n,T}, \end{aligned}$$

where C_1, C_2 are positive constants and $M_{n,T} = \mathcal{O}_{\mathbb{P}}(b_T^{1/2} a_{n,T})$, $m_{n,T} = o_{\mathbb{P}}(b_T^{1/2})$.

Proof of Lemma 10.2. Assume $i \in I_k^*, j \in I_l^*$ for some $k, l \in \{1, \dots, G\}$. When $l = k$, it holds that $V_{ij} = 0$. It then follows that

$$\max_{i,j \text{ in the same group}} \hat{V}_{ij} \leq b_T^{1/2} (\|b_T \hat{\Sigma}_{i,j}\|_\infty)^{-1/2} a_{n,T} = \mathcal{O}_{\mathbb{P}}(b_T^{1/2} a_{n,T}).$$

When $l \neq k$, we have

$$\begin{aligned} V_{ij} &= \|b_T^{1/2} \Sigma_{i,j}^{-1/2} (\beta_l^* - \beta_k^*)\|_\infty \\ &\leq \|b_T^{1/2} \Sigma_{i,j}^{-1/2} (\beta_l^* - \beta_k^*)\|_2 \\ &\leq b_T^{1/2} \lambda_{\max}((\Sigma_{i,j})^{-1/2}) \max_i \|\beta_i^*\|_2 \\ &= b_T^{1/2} (\lambda_{\min}(\Sigma_{i,j}))^{-1/2} \max_i \|\beta_i^*\|_2. \end{aligned}$$

By Assumption 3.3, we have

$$(\lambda_{\min}(\Sigma_{i,j}))^{-1/2} \leq m^{-1/2}.$$

Setting $C_1 := m^{-1/2} \max_i \|\beta_i^*\|_2$, we then obtain

$$V_{ij} \leq C_1 b_T^{1/2}.$$

Similarly, we can derive the lower bound for V_{ij} as following

$$\begin{aligned} V_{ij} &= b_T^{1/2} \|\Sigma_{i,j}^{-1/2}(\beta_l^* - \beta_k^*)\|_\infty \\ &\geq b_T^{1/2} \sqrt{p} \|\Sigma_{i,j}^{-1/2}(\beta_l^* - \beta_k^*)\|_2 \\ &\geq b_T^{1/2} \sqrt{p} (\lambda_{\max}(\Sigma_{i,j}))^{-1/2} \inf_{l \neq k} \|\beta_l^* - \beta_k^*\|_2. \end{aligned}$$

By Assumption 3.3, we have

$$(\lambda_{\max}(\Sigma_{i,j}))^{-1/2} \geq M^{-1/2}.$$

Set $C_2 := \sqrt{\frac{p}{M}} \inf_{l \neq k} \|\beta_l^* - \beta_k^*\|_2$. It then follows that

$$V_{ij} \geq C_2 b_T^{1/2}.$$

Now, we quantify the difference between V_{ij} and \hat{V}_{ij} . By the reverse triangle inequality, it holds for any $i \in I_l^*, j \in I_k^*$ that

$$\begin{aligned} &|V_{ij} - \hat{V}_{ij}| \\ &= \left| \|b_T^{1/2} \Sigma_{i,j}^{-1/2}(\beta_l^* - \beta_k^*)\|_\infty - \|\hat{\Sigma}_{i,j}^{-1/2}(\hat{\beta}_i - \hat{\beta}_j)\|_\infty \right| \\ &\leq \|b_T^{1/2} \Sigma_{i,j}^{-1/2}(\beta_l^* - \beta_k^*) - \hat{\Sigma}_{i,j}^{-1/2}(\hat{\beta}_i - \hat{\beta}_j)\|_\infty \\ &= \|b_T^{1/2} \Sigma_{i,j}^{-1/2}(\beta_l^* - \beta_k^*) - b_T^{1/2} \Sigma_{i,j}^{-1/2}(\hat{\beta}_i - \hat{\beta}_j) + b_T^{1/2} \Sigma_{i,j}^{-1/2}(\hat{\beta}_i - \hat{\beta}_j) - \hat{\Sigma}_{i,j}^{-1/2}(\hat{\beta}_i - \hat{\beta}_j)\|_\infty \\ &\leq b_T^{1/2} \|\Sigma_{i,j}^{-1/2}(\beta_l^* - \hat{\beta}_i - \beta_k^* + \hat{\beta}_j)\|_\infty + b_T^{1/2} \|(\Sigma_{i,j}^{-1/2} - b_T^{-1/2} \hat{\Sigma}_{i,j}^{-1/2})(\hat{\beta}_i - \hat{\beta}_j)\|_\infty \\ &\leq b_T^{1/2} \|\Sigma_{i,j}^{-1/2}(\beta_l^* - \hat{\beta}_i - \beta_k^* + \hat{\beta}_j)\|_\infty + b_T^{1/2} \|(\Sigma_{i,j}^{-1/2} - b_T^{-1/2} \hat{\Sigma}_{i,j}^{-1/2})(\hat{\beta}_i - \beta_l^* - \hat{\beta}_j + \beta_k^*)\|_\infty \\ &\quad + b_T^{1/2} \|(\Sigma_{i,j}^{-1/2} - b_T^{-1/2} \hat{\Sigma}_{i,j}^{-1/2})(\beta_l^* - \beta_k^*)\|_\infty. \end{aligned}$$

By Assumption 3.2 and Assumption 3.3, it follows that

$$\max_{i,j} |\hat{V}_{ij} - V_{ij}| \leq \begin{cases} b_T^{1/2} o_{\mathbb{P}}(1) & i, j \text{ in different groups} \\ b_T^{1/2} \mathcal{O}_{\mathbb{P}}(a_{n,T}) & i, j \text{ in the same group.} \end{cases}$$

This completes the proof. \square

Now we consider the distance between \hat{L} and \hat{L}_{diag} in operator norm.

Lemma 10.3. *Under Assumption 3.1-Assumption 3.3, it holds that*

$$\left\| \hat{L} - \hat{L}_{\text{diag}} \right\|_\infty \lesssim \exp\left(-C_2 \sqrt{b_T} + m_{n,T} + \frac{3}{2} M_{n,T}\right),$$

where \lesssim depends only on the ratio $n / \min_k |I_k^*|$, and $C_2, m_{n,T}, M_{n,T}$ are from Lemma 10.2.

Proof of Lemma 10.3. The proof follows a similar strategy as in Chung and Radcliffe (2011),

and Lemma 3.1 of van Delft and Dette (2021) but modified to account for the fact that n can diverge while it is fixed in the latter paper. Decompose the difference $\hat{L} - \hat{L}_{\text{diag}}$ as follows

$$\begin{aligned}
& \hat{L} - \hat{L}_{\text{diag}} \\
&= (\hat{D}^{-1/2} - \hat{D}_{\text{diag}}^{-1/2}) \hat{A} \hat{D}^{-1/2} + \hat{D}_{\text{diag}}^{-1/2} \hat{A} (\hat{D}^{-1/2} - \hat{D}_{\text{diag}}^{-1/2}) + \hat{D}_{\text{diag}}^{-1/2} (\hat{A} - \hat{A}_{\text{diag}}) \hat{D}_{\text{diag}}^{-1/2} \\
&= (I - \hat{D}_{\text{diag}}^{-1/2} \hat{D}^{1/2}) \hat{D}^{-1/2} \hat{A} \hat{D}^{-1/2} + (\hat{D}_{\text{diag}}^{-1/2} \hat{D}^{1/2}) \hat{D}^{-1/2} \hat{A} \hat{D}^{-1/2} (I - \hat{D}^{1/2} \hat{D}_{\text{diag}}^{-1/2}) \\
&\quad + \hat{D}_{\text{diag}}^{-1/2} (\hat{A} - \hat{A}_{\text{diag}}) \hat{D}_{\text{diag}}^{-1/2}.
\end{aligned}$$

Now, we bound the terms on the right hand side separately. Define the i -th diagonal elements of the diagonal matrix D by $(D)_i$. By definition of the norm $\|\cdot\|_\infty$, we have

$$\begin{aligned}
\|I - \hat{D}_{\text{diag}}^{-1/2} \hat{D}^{1/2}\|_\infty &= \max_i \left| 1 - \sqrt{\frac{\hat{D}_i}{(\hat{D}_{\text{diag}})_i}} \right| \\
&\leq \max_i \left| 1 - \frac{\hat{D}_i}{(\hat{D}_{\text{diag}})_i} \right| \\
&\leq \frac{\max_i |(\hat{D}_{\text{diag}})_i - \hat{D}_i|}{\min_i (\hat{D}_{\text{diag}})_i},
\end{aligned}$$

where we used the fact that $|1 - x| = |1 - \sqrt{x}| |1 + \sqrt{x}| \geq |1 - \sqrt{x}|, \forall x > 0$. We also have

$$\|\hat{D}_{\text{diag}}^{-1/2} \hat{D}^{-1/2}\|_\infty = \|I - (I - \hat{D}_{\text{diag}}^{-1/2} \hat{D}^{-1/2})\|_\infty \leq 1 + \frac{\max_i |(\hat{D}_{\text{diag}})_i - \hat{D}_i|}{\min_i (\hat{D}_{\text{diag}})_i},$$

and

$$\begin{aligned}
\|\hat{D}^{-1/2} \hat{A} \hat{D}^{-1/2}\|_\infty &= \max_i \left\{ \sum_{j=1}^n \frac{\hat{A}_{ij}}{\sqrt{\hat{D}_i} \sqrt{\hat{D}_j}} \right\} \\
&\leq \max_i \left\{ \frac{1}{\sqrt{\hat{D}_i}} \frac{1}{\min_k \sqrt{\hat{D}_k}} \sum_{j=1}^n \hat{A}_{ij} \right\} \\
&= \frac{\max_i \sqrt{\hat{D}_i}}{\min_j \sqrt{\hat{D}_j}}.
\end{aligned}$$

Moreover, by the sub-multiplicativity of the norm $\|\cdot\|_\infty$, it holds that

$$\|\hat{D}_{\text{diag}}^{-1/2} (\hat{A} - \hat{A}_{\text{diag}}) \hat{D}_{\text{diag}}^{-1/2}\|_\infty \leq \frac{1}{\min_i (\hat{D}_{\text{diag}})_i} \|\hat{A} - \hat{A}_{\text{diag}}\|_\infty.$$

Collecting pieces gives

$$\begin{aligned} & \left\| \hat{L} - \hat{L}_{\text{diag}} \right\|_{\infty} \\ & \leq \frac{\max_i |(\hat{D}_{\text{diag}})_i - \hat{D}_i|}{\min_i (\hat{D}_{\text{diag}})_i} \frac{\max_i \sqrt{\hat{D}_i}}{\min_j \sqrt{\hat{D}_j}} \left(2 + \frac{\max_i |(\hat{D}_{\text{diag}})_i - \hat{D}_i|}{\min_i (\hat{D}_{\text{diag}})_i} \right) + \frac{1}{\min_i (\hat{D}_{\text{diag}})_i} \left\| \hat{A}_{\text{diag}} - \hat{A} \right\|_{\infty}. \end{aligned}$$

Now, we handle with the term $\frac{\max_i |(\hat{D}_{\text{diag}})_i - \hat{D}_i|}{\min_i (\hat{D}_{\text{diag}})_i}$. By definitions of $(\hat{D}_{\text{diag}})_i$ and \hat{D}_i , Assumption 3.1, and Lemma 10.2, we have

$$|(\hat{D}_{\text{diag}})_i - \hat{D}_i| = \sum_{j:i,j \text{ in different groups}} \hat{A}_{ij} \leq n \exp(-C_2 \sqrt{b_T} + m_{n,T}),$$

and

$$(\hat{D}_{\text{diag}})_i = \sum_{j:i,j \text{ in the same group}} \hat{A}_{ij} \geq \min_k |I_k^*| \exp(-M_{n,T}) \gtrsim n \exp(-M_{n,T}). \quad (15)$$

This implies

$$\frac{\max_i |(\hat{D}_{\text{diag}})_i - \hat{D}_i|}{\min_i (\hat{D}_{\text{diag}})_i} \lesssim \exp(-C_2 \sqrt{b_T} + M_{n,T} + m_{n,T}).$$

Next, we deal with the term $\frac{\max_i \sqrt{\hat{D}_i}}{\min_j \sqrt{\hat{D}_j}}$. By definition of \hat{D}_i , Assumption 3.1, and Lemma 10.2, it holds for any $i \in \{1, \dots, n\}$ that

$$\begin{aligned} \hat{D}_i &= \sum_{j:i,j \text{ in the same group}} \hat{A}_{ij} + \sum_{j:i,j \text{ in different groups}} \hat{A}_{ij} \\ &\gtrsim n \min_{i,j \text{ in the same group}} \hat{A}_{ij} + n \min_{i,j \text{ in different groups}} \hat{A}_{ij}, \end{aligned}$$

which implies

$$\hat{D}_i \gtrsim n \exp(-M_{n,T}) + n \exp(-C_1 \sqrt{b_T} - m_{n,T}) \geq n \exp(-M_{n,T}).$$

Combing this with the fact that $\hat{D}_i \leq n$ gives

$$\frac{\max_i \sqrt{\hat{D}_i}}{\min_j \sqrt{\hat{D}_j}} \lesssim \exp(M_{n,T}/2).$$

Now, we consider the term $\left\| \hat{A}_{\text{diag}} - \hat{A} \right\|_{\infty}$. By definition of operator norm, Assumption 3.1, and Lemma 10.2, we have

$$\left\| \hat{A}_{\text{diag}} - \hat{A} \right\|_{\infty} = \max_i \sum_{j:i,j \text{ in different groups}} \hat{A}_{ij} \leq n \exp(-C_2 \sqrt{b_T} + m_{n,T}).$$

Recall the Assumption 3.2 that $a_{n,T} = o(1)$, we finally obtain

$$\left\| \hat{L} - \hat{L}_{\text{diag}} \right\|_{\infty} \lesssim \exp \left(-C_2 \sqrt{b_T} + m_{n,T} + \frac{3}{2} M_{n,T} \right)$$

as claimed. \square

Step 3: *Bounding the $G+1$ 'st smallest eigenvalue of \hat{L}_{diag} .*

Denote the i -th smallest eigenvalue of \hat{L}_{diag} by λ_i . By Lemma 10.1, we know that $\lambda_1 = \dots = \lambda_G = 0$. Thus, we need to find a lower bound on the $G+1$ 'st smallest eigenvalue λ_{G+1} . This is done in the following Lemma.

Lemma 10.4. *Under Assumption 3.1-Assumption 3.3 we have*

$$\lambda_{G+1} \geq 1/8.$$

Proof of Lemma 10.4. Recall the *Cheeger constant* (see for instance equation (2.2) in Chung and Graham (1997)) of a undirected graph $\mathcal{G} = (V, E)$ (V denotes the set of vertices and E denotes the set of edges) with weights $w_{i,j}$ on the vertices $(i, j) \in E$:

$$\mathfrak{H} := \min_{\mathcal{I} \subset V} \frac{\sum_{j \in \mathcal{I}, k \notin \mathcal{I}} w_{j,k}}{\min \left\{ \sum_{j \in \mathcal{I}} d_j, \sum_{k \in V \setminus \mathcal{I}} d_k \right\}},$$

where

$$d_k := \sum_{(i,j) \in E: i \in \mathcal{I}} w_{i,j}.$$

Then, Theorem 2.2 in Chung and Graham (1997) implies that the eigengap of the normalized graph Laplacian is bounded below by $\mathfrak{H}^2/2$. To translate this result to our setting consider the fully connected graph with vertices given by $V = I_k^*$ and edge weights $w_{i,j} := \hat{A}_{ij}, i, j \in V$. Hence, the Cheeger constant corresponding to block $\hat{L}^{(mm)}$ on the diagonal of \hat{L}_{diag} is defined as

$$\mathfrak{H}_m := \min_{\mathcal{I} \subset I_m^*} \frac{|\mathcal{I}|(|I_m^*| - |\mathcal{I}|)}{\min \left\{ \sum_{j \in \mathcal{I}} \hat{d}_j(m), \sum_{k \in I_m^* \setminus \mathcal{I}} \hat{d}_k(m) \right\}},$$

where $\hat{d}_j(m) := \sum_{i \in I_m} \hat{A}_{ij}$. Since the non-zero eigenvalues of \hat{L}_{diag} are exactly the eigenvalues of the corresponding block diagonal pieces, it follows that

$$\lambda_{G+1} \geq \frac{\min_{m=1,\dots,G} \mathfrak{H}_m^2}{2}.$$

Hence, it suffices to prove that

$$\min_{m=1,\dots,G} \mathfrak{H}_m \geq 1/2.$$

By definition we have $\hat{A}_{ij} \leq 1$ and thus

$$\sum_{j \in \mathcal{I}} \hat{d}_j(m) \leq |\mathcal{I}| |I_m^*|.$$

Let $\bar{\mathcal{I}} := I_m^* \setminus \mathcal{I}$. It then holds that

$$\mathfrak{H}_m \geq \min_{\mathcal{I} \subset I_m^*} \frac{|\mathcal{I}| |\bar{\mathcal{I}}|}{|I_m^*| \min\{|\mathcal{I}|, |\bar{\mathcal{I}}|\}} = \min_{\mathcal{I} \subset I_m^*} \frac{|\mathcal{I}| \vee |\bar{\mathcal{I}}|}{|I_m^*|} \geq 1/2, \quad m = 1, \dots, G.$$

This completes the proof. \square

Step 4: *Frobenius norm convergence of \hat{U} to a transformation of U .*

Lemma 10.5. *Under Assumptions 3.1-3.3, there exists a orthogonal matrix $O_{n,T} \in \mathbb{R}^{G \times G}$ such that*

$$\left\| \hat{U} - U O_{n,T} \right\|_{\text{F}}^2 \lesssim \exp \left(\log n - 2C_2 \sqrt{b_T} + 8M_{n,T} + 2m_{n,T} \right),$$

where \lesssim depends only on $|I_k^*|/n$, $k = 1, \dots, G^*$ and $C_2, M_{n,T}, m_{n,T}$ are from Lemma 10.2..

Proof of Lemma 10.5. In the first step we apply Theorem 2 from Yu et al. (2015). In the notation of the latter paper let $d = G, s = n, r = n - G + 1$, $\hat{\Sigma} = \hat{L}, \Sigma = \hat{L}_{\text{diag}}$. Let \hat{Z}, Z denote the matrices which contain the eigenvectors corresponding to the G smallest eigenvalues of \hat{L}_{diag} and \hat{L} , respectively (in the notation of Yu et al. (2015) we have $\hat{V} = \hat{Z}, V = Z$). Note that by Lemma 10.1 we can choose Z to have columns $\hat{D}_{\text{diag}} \mathbb{1}_{I_j^*}, j = 1, \dots, G$. By equation (3) in Theorem 2 from Yu et al. (2015) there exists an orthonormal matrix $\hat{O} \in \mathbb{R}^{G \times G}$ with

$$\left\| \hat{Z} \hat{O} - Z \right\|_{\text{F}} \leq \frac{2^{3/2} \sqrt{G} \left\| \hat{L} - \hat{L}_{\text{diag}} \right\|_{\infty}}{\lambda_{G+1}}. \quad (16)$$

Here we note that for symmetric matrices the operator norm $\|\cdot\|_{\text{op}}$ used in Yu et al. (2015) coincides with our $\|\cdot\|_2$ and the latter satisfies $\|A\|_2 \leq \|A\|_{\infty}$ for symmetric matrices A . Let $O_{n,T} := \hat{O}^{\top}$ and note that by orthogonality of \hat{O} we have $\left\| \hat{Z} \hat{O} - Z \right\|_{\text{F}} = \left\| \hat{Z} - Z O_{n,T} \right\|_{\text{F}}$. In what follows write O for $O_{n,T}$ to simplify notation. Note that $\hat{U}_{i,\cdot} = \frac{\hat{Z}_{i,\cdot}}{\|\hat{Z}_{i,\cdot}\|_2}$, and $(UO)_{i,\cdot} = \frac{(ZO)_{i,\cdot}}{\|Z_{i,\cdot}\|_2}$. Similarly to Lemma 3.2 in van Delft and Dette (2021), it

follows that

$$\begin{aligned}
\|\hat{U} - UO\|_{\text{F}}^2 &= \sum_{i=1}^n \left\| \frac{\hat{Z}_{i,\cdot}}{\|\hat{Z}_{i,\cdot}\|_2} - \frac{(ZO)_{i,\cdot}}{\|Z_{i,\cdot}\|_2} \right\|_2^2 \\
&= \sum_{i=1}^n \left\| \frac{\hat{Z}_{i,\cdot} \|Z_{i,\cdot}\|_2 - \hat{Z}_{i,\cdot} \|\hat{Z}_{i,\cdot}\|_2 + \hat{Z}_{i,\cdot} \|\hat{Z}_{i,\cdot}\|_2 - (ZO)_{i,\cdot} \|\hat{Z}_{i,\cdot}\|_2}{\|\hat{Z}_{i,\cdot}\|_2 \|Z_{i,\cdot}\|_2} \right\|_2^2 \\
&\leq 2 \sum_{i=1}^n \left\| \frac{\hat{Z}_{i,\cdot} (\|Z_{i,\cdot}\|_2 - \|\hat{Z}_{i,\cdot}\|_2)}{\|\hat{Z}_{i,\cdot}\|_2 \|Z_{i,\cdot}\|_2} \right\|_2^2 + \left\| \frac{\hat{Z}_{i,\cdot} - (ZO)_{i,\cdot}}{\|Z_{i,\cdot}\|_2} \right\|_2^2 \\
&= 2 \sum_{i=1}^n \frac{(\|Z_{i,\cdot}\|_2 - \|\hat{Z}_{i,\cdot}\|_2)^2}{\|Z_{i,\cdot}\|_2^2} + \frac{\|\hat{Z}_{i,\cdot} - (ZO)_{i,\cdot}\|_2^2}{\|Z_{i,\cdot}\|_2^2} \\
&\leq 4 \sum_{i=1}^n \frac{\|\hat{Z}_{i,\cdot} - (ZO)_{i,\cdot}\|_2^2}{\|Z_{i,\cdot}\|_2^2} \\
&\leq \frac{4}{\min_i \|Z_{i,\cdot}\|_2^2} \|\hat{Z} - (ZO)\|_{\text{F}}^2.
\end{aligned}$$

Combining this with (16) yields

$$\|\hat{U} - UO\|_{\text{F}}^2 \leq \frac{32G}{(\lambda_{G+1})^2 \min_i \|Z_{i,\cdot}\|_2^2} \|\hat{L} - \hat{L}_{\text{diag}}\|_{\infty}^2. \quad (17)$$

Recalling the definition of Z , we obtain

$$\|Z_{i,\cdot}\|_2^2 = \frac{(\hat{D}_{\text{diag}})_i}{\sum_{j \in I_k^*} (\hat{D}_{\text{diag}})_j}, \quad \forall i \in I_k^*.$$

By inequality (15), we have

$$(\hat{D}_{\text{diag}})_i \gtrsim n \exp(-M_{n,T}),$$

and we also have

$$(\hat{D}_{\text{diag}})_i \leq n.$$

Combining these with previous display yields

$$\|Z_{i,\cdot}\|_2^2 \gtrsim \exp(-\log n - M_{n,T}),$$

which implies

$$\frac{1}{\min_i \|Z_{i,\cdot}\|_2^2} \lesssim \exp(\log n + M_{n,T}), \quad \forall i \in I_k^*.$$

Plugging this into the inequality (17), and combining it with Lemma 10.3 and $\lambda_{G+1} \geq 1/8$

yields

$$\begin{aligned} \left\| \hat{U} - UO \right\|_{\text{F}}^2 &\leq \frac{32G}{\min_i \|Z_{i,\cdot}\|_2^2 (\lambda_{G+1})^2} \left\| \hat{L} - \hat{L}_{\text{diag}} \right\|_{\infty}^2 \\ &\lesssim \exp(\log n + M_{n,T}) \exp(-2C_2 \sqrt{b_T} + 2m_{n,T} + 3M_{n,T}). \end{aligned}$$

Collecting terms completes the proof. \square

Step 5: Completing the argument

Recall that the last step of the algorithm consists of applying k -means clustering to the n embedded points $\hat{U}_{1,\cdot}, \dots, \hat{U}_{n,\cdot}$. In other words, this step determines group centers $\hat{c}_1, \dots, \hat{c}_G$ through

$$\{\hat{c}_1, \dots, \hat{c}_G\} \in \arg \min_{c_1, \dots, c_G \in \mathbb{R}^G} \left\{ \sum_{i=1}^n \min_{j \in \{1, \dots, G\}} \left\| \hat{U}_{i,\cdot} - c_j \right\|_2^2 \right\}.$$

The data points $\hat{U}_{i,\cdot}$ and $\hat{U}_{j,\cdot}$ are grouped together if and only if

$$\arg \min_k \left\| \hat{c}_k - \hat{U}_{i,\cdot} \right\|_2 = \arg \min_k \left\| \hat{c}_k - \hat{U}_{j,\cdot} \right\|_2.$$

We will prove that as soon as $\left\| \hat{U} - UO_{n,T} \right\|_{\text{F}} < 1/2$ all individuals are clustered correctly. Since $\left\| \hat{U} - UO_{n,T} \right\|_{\text{F}} = o_{\mathbb{P}}(1)$ by Lemma 10.5 and Assumption 3.4, this will complete the proof. By orthogonality of $O_{n,T}$ and the definition of U we have for i, j in different groups

$$\left\| (UO_{n,T})_{i,\cdot} - (UO_{n,T})_{j,\cdot} \right\|_2 = \left\| U_{i,\cdot} - U_{j,\cdot} \right\|_2 = \sqrt{2}.$$

Note that by definition of the Frobenius norm

$$\max_{i \neq j} \left\{ \left\| \hat{U}_{i,\cdot} - (UO_{n,T})_{i,\cdot} \right\|_2 + \left\| \hat{U}_{j,\cdot} - (UO_{n,T})_{j,\cdot} \right\|_2 \right\} \leq \sqrt{2} \left\| \hat{U} - UO_{n,T} \right\|_{\text{F}} < 1/\sqrt{2}.$$

Combining the above inequality with the reverse triangle inequality we have for i, j in different groups

$$\min_{i,j \text{ in different groups}} \left\| \hat{U}_{i,\cdot} - \hat{U}_{j,\cdot} \right\|_2 \geq \left\| U_{i,\cdot} - U_{j,\cdot} \right\|_2 - \sqrt{2} \left\| \hat{U} - UO_{n,T} \right\|_{\text{F}} > 1/\sqrt{2}.$$

Similarly, we have

$$\max_{i,j \text{ in the same group}} \left\| \hat{U}_{i,\cdot} - \hat{U}_{j,\cdot} \right\|_2 \leq \sqrt{2} \left\| \hat{U} - UO_{n,T} \right\|_{\text{F}} < 1/\sqrt{2}.$$

Hence any two points in the same group are closer to each other than to any point outside of that group. This implies that \hat{c}_j are just the group means of group I_j^* (modulo permutation of group labels) and that individuals i, j are grouped together if and only if $i, j \in I_k^*$ for

some k . This completes step 5 and thus the proof of Theorem 3.1. \square

10.3 Proofs for examples section

Throughout this section, we will use the following empirical process notation: let $\mathbb{P}_{T,i}$ denote the empirical measure of the sample $(\mathbf{z}_{it}, Y_{it})_{t=1,\dots,T}$ and let \mathbb{P}_i denote the measure corresponding to the distribution of $(\mathbf{z}_{i1}, Y_{i1})$ and let $\mathbb{G}_{T,i} := \sqrt{T}(\mathbb{P}_{T,i} - \mathbb{P}_i)$ denote the corresponding empirical process. For a function $f : (\mathbf{z}, y) \mapsto f(\mathbf{z}, y)$ and a signed measure \mathbb{P} let $\mathbb{P}f$ stand for $\int f d\mathbb{P}$. For a class of functions \mathcal{G} define $\|\mathbb{G}_{T,i}\|_{\mathcal{G}} := \sup_{g \in \mathcal{G}} |\mathbb{G}_{T,i}g|$.

10.3.1 Proofs for logistic regression (Theorem 3.2)

Throughout this section we will use the following additional notation. Let $f(y; \boldsymbol{\gamma}, \mathbf{z}) = \exp\{y\mathbf{z}^\top \boldsymbol{\gamma} - g(\mathbf{z}^\top \boldsymbol{\gamma})\}$, denote the pmf of $y \in \mathbb{R}$ conditional on $\mathbf{z} \in \mathbb{R}^{p+1}$; here the function g is defined via

$$\begin{aligned} g : \mathbb{R} &\rightarrow \mathbb{R} \\ z &\mapsto \log(1 + e^z). \end{aligned}$$

We abbreviate the corresponding log-likelihood as $\ell(\mathbf{z}, y; \boldsymbol{\gamma}) := y\mathbf{z}^\top \boldsymbol{\gamma} - g(\mathbf{z}^\top \boldsymbol{\gamma})$. Define

$$\mathbb{M}_{i,T}(\boldsymbol{\gamma}) := \frac{1}{T} \sum_t [Y_{it} \mathbf{z}_{it}^\top \boldsymbol{\gamma} - g(\mathbf{z}_{it}^\top \boldsymbol{\gamma})]$$

and

$$\mathbb{M}_i(\boldsymbol{\gamma}) := \mathbb{E}[\mathbb{M}_{i,T}(\boldsymbol{\gamma})], i = 1, \dots, n.$$

Lemma 10.6. *Given $p \in \mathbb{Z}^+$, we have $\int_0^1 \sqrt{1 + \log(\epsilon^{-p})} d\epsilon \leq 1 + \sqrt{2\pi p} e^{1/p}$.*

Proof of Lemma 10.6. Set $t = \sqrt{1 + \log(\epsilon^{-p})}$, we then have

$$\begin{aligned} &\int_0^1 \sqrt{1 + \log(\epsilon^{-p})} d\epsilon \\ &\leq \frac{2}{p} e^{\frac{1}{p}} \int_1^\infty t^2 e^{\frac{-t^2}{p}} dt \\ &= -e^{\frac{1}{p}} \int_1^\infty t d(e^{-\frac{t^2}{p}}) \\ &= -e^{\frac{1}{p}} \left(t e^{-\frac{t^2}{p}} \Big|_1^\infty - \int_1^\infty e^{-\frac{t^2}{p}} dt \right) \\ &= 1 + e^{\frac{1}{p}} \int_1^\infty e^{-\frac{t^2}{p}} dt \\ &\leq 1 + \sqrt{2\pi p} e^{1/p}. \end{aligned}$$

\square

Proof of Theorem 3.2, equation (5). Define set $\Gamma_i(\delta) := \{\gamma \in \mathbb{R}^{p+1} : \|\gamma - \gamma_i^*\|_2 \leq \delta\}$. By the concavity of function $\mathbb{M}_{i,T}$ and definition of $\hat{\gamma}_i$, when all the directional derivatives on the boundary of the set $\Gamma_i(\delta)$ is negative, that is,

$$\sup_{\gamma: \|\gamma - \gamma_i^*\|_2 = \delta} (\gamma - \gamma_i^*)^\top \nabla \mathbb{M}_{i,T}(\gamma) < 0,$$

it follows that $\hat{\gamma}_i \in \Gamma_i(\delta)$. This implies

$$\mathbb{P} \left(\sup_i \sup_{\gamma: \|\gamma - \gamma_i^*\|_2 = \tilde{C} \sqrt{\frac{\log n}{T}}} (\gamma - \gamma_i^*)^\top \nabla \mathbb{M}_{i,T}(\gamma) < 0 \right) \leq \mathbb{P} \left(\sup_i \|\hat{\gamma}_i - \gamma_i^*\|_2 \leq \tilde{C} \sqrt{\frac{\log n}{T}} \right).$$

Hence it suffices to show that under the stated assumptions it holds that

$$\mathbb{P} \left(\sup_i \sup_{\gamma: \|\gamma - \gamma_i^*\|_2 = \tilde{C} \sqrt{\frac{\log n}{T}}} (\gamma - \gamma_i^*)^\top \nabla \mathbb{M}_{i,T}(\gamma) < 0 \right) \rightarrow 1 \quad (18)$$

provided that \tilde{C} is picked sufficiently large. Note that

$$(\gamma - \gamma_i^*)^\top \nabla \mathbb{M}_{i,T}(\gamma) = (\gamma - \gamma_i^*)^\top \left(\nabla \mathbb{M}_{i,T}(\gamma) - \nabla \mathbb{M}_i(\gamma) \right) + (\gamma - \gamma_i^*)^\top \nabla \mathbb{M}_i(\gamma). \quad (19)$$

We now handle the last two terms on the right hand side of the last equality separately. More precisely, we will show that for any $\tilde{C} > 0$ there exists $\delta > 0$ such that for $\log n/T < \delta$ we have

$$\sup_{\gamma: \|\gamma - \gamma_i^*\|_2 = \tilde{C} \sqrt{\frac{\log n}{T}}} (\gamma - \gamma_i^*)^\top \nabla \mathbb{M}_i(\gamma) \leq -C_1 \frac{\log n}{T}, \quad i = 1, \dots, n, \quad (20)$$

where $C_1 = \tilde{C}^2 \kappa_2 \inf_i \{\lambda_{\min}(\mathbb{E}[\mathbf{z}_{it} \mathbf{z}_{it}^\top])\}$ with $\kappa_1 := \max_i \{\|\gamma_i^*\|_2\}$ and $\kappa_2 := \frac{e^{\kappa(1+\kappa_1)}}{(1+e^{\kappa(1+\kappa_1)})^2}$.

Additionally, we will prove that for \tilde{C} sufficiently large (where ‘‘sufficiently large’’ does not depend on n, T), it holds that

$$\mathbb{P} \left(\sup_i \sup_{\gamma: \|\gamma - \gamma_i^*\|_2 = \tilde{C} \sqrt{\frac{\log n}{T}}} (\gamma - \gamma_i^*)^\top \left(\nabla \mathbb{M}_{i,T}(\gamma) - \nabla \mathbb{M}_i(\gamma) \right) > \frac{C_1 \log n}{2} \right) \rightarrow 0. \quad (21)$$

Combining the above statements with the decomposition in (19) yields (18).

Proof of display (20). In what follows assume that the vector $\gamma \in \mathbb{R}^{p+1}$ satisfies $\|\gamma - \gamma_i^*\|_2 = \tilde{C} \sqrt{\frac{\log n}{T}}$. Using Taylor expansion, we have

$$\nabla \mathbb{M}_i(\gamma) = \nabla \mathbb{M}_i(\gamma_i^*) + \nabla^2 \mathbb{M}_i(\tilde{\gamma})(\gamma - \gamma_i^*),$$

where $\tilde{\gamma} \in \mathbb{R}^{p+1}$ is on the line connecting γ and γ_i^* . Note that $\nabla \mathbb{M}_i(\gamma_i^*) = \mathbf{0}$. Multiplying both sides of the equation by $(\gamma - \gamma_i^*)$ gives

$$(\gamma - \gamma_i^*)^\top \nabla \mathbb{M}_i(\gamma) = (\gamma - \gamma_i^*)^\top \nabla^2 \mathbb{M}_i(\tilde{\gamma})(\gamma - \gamma_i^*).$$

Note that $\nabla^2 \mathbb{M}_i(\tilde{\gamma}) = -\mathbb{E}[g''(\mathbf{z}_{it}^\top \tilde{\gamma}) \mathbf{z}_{it} \mathbf{z}_{it}^\top]$. It then follows that

$$(\gamma - \gamma_i^*)^\top \nabla \mathbb{M}_i(\gamma) = -(\gamma - \gamma_i^*)^\top \mathbb{E}[g''(\mathbf{z}_{it}^\top \tilde{\gamma}) \mathbf{z}_{it} \mathbf{z}_{it}^\top](\gamma - \gamma_i^*).$$

This implies

$$(\gamma - \gamma_i^*)^\top \nabla \mathbb{M}_i(\gamma) \leq -\|\gamma - \gamma_i^*\|_2^2 \lambda_{\min}(\mathbb{E}[g''(\mathbf{z}_{it}^\top \tilde{\gamma}) \mathbf{z}_{it} \mathbf{z}_{it}^\top]). \quad (22)$$

For any \tilde{C} we have $\tilde{C} \sqrt{\frac{\log n}{T}} < 1$ provided that $\log n/T$ is small enough. Note that $\tilde{\gamma}$ is in between γ and γ_i^* and $\|\gamma - \gamma_i^*\|_2 = \tilde{C} \sqrt{\frac{\log n}{T}}$. We then find $\|\tilde{\gamma}\|_2 \leq 1 + \kappa_1$. Combining this with Assumption 3.6 yields

$$\left\| \mathbf{z}_{it}^\top \tilde{\gamma} \right\|_2 \leq \sup_{i,t} \|\mathbf{z}_{it}\|_2 \|\tilde{\gamma}\|_2 \leq \kappa(1 + \kappa_1).$$

Note that the function $z \mapsto g''(z) = \frac{e^z}{(1+e^z)^2}$ is positive and decreasing on \mathbb{R}_+ . It then follows that

$$g''(\mathbf{z}_{it}^\top \tilde{\gamma}) \geq \frac{e^{\kappa(1+\kappa_1)}}{(1+e^{\kappa(1+\kappa_1)})^2}.$$

Define $\kappa_2 := \frac{e^{\kappa(1+\kappa_1)}}{(1+e^{\kappa(1+\kappa_1)})^2}$. Plugging the last display into the inequality (22) and using $\|\gamma - \gamma_i^*\|_2 = \tilde{C} \sqrt{\frac{\log n}{T}}$ yields

$$(\gamma - \gamma_i^*)^\top \nabla \mathbb{M}_i(\gamma) \leq -\kappa_2 \tilde{C}^2 \frac{\log n}{T} \lambda_{\min}(\mathbb{E}[\mathbf{z}_{it} \mathbf{z}_{it}^\top]).$$

By Assumption 3.5 that $\inf_i \{\lambda_{\min}(\mathbb{E}[\mathbf{z}_{it} \mathbf{z}_{it}^\top])\}$ is bounded from zero, we obtain (20) by setting $C_1 := \kappa_2 \tilde{C}^2 \inf_i \{\lambda_{\min}(\mathbb{E}[\mathbf{z}_{it} \mathbf{z}_{it}^\top])\}$.

Proof of display (21) We will show

$$\mathbb{P} \left(\sup_i \sup_{\gamma: \|\gamma - \gamma_i^*\|_2 = \tilde{C} \sqrt{\frac{\log n}{T}}} (\gamma - \gamma_i^*)^\top (\nabla \mathbb{M}_{i,T}(\gamma) - \nabla \mathbb{M}_i(\gamma)) > \frac{C_1 \log n}{2} \right) \rightarrow 0.$$

By Cauchy-Schwaz inequality, it holds that

$$(\gamma - \gamma_i^*)^\top (\nabla \mathbb{M}_{i,T}(\gamma) - \nabla \mathbb{M}_i(\gamma)) \leq \|\gamma - \gamma_i^*\|_2 \|\nabla \mathbb{M}_{i,T}(\gamma) - \nabla \mathbb{M}_i(\gamma)\|_2,$$

which implies

$$\begin{aligned}
& \mathbb{P} \left(\sup_i \sup_{\gamma: \|\gamma - \gamma_i^*\|_2 = \tilde{C} \sqrt{\frac{\log n}{T}}} (\gamma - \gamma_i^*)^\top (\nabla \mathbb{M}_{i,T}(\gamma) - \nabla \mathbb{M}_i(\gamma)) > \frac{C_1 \log n}{2} \frac{1}{T} \right) \\
& \leq \mathbb{P} \left(\sup_i \sup_{\gamma: \|\gamma - \gamma_i^*\|_2 = \tilde{C} \sqrt{\frac{\log n}{T}}} \|\gamma - \gamma_i^*\|_2 \|\nabla \mathbb{M}_{i,T}(\gamma) - \nabla \mathbb{M}_i(\gamma)\|_2 > \frac{C_1 \log n}{2} \frac{1}{T} \right) \\
& = \mathbb{P} \left(\sup_i \sup_{\gamma: \|\gamma - \gamma_i^*\|_2 = \tilde{C} \sqrt{\frac{\log n}{T}}} \|\nabla \mathbb{M}_{i,T}(\gamma) - \nabla \mathbb{M}_i(\gamma)\|_2 > \frac{C_1}{2\tilde{C}} \sqrt{\frac{\log n}{T}} \right) \\
& \leq \mathbb{P} \left(\sup_i \sup_{\gamma: \|\gamma - \gamma_i^*\|_2 \leq 1} \|\gamma - \gamma_i^*\|_2 \|\nabla \mathbb{M}_{i,T}(\gamma) - \nabla \mathbb{M}_i(\gamma)\|_2 > C_2 \sqrt{\frac{\log n}{T}} \right),
\end{aligned}$$

where $C_2 := \frac{C_1}{2\tilde{C}} = \tilde{C} \kappa_2 \inf_i \{\lambda_{\min}(\mathbb{E}[\mathbf{z}_{it} \mathbf{z}_{it}^\top])\}/2$. We will show that the last line in the display above converges to zero provided that \tilde{C} is large enough. Define the vector

$$M_{it}(\gamma) := Y_{it} \mathbf{z}_{it} - \frac{\mathbf{z}_{it} e^{\mathbf{z}_{it}^\top \gamma}}{1 + e^{\mathbf{z}_{it}^\top \gamma}} - \mathbb{E} \left[Y_{it} \mathbf{z}_{it} - \frac{\mathbf{z}_{it} e^{\mathbf{z}_{it}^\top \gamma}}{1 + e^{\mathbf{z}_{it}^\top \gamma}} \right].$$

Denote the j -th entry of the vector $M_{it}(\gamma)$ by $M_{it,j}(\gamma)$. We now show that

$$\mathbb{P} \left(\sup_i \sup_{\gamma: \|\gamma - \gamma_i^*\|_2 \leq 1} \frac{1}{T} \sum_{t=1}^T |M_{it,j}(\gamma)| > C_2 \sqrt{\frac{\log n}{T}} \right) \rightarrow 0,$$

Define the function $h_\gamma^j(\mathbf{z}, y)$ via

$$\begin{aligned}
h_\gamma^j : \mathbb{R}^{p+1} \times \{0, 1\} & \rightarrow \mathbb{R} \\
(\mathbf{z}, y) & \mapsto h_\gamma^j(\mathbf{z}, y) := z_j \left(y - \frac{e^{\mathbf{z}^\top \gamma}}{1 + e^{\mathbf{z}^\top \gamma}} \right) \mathbb{1}\{\|\mathbf{z}\|_2 \leq \kappa\},
\end{aligned}$$

where z_j denotes the j -th element of the vector \mathbf{z} . Consider the function class $\mathcal{H}_i^j(\delta) := \{h_\gamma^j(\mathbf{z}, y) : \|\gamma - \gamma_i^*\|_2 \leq \delta\}$. It follows that

$$\mathbb{P} \left(\sup_{\gamma: \|\gamma - \gamma^*\|_2 \leq 1} \left| \frac{1}{T} \sum_{t=1}^T M_{it,j}(\gamma) \right| > C_2 \sqrt{\frac{\log n}{T}} \right) = \mathbb{P} \left(\|\mathbb{G}_{T,i}\|_{\mathcal{H}_i^j(1)} > C_2 \sqrt{\log n} \right).$$

Now, we study the probability

$$\mathbb{P} \left(\|\mathbb{G}_{T,i}\|_{\mathcal{H}_i^j(1)} > C_2 \sqrt{\log n} \right).$$

Note that for any $\gamma \in \mathbb{R}^{p+1}$ satisfying $\|\gamma - \gamma_i^*\|_2 < 1$, it holds that

$$\left| yz_j - \frac{e^{\mathbf{z}^\top \gamma} z_j}{1 + e^{\mathbf{z}^\top \gamma}} \right| = |z_j| \left| y - \frac{e^{\mathbf{z}^\top \gamma}}{1 + e^{\mathbf{z}^\top \gamma}} \right| \leq \|\mathbf{z}\|_2,$$

and thus an envelope for the class $\mathcal{H}_i^j(1)$ is given by κ . Moreover, for any functions $h_\gamma^j(\mathbf{z}, y), h_{\tilde{\gamma}}^j(\mathbf{z}, y) \in \mathcal{H}_i^j(1)$, it holds that

$$\begin{aligned} & \left| yz_j - \frac{e^{\mathbf{z}^\top \gamma} z_j}{1 + e^{\mathbf{z}^\top \gamma}} - yz_j + \frac{e^{\mathbf{z}^\top \tilde{\gamma}} z_j}{1 + e^{\mathbf{z}^\top \tilde{\gamma}}} \right| \\ & \leq \|\mathbf{z}\|_2 \left| \frac{e^{\mathbf{z}^\top \gamma} z_j}{1 + e^{\mathbf{z}^\top \gamma}} - \frac{e^{\mathbf{z}^\top \tilde{\gamma}} z_j}{1 + e^{\mathbf{z}^\top \tilde{\gamma}}} \right| \\ & \leq \|\mathbf{z}\|_2^2 \|\gamma - \tilde{\gamma}\|_2, \end{aligned}$$

where the last inequality follows from the mean value theorem and the bound $e^z/(1+e^z)^2 \leq 1$. Thus, the ϵ -bracketing number of the function class $\mathcal{H}_i^j(1)$ satisfies

$$\sup_{i,j} N_{[]}(\epsilon, \mathcal{H}_i^j(1), \|\cdot\|_2) \leq C_4 \epsilon^{-p-1}$$

for a constant C_4 independent of n . By Theorem 2.14.2 in van der Vaart and Wellner (1996) and Assumption 3.6, we have

$$\mathbb{E} \sup_{\gamma: \|\gamma - \gamma_i^*\|_2 < 1} \left(\sqrt{T} \left| \frac{1}{T} \sum_{t=1}^T M_{it,j}(\gamma) \right| \right) \lesssim 2\kappa J_{[]} (1, \mathcal{H}_i^1(1)),$$

where

$$J_{[]} (1, \mathcal{H}_i^j(1)) := \int_0^1 \sqrt{1 + \log N_{[]}(\epsilon, \mathcal{H}_i^j(1), \|\cdot\|_2)} d\epsilon \leq \int_0^1 \sqrt{1 + \log(C_4 \epsilon^{-p-1})} d\epsilon < \infty$$

by Lemma 10.6. This implies

$$\mu := \sup_{i,j} \mathbb{E} \left[\sup_{\gamma: \|\gamma - \gamma_i^*\|_2 < 1} \left(\sqrt{T} \left| \frac{1}{T} \sum_{t=1}^T M_{it,j}(\gamma) \right| \right) \right] \leq C_5 \kappa \quad (23)$$

for a constant C_5 independent of n . For a function class \mathcal{H} define $\mu_i(\mathcal{H}) := \mathbb{E} [\mathbb{G}_{T,i} \mathcal{H}]$, and $\sigma_i^2(\mathcal{H}) := \|\mathbb{P}_i[(h - \mathbb{P}_i h)^2]\|_{\mathcal{H}}$. By (23) we have $\mu_i(\mathcal{H}_i^j(1)) \leq \mu$. Since the envelope for the class $\mathcal{H}_i^j(1)$ is κ , it holds by Assumption 3.6 that

$$\sigma^2 := \sup_{i,j} \sigma^2(\mathcal{H}_i^j(1)) \leq \kappa^2.$$

Define $\tilde{C}_2 := C_2 C^*$ where C^* denotes the universal constant C from Theorem 2.14.25 in

van der Vaart and Wellner (1996). Set $t = C_2\sqrt{\log n} - \mu$ to obtain for $\log n > \mu^2/\tilde{C}_2^2$, it holds that

$$\sup_{i,j} \mathbb{P}\left(\|\mathbb{G}_{T,i}\|_{\mathcal{H}_i^j(1)} > \tilde{C}_2\sqrt{\log n}\right) \leq \sup_{i,j} \mathbb{P}\left(\|\mathbb{G}_{T,i}\|_{\mathcal{H}_i^j(1)} > C^*\{\mu_i(\mathcal{H}_i^j(1)) + t\}\right).$$

Invoking Theorem 2.14.25 in van der Vaart and Wellner (1996) yields

$$\begin{aligned} & \sup_{i,j} \mathbb{P}\left(\|\mathbb{G}_{T,i}\|_{\mathcal{H}_i^j(1)} > C^*\{\mu_i(\mathcal{H}_i^j(1)) + t\}\right) \\ & \leq \exp\left(-D\left(\frac{(C_2\sqrt{\log n} - \mu)^2}{\sigma^2} \wedge \frac{(C_2\sqrt{\log n} - \mu)\sqrt{T}}{\kappa}\right)\right), \end{aligned}$$

where D is a universal constant independent of n, T, C_2 . Collecting pieces gives

$$\begin{aligned} & \mathbb{P}\left(\sup_i \sup_{\gamma: \|\gamma - \gamma^*\|_2 \leq 1} \left|\frac{1}{T} \sum_{t=1}^T M_{it,j}(\gamma)\right| > C_2\sqrt{\frac{\log n}{T}}\right) \\ & \leq \sum_{i=1}^n \mathbb{P}\left(\sup_{\gamma: \|\gamma - \gamma^*\|_2 \leq 1} \left|\frac{1}{T} \sum_{t=1}^T M_{it,j}(\gamma)\right| > C_2\sqrt{\frac{\log n}{T}}\right) \\ & \leq \exp\left(\log n - D\left(\frac{(C_2\sqrt{\log n} - \mu)^2}{\sigma^2} \wedge \frac{(C_2\sqrt{\log n} - \mu)\sqrt{T}}{\kappa}\right)\right). \end{aligned}$$

By assumption that $\log n/T \rightarrow 0$ and $n, T \rightarrow \infty$, we can pick a \tilde{C} sufficiently large such that C_2 is large enough to obtain

$$\mathbb{P}\left(\sup_i \sup_{\gamma: \|\gamma - \gamma^*\|_2 \leq 1} \left|\frac{1}{T} \sum_{t=1}^T M_{it,j}(\gamma)\right| > C_2\sqrt{\frac{\log n}{T}}\right) \rightarrow 0.$$

This completes the proof. \square

Proof of Theorem 3.2, equation (6). Define the functions $h_i : \mathbb{R}^{p+1} \rightarrow \mathbb{R}^{(p+1) \times (p+1)}$ through

$$h_i(\gamma) := \mathbb{E}\left[\frac{e^{\mathbf{z}_{it}^\top \gamma}}{(1 + e^{\mathbf{z}_{it}^\top \gamma})^2} \mathbf{z}_{it} \mathbf{z}_{it}^\top\right].$$

Note that

$$\sup_i \left\| \tilde{\Sigma}_i^{-1} - h_i(\hat{\gamma}_i) \right\|_2 \leq \kappa \sup_i \lambda_{\max}(\mathbb{E}[\mathbf{z}_{it} \mathbf{z}_{it}^\top]) \sup_i \|\hat{\gamma}_i - \gamma_i^*\|_2.$$

By Theorem 3.2 and Assumption 3.5, we obtain

$$\sup_i \left\| \tilde{\Sigma}_i^{-1} - h_i(\hat{\gamma}_i) \right\|_2 = \mathcal{O}_{\mathbb{P}}\left(\sqrt{\frac{\log n}{T}}\right).$$

Since

$$\sup_i \left\| \hat{\tilde{\Sigma}}_i^{-1} - \tilde{\Sigma}_i^{-1} \right\|_2 \leq \sup_i \left\| \hat{\tilde{\Sigma}}_i^{-1} - h_i(\hat{\gamma}_i) \right\|_2 + \sup_i \left\| h_i(\hat{\gamma}_i) - \tilde{\Sigma}_i^{-1} \right\|_2,$$

it remains to show that

$$\sup_i \left\| \hat{\tilde{\Sigma}}_i^{-1} - h_i(\hat{\gamma}_i) \right\|_2 = \mathcal{O}_{\mathbb{P}} \left(\sqrt{\frac{\log n}{T}} \right). \quad (24)$$

For ease of notation, we define the matrix $N_{it}(\gamma) \in \mathbb{R}^{(p+1) \times (p+1)}$ via

$$N_{it}(\gamma) := \frac{e^{\mathbf{z}_{it}^\top \gamma}}{(1 + e^{\mathbf{z}_{it}^\top \gamma})^2} \mathbf{z}_{it} \mathbf{z}_{it}^\top - \mathbb{E} \left[\frac{e^{\mathbf{z}_{it}^\top \gamma}}{(1 + e^{\mathbf{z}_{it}^\top \gamma})^2} \mathbf{z}_{it} \mathbf{z}_{it}^\top \right].$$

Define the (j, l) -th entry of matrix $N_{it}(\gamma)$ by $N_{it,j,l}(\gamma)$. Given $\delta > 0$, it holds that

$$\begin{aligned} & \mathbb{P} \left(\sup_i \left| \frac{1}{T} \sum_{t=1}^T N_{it,j,l}(\hat{\gamma}_i) \right| > C \sqrt{\frac{\log n}{T}} \right) \\ & \leq \mathbb{P} \left(\sup_i \sup_{\gamma: \|\gamma - \gamma_i^*\|_2 \leq \delta} \left| \frac{1}{T} \sum_{t=1}^T N_{it,j,l}(\gamma) \right| > C \sqrt{\frac{\log n}{T}} \right) + \mathbb{P} \left(\sup_i \|\hat{\gamma}_i - \gamma_i^*\|_2 > \delta \right). \end{aligned}$$

By equation (5) of Theorem 3.2, it holds that

$$\mathbb{P} \left(\sup_i \|\hat{\gamma}_i - \gamma_i^*\|_2 > \delta \right) \rightarrow 0.$$

It remains to bound the probability

$$\mathbb{P} \left(\sup_i \sup_{\gamma: \|\gamma - \gamma_i^*\|_2 \leq \delta} \left| \frac{1}{T} \sum_{t=1}^T N_{it,j,l}(\gamma) \right| > C \sqrt{\frac{\log n}{T}} \right).$$

Define the function $h_{\gamma}^{j,l}(\mathbf{z})$ via

$$\begin{aligned} h_{\gamma}^{j,l} : \mathbb{R}^{p+1} & \rightarrow \mathbb{R} \\ \mathbf{z} & \mapsto h_{\gamma}^{j,l}(\mathbf{z}) := \frac{e^{\mathbf{z}^\top \gamma}}{(1 + e^{\mathbf{z}^\top \gamma})^2} z_j z_l \mathbb{1}\{\|\mathbf{z}\|_2 \leq \kappa\}, \end{aligned}$$

where z_j denotes the j -th element of the vector \mathbf{z} . Consider the function class $\mathcal{H}_i^{j,l}(\delta) := \{h_{\gamma}^{j,l}(\mathbf{z}) : \|\gamma - \gamma_i^*\|_2 \leq \delta\}$. It follows that

$$\mathbb{P} \left(\sup_{\gamma: \|\gamma - \gamma^*\|_2 \leq \delta} \left| \frac{1}{T} \sum_{t=1}^T N_{it,j,l}(\gamma) \right| > C \sqrt{\frac{\log n}{T}} \right) = \mathbb{P} \left(\|\mathbb{G}_{T,i}\|_{\mathcal{H}_i^{j,l}(\delta)} > C \sqrt{\log n} \right).$$

Moreover, by Assumption 3.6, it holds for any function $h_{\gamma}^{j,l}(\mathbf{z}) \in \mathcal{H}_i^{j,l}(\delta)$ that $|h_{\gamma}^{j,l}(\mathbf{z})| \leq \kappa^2/4$.

Employing the similar entropy method as in the proof of equation (5) of Theorem 3.2, we obtain

$$\mathbb{E} \sup_{\gamma: \|\gamma - \gamma^*\|_2 \leq \delta} \left(\sqrt{T} \left| \frac{1}{T} \sum_{t=1}^T N_{it,j,l}(\gamma) \right| \right) \leq C_6 \kappa^2$$

for a constant C_6 independent of n, T . Defining $\mu_i(\mathcal{H}) := \mathbb{E}[\|\mathbb{G}_{T,i}\|_{\mathcal{H}}]$, and $\sigma_i^2(\mathcal{H}) := \mathbb{P}_i[(h - \mathbb{P}_i h)^2]_{\mathcal{H}}$ we have

$$\begin{aligned} \mu &:= \sup_i \mu_i(\mathcal{H}_i^{j,l}(\delta)) \leq C_6 \kappa^2, \\ \sigma^2 &:= \sup_i \sigma_i^2(\mathcal{H}_i^{j,l}(\delta)) \leq \kappa^4. \end{aligned}$$

Denote the universal constant C from Theorem 2.14.25 in van der Vaart and Wellner (1996) by C^* and set $t = \tilde{C}\sqrt{\log n} - \mu$ with $\tilde{C} := C/C^*$ for $\log n > \mu_1^2/\tilde{C}^2$ to obtain

$$\mathbb{P}(\|\mathbb{G}_{T,i}\|_{\mathcal{H}_i^{j,l}(\delta)} > C\sqrt{\log n}) \leq \mathbb{P}(\|\mathbb{G}_{T,i}\|_{\mathcal{H}_i^{j,l}(\delta)} > C^* \{\mu_i(\mathcal{H}_i^{j,l}(\delta)) + t\}).$$

Invoking Theorem 2.14.25 in van der Vaart and Wellner (1996) yields

$$\begin{aligned} &\mathbb{P}(\|\mathbb{G}_{T,i}\|_{\mathcal{H}_i^{j,l}(\delta)} > C^* \{\mu_i(\mathcal{H}_i^{j,l}(\delta)) + t\}) \\ &\leq \exp \left(-D \left(\frac{(\tilde{C}\sqrt{\log n} - \mu)^2}{\sigma^2} \wedge \frac{(\tilde{C}\sqrt{\log n} - \mu)\sqrt{T}}{\kappa^2} \right) \right), \end{aligned}$$

where D is an universal constant independent of n, T, C . Collecting pieces gives

$$\begin{aligned} &\mathbb{P} \left(\sup_i \sup_{\gamma: \|\gamma - \gamma^*\|_2 \leq \delta} \left| \frac{1}{T} \sum_{t=1}^T N_{it,j,l}(\gamma) \right| > C \sqrt{\frac{\log n}{T}} \right) \\ &\leq \sum_{i=1}^n \mathbb{P} \left(\sup_{\gamma: \|\gamma - \gamma^*\|_2 \leq \delta} \left| \frac{1}{T} \sum_{t=1}^T N_{it,j,l}(\gamma) \right| > C \sqrt{\frac{\log n}{T}} \right) \\ &\leq \exp \left(\log n - D \left(\frac{(\tilde{C}\sqrt{\log n} - \mu)^2}{\sigma^2} \wedge \frac{(\tilde{C}\sqrt{\log n} - \mu)\sqrt{T}}{\kappa^2} \right) \right). \end{aligned}$$

By assumption $\log n/T \rightarrow 0$, and hence we can pick C sufficiently large to obtain as $\min(n, T) \rightarrow \infty$

$$\mathbb{P} \left(\sup_i \sup_{\gamma: \|\gamma - \gamma^*\|_2 \leq \delta} \left| \frac{1}{T} \sum_{t=1}^T N_{it,j,l}(\gamma) \right| > C \sqrt{\frac{\log n}{T}} \right) \rightarrow 0.$$

This establishes (24). Note that the eigenvalues of $\mathbb{E} \left[\frac{e^{\mathbf{z}_{it}^\top \gamma_i^*}}{(1 + e^{\mathbf{z}_{it}^\top \gamma_i^*})^2} \mathbf{z}_{it} \mathbf{z}_{it}^\top \right]$ are bounded uniformly away from zero and from above – indeed, boundedness from above follows since $\|\mathbf{z}_{it}\|_2 \leq \kappa$ by assumption, for boundedness from below recall that $z \mapsto e^z/(1 + e^z)^2$ is

decreasing and non-negative on \mathbb{R}_+ so that for $\kappa_1 := \max_i \{\|\boldsymbol{\gamma}_i^*\|_2\} < \infty$, it holds that

$$\frac{e^{\mathbf{z}_{it}^\top \boldsymbol{\gamma}_i^*}}{(1 + e^{\mathbf{z}_{it}^\top \boldsymbol{\gamma}_i^*})^2} \geq \frac{e^{\kappa \kappa_1}}{(1 + e^{\kappa \kappa_1})^2} > 0.$$

A Taylor expansion of the map $A \mapsto A^{-1}$ together completes the proof. \square

10.3.2 Proofs for quantile regression (Theorem 3.3 and Theorem 3.4)

Proof of Theorem 3.3(i). Define $\boldsymbol{\gamma}_{n,T,i} := \hat{\boldsymbol{\gamma}}_i - \boldsymbol{\gamma}_i^*$. The Theorem 5.1 in Chao et al. (2017) can be used in our framework by setting $n = T, m = p, \xi_m = \kappa, g_n = 0$, and $c_n = 0$. We then find

$$\boldsymbol{\gamma}_{n,T,i} = -\frac{1}{T} B_i^{-1} \sum_{t=1}^T \psi_{i,\tau}(\mathbf{z}_{it}, Y_{it}) + \boldsymbol{\gamma}_{n,T,i,1} + \boldsymbol{\gamma}_{n,T,i,2} + \boldsymbol{\gamma}_{n,T,i,3}, \quad (25)$$

where $B_i := \mathbb{E}[f_{Y|\mathbf{z}}(q_{i,\tau}(\mathbf{z}_{i1}) \mid \mathbf{z}_{i1}) \mathbf{z}_{i1} \mathbf{z}_{i1}^\top]$ and $\psi_{i,\tau}(\mathbf{z}, Y) := \mathbf{z}(\mathbb{1}(Y \leq q_{i,\tau}(\mathbf{z})) - \tau)$. Define $\tilde{\boldsymbol{\gamma}}_{n,T,i} := \boldsymbol{\gamma}_{n,T,i,1} + \boldsymbol{\gamma}_{n,T,i,2} + \boldsymbol{\gamma}_{n,T,i,3}$. We now prove that

$$\sup_i \|\tilde{\boldsymbol{\gamma}}_{n,T,i}\|_2 = o_{\mathbb{P}}\left(\sqrt{\frac{\log n}{T}}\right). \quad (26)$$

For this, we show that

$$\sup_i \|\boldsymbol{\gamma}_{n,T,i,k}\|_2 = o_{\mathbb{P}}\left(\sqrt{\frac{\log n}{T}}\right), \quad k = 1, 2, 3.$$

Now, we handle the three remainder terms $\boldsymbol{\gamma}_{n,T,i,1}, \boldsymbol{\gamma}_{n,T,i,2}, \boldsymbol{\gamma}_{n,T,i,3}$ separately. By equation (5.1) in Theorem 5.1 of Chao et al. (2017), we have almost surely

$$\sup_i \|\boldsymbol{\gamma}_{n,T,i,1}\|_2 \leq C/T$$

for a constant C independent of n, T, i . Since $1/T = o(\sqrt{\log n/T})$ it follows that

$$\sup_i \|\boldsymbol{\gamma}_{n,T,i,1}\|_2 = o_{\mathbb{P}}\left(\sqrt{\frac{\log n}{T}}\right).$$

By equation (5.2) in Theorem 5.1 of Chao et al. (2017) applied with $\kappa_n = 2 \log n \ll T$, there exists a constant C_1 independent of n, T (and bounded uniformly in i as seen by a close inspection of the corresponding proof in Chao et al. (2017)) such that for all sufficiently large T

$$\mathbb{P}\left(\|\boldsymbol{\gamma}_{n,T,i,2}\|_2 > C_1 \left(\sqrt{\frac{\log T}{T}} + \sqrt{\frac{2 \log n}{T}}\right)^2\right) \leq 2 \exp(-\kappa_n) = 2/n^2. \quad (27)$$

Since

$$\left(\sqrt{\frac{\log T}{T}} + \sqrt{\frac{2 \log n}{T}} \right)^2 \leq 2 \frac{2 \log n + \log T}{T} = o\left(\sqrt{\frac{\log n}{T}}\right),$$

an application of the union bound shows that

$$\sup_i \|\gamma_{n,T,i,2}\|_2 = o_{\mathbb{P}}\left(\sqrt{\frac{\log n}{T}}\right).$$

Next apply (5.2) in Theorem 5.1 from Chao et al. (2017) with $\kappa_n = 2 \log n \ll T$ to obtain the existence of a constant C_2 independent of T (and bounded uniformly in i as seen by a close inspection of the corresponding proof in Chao et al. (2017)) such that for all sufficiently large T

$$\mathbb{P}\left(\|\gamma_{n,T,i,3}\|_2 > C_2 \left(\sqrt{\frac{\log T}{T}} + \sqrt{\frac{2 \log n}{T}}\right)^{3/2}\right) < 2/n^2. \quad (28)$$

Note that

$$\left(\sqrt{\frac{\log T}{T}} + \sqrt{\frac{2 \log n}{T}}\right)^3 \leq 8 \frac{(2 \log n)^{3/2} + (\log T)^{3/2}}{T^{3/2}} = o\left(\frac{\log n}{T}\right)$$

by the assumption that $\log n = o(T)$. Combining this with the union bound and (28) shows that

$$\sup_i \|\gamma_{n,T,i,3}\|_2 = o_{\mathbb{P}}\left(\sqrt{\frac{\log n}{T}}\right),$$

and collecting pieces yields (26).

To complete the proof, define the classes of functions

$$\mathcal{G}_i := \left\{ (\mathbf{z}, y) \mapsto \mathbf{a}^\top \mathbf{z} (\mathbb{1}\{y \leq \mathbf{z}^\top \mathbf{b}\} - \tau) \mathbb{1}\{\|\mathbf{z}\|_2 \leq \kappa\} : \mathbf{b} \in \mathbb{R}^{p+1}, \mathbf{a} \in \mathbb{R}^{p+1}, \|\mathbf{a}\|_2 = 1 \right\}$$

and note that

$$\sup_i \left\| \frac{1}{T} B_i^{-1} \sum_{t=1}^T \psi_{i,\tau}(\mathbf{z}_{it}, Y_{it}) \right\|_2 \leq \sup_i \|B_i^{-1}\|_2 \sup_i \|\mathbb{P}_{T,i} - \mathbb{P}_i\|_{\mathcal{G}_i}$$

for \mathbb{P}_i denoting the measure of and $\mathbb{P}_{T,i}$ corresponding to the empirical measure of $\{(\mathbf{z}_{it}, Y_{it}), t = 1, \dots, T\}$. Under the assumptions made we have $\sup_i \|B_i^{-1}\|_2 = O(1)$, and Lemma C.3 from Chao et al. (2017) applied with $\kappa_n = 2 \log n \ll T$ shows that there exists a constant C_3 , independent of n, T (and bounded uniformly in i as revealed by a close look at the corresponding proof) such that

$$\mathbb{P}\left(\|\mathbb{P}_{T,i} - \mathbb{P}_i\|_{\mathcal{G}_i} > C_3 \sqrt{\frac{\log n}{T}}\right) \leq n^{-2}.$$

Applying the union bound shows that

$$\sup_i \|\mathbb{P}_{T,i} - \mathbb{P}_i\|_{\mathcal{G}_i} = \mathcal{O}_{\mathbb{P}}\left(\sqrt{\frac{\log n}{T}}\right).$$

Combining this with (26) completes the proof. \square

Next we proceed to the proof of Theorem 3.3(ii). The proof will make use of the following additional notation

$$\begin{aligned}\psi_{i,\tau}(\mathbf{z}, Y) &= \mathbf{z}(\mathbb{1}(Y \leq q_{i,\tau}(\mathbf{z})) - \tau) \\ f_{it} &:= \frac{2d_T}{q_{i,\tau+d_T}(\mathbf{z}_{it}) - q_{i,\tau-d_T}(\mathbf{z}_{it})} \\ e_{it} &:= 1/f_{it} \\ B_{iT} &= \frac{1}{T} \sum_{t=1}^T f_{it} \mathbf{z}_{it} \mathbf{z}_{it}^\top \\ \tilde{\Sigma}_{iT}^{-1} &= \mathbb{E}[B_{iT}] H_i^{-1} \mathbb{E}[B_{iT}].\end{aligned}$$

We begin by stating and proving an intermediate technical result.

Lemma 10.7. *Let Assumptions (A0)–(A4) hold and assume $\log n = o(T)$. Let $\hat{e}_{it} := \hat{f}_{it}^{-1}$, then $\sup_{i,t} |\hat{e}_{it} - e_{it}| = \mathcal{O}_{\mathbb{P}}(b_{n,T})$ with $b_{n,T} = \sqrt{\frac{\log n}{Td_T}}$.*

Proof of Lemma 10.7. The proof essentially follows from the arguments in the proof of Lemma 9 of Galvao et al. (2020), but modifications are needed to take into account that $n(\log T)^2/T = o(1)$ made in that paper is replaced by $\log n = o(T)$ and that the rate changes accordingly. By definitions of \hat{e}_{is} and e_{is} , it holds that

$$\hat{e}_{is} - e_{is} = \mathbf{z}_{is}^\top \left((\hat{\gamma}_i(\tau + d_T) - \gamma_i^*(\tau + d_T)) - (\hat{\gamma}_i(\tau - d_T) - \gamma_i^*(\tau - d_T)) \right) / 2d_T.$$

We know from the display (25) and Theorem 3.3 that

$$\begin{aligned}\mathbf{z}_{is}^\top (\hat{\gamma}_i(\tau \pm d_T) - \gamma_i^*(\tau \pm d_T)) \\ = -\frac{1}{T} \mathbf{z}_{is}^\top B_i^{-1} \sum_{t=1}^T \mathbf{z}_{it} \left(\mathbb{1}\{Y_{it} \leq q_{i,\tau \pm d_T}(\mathbf{z}_{it})\} - (\tau \pm d_T) \right) + \mathcal{O}_{\mathbb{P}}\left(\sqrt{\frac{\log n}{T}}\right).\end{aligned}$$

Hence with $U_{it} := F_{Y|\mathbf{z}}(Y_{it}|\mathbf{z}_{it}) \sim U[0, 1]$ independent of \mathbf{z}_{it} , it holds that

$$\hat{e}_{is} - e_{is} = -\frac{1}{2Td_T} \mathbf{z}_{is}^\top B_i^{-1} \sum_{t=1}^T \mathbf{z}_{it} \left(\mathbb{1}\{U_{it} \leq \tau + d_T\} - \mathbb{1}\{U_{it} \leq \tau - d_T\} - 2d_T \right) + \mathcal{O}_{\mathbb{P}}\left(\sqrt{\frac{\log n}{T}}\right). \quad (29)$$

Define the vectors $M_{it} \in \mathbb{R}^{p+1}$ via

$$M_{it} := \mathbf{z}_{it} \left(\mathbb{1}\{U_{it} \leq \tau + d_T\} - \mathbb{1}\{U_{it} \leq \tau - d_T\} - 2d_T \right) / 2d_T.$$

Fix an arbitrary $k \in \{1, \dots, p+1\}$ and let $M_{it,k}$ denote the k -th entry of the vector M_{it} . It then follows that $\mathbb{E}[M_{it,k}] = 0$ and $\sup_i \text{Var}[M_{it,k}] \leq \frac{C_1}{d_T}$ for some constant C_1 under Assumption (A1). Under Assumption (A1), we also have $\sup_{i,t,k} |M_{it,k}| \leq C_2/d_T$ for some constant $C_2 > 0$. Invoking the Bernstein inequality yields

$$\begin{aligned} \mathbb{P}\left(\left|\sum_{t=1}^T M_{it,k}\right| > T\epsilon\right) &\leq 2 \exp\left(-\frac{\frac{1}{2}T^2\epsilon^2}{\sum_{t=1}^T \mathbb{E}[M_{it,k}^2] + \frac{1}{3}C_2d_T^{-1}T\epsilon}\right) \\ &= 2 \exp\left(-\frac{\frac{1}{2}T^2\epsilon^2}{C_1Td_T^{-1} + \frac{1}{3}C_2d_T^{-1}T\epsilon}\right). \end{aligned}$$

Take $\epsilon = C_3 T^{-1/2} d_T^{-1/2} (\log n)^{1/2}$ for a constant C_3 which will be determined later. Under the assumption $\frac{\log n}{Td_T} \rightarrow 0$, it follows that $\epsilon \rightarrow 0$ and the right hand side of the inequality becomes

$$2 \exp\left(-\frac{1}{2} \frac{(C_3)^2 d_T^{-1} \log n}{C_1 d_T^{-1} + \frac{1}{3} C_2 C_3 d_T^{-1} T^{-1/2} d_T^{-1/2} (\log n)^{1/2}}\right) \leq 2 \exp\left(-\frac{1}{4} (C_3)^2 \log n / C_1\right),$$

where the last inequality holds for $\log n / (Td_T)$ sufficiently small. Then, we have

$$\begin{aligned} \mathbb{P}\left(\sup_k \sup_i \left|\frac{1}{T} \sum_{t=1}^T M_{it,k}\right| > \epsilon\right) &\leq \sum_k \sum_i \mathbb{P}\left(\left|\frac{1}{T} \sum_{t=1}^T M_{it,k}\right| > \epsilon\right) \\ &\leq 2np \exp\left(-\frac{(C_3)^2}{4C_1} \log n\right) \rightarrow 0 \end{aligned}$$

by taking $(C_3)^2 > 4C_1$. Hence, we obtain

$$\sup_i \left\| \frac{1}{T} \sum_{t=1}^T M_{it} \right\|_2 = \mathcal{O}_{\mathbb{P}}\left(\sqrt{\frac{\log n}{Td_T}}\right).$$

Combining this with (29), the fact that $\sup_i \|B_i^{-1}\|_2 = \mathcal{O}(1)$, and Assumption (A4) gives

$$\sup_{i,s} |\hat{e}_{is} - e_{is}| = \mathcal{O}_{\mathbb{P}}\left(\sqrt{\frac{\log n}{Td_T}} + \sqrt{\frac{\log n}{T}}\right) = \mathcal{O}_{\mathbb{P}}\left(\sqrt{\frac{\log n}{Td_T}}\right)$$

as desired. \square

Proof of Theorem 3.3(ii). The following bound follows by the same arguments as Lemma 8 of Galvao et al. (2020) (note that the condition $n(\log T)^2/T = o(1)$ made in that paper

is not used in their proof of Lemma 8):

$$\sup_i \|\mathbb{E}[B_{iT}] - B_i\|_2 = o(1). \quad (30)$$

In addition, we will prove the following bounds

$$\sup_i \|\widehat{B}_{iT} - B_{iT}\|_2 = \mathcal{O}_{\mathbb{P}}(b_{n,T}) \quad (31)$$

with $b_{n,T} = \sqrt{\frac{\log n}{Td_T}}$,

$$\sup_i \|\mathbb{E}[B_{iT}] - \mathbb{E}[B_{iT}]\|_2 = \mathcal{O}_{\mathbb{P}}\left(\sqrt{\frac{\log n}{T}}\right), \quad (32)$$

and

$$\sup_i \|\widehat{H}_{iT}^{-1} - H_i^{-1}\|_2 = \mathcal{O}_{\mathbb{P}}\left(\sqrt{\frac{\log n}{T}}\right). \quad (33)$$

The remaining proof follows from similar arguments as the proof of Lemma 10 of Galvao et al. (2020), but modifications are needed to take into account that $n(\log T)^2/T = o(1)$ made in that paper is replaced by $\log n = o(T)$ and that the rate changes accordingly. We note that

$$\widehat{B}_{iT} - B_{iT} = \frac{1}{T} \sum_{t=1}^T (\widehat{f}_{it} - f_{it}) \mathbf{z}_{it} \mathbf{z}_{it}^\top.$$

Using Taylor expansion, we have

$$\widehat{f}_{it} - f_{it} = \widehat{e}_{it}^{-1} - e_{it}^{-1} = \frac{e_{it} - \widehat{e}_{it}}{e_{it}^2} + \mathcal{O}(|\widehat{e}_{it} - e_{it}|^2),$$

where the remainder term is uniform in i, t since under Assumption (A2), it holds that

$$\begin{aligned} \inf_{i,t} e_{i,t} &= \inf_{i,t} \frac{q_{i,\tau+d_T}(\mathbf{z}_{it}) - q_{i,\tau-d_T}(\mathbf{z}_{it})}{2d_T} \geq \inf_{i,t} \inf_{|\eta-\tau| \leq d_T} \frac{1}{f_{Y|\mathbf{z}}(q_{i,\eta}(\mathbf{z}_{it}) \mid \mathbf{z}_{it})} \\ &= \frac{1}{\sup_{i,t} \sup_{\eta,\mathbf{z}} f_{Y|\mathbf{z}}(q_{i,\eta}(\mathbf{z}_{it}) \mid \mathbf{z}_{it})} \geq 1/f_{max}, \end{aligned} \quad (34)$$

almost surely. By Assumption (A1) and Lemma 10.7, the bound in (31) follows.

Next we prove (32). Define the matrix $N_{it} \in \mathbb{R}^{(p+1) \times (p+1)}$ via

$$N_{it} := f_{it} \mathbf{z}_{it} \mathbf{z}_{it}^\top - \mathbb{E}[f_{it} \mathbf{z}_{it} \mathbf{z}_{it}^\top].$$

It then follows that $\mathbb{E}[N_{it}] = \mathbf{0}$. We denote by $N_{it,j,\ell}$ the (j, ℓ) -th entry of the matrix N_{it} . By Assumption (A1) and the inequality (34), we have $\sup_{i,t,j,\ell} |N_{it,j,\ell}| \leq C_5$ and $\sup_{i,t,j,\ell} \text{Var}[N_{it,j,\ell}] \leq$

C_6 for some constants $C_5, C_6 > 0$. Applying the Bernstein inequality gives, for any $\epsilon_2 > 0$,

$$\begin{aligned}\mathbb{P}\left(\left|\sum_{t=1}^T N_{it,j,\ell}\right| > T\epsilon_2\right) &\leq 2\exp\left(-\frac{\frac{1}{2}T^2\epsilon_2^2}{\sum_{t=1}^T \mathbb{E}[N_{it,j,\ell}^2] + \frac{1}{3}C_5T\epsilon_2}\right) \\ &\leq 2\exp\left(-\frac{\frac{1}{2}T^2\epsilon_2^2}{TC_6 + \frac{1}{3}C_5T\epsilon_2}\right).\end{aligned}$$

Take $\epsilon_2 = C_7T^{-1/2}(\log n)^{1/2}$ for some constant $C_7 > 0$ to be determined later, and the right hand side of the inequality becomes, for $\log n/T$ sufficiently small,

$$2\exp\left(-\frac{1}{2}\frac{(C_7)^2 \log n}{C_6 + \frac{1}{3}C_5C_7T^{-1/2}(\log n)^{1/2}}\right) \leq 2\exp\left(-\frac{(C_7)^2 \log n}{4C_6}\right).$$

Choosing $(C_7)^2 > 4C_6$, then for every j, ℓ , it holds that

$$\mathbb{P}\left(\sup_i \left|\frac{1}{T} \sum_{t=1}^T N_{it,j,\ell}\right| > \epsilon_2\right) \leq \sum_{i=1}^n \mathbb{P}\left(\left|\frac{1}{T} \sum_{t=1}^T N_{it,j,\ell}\right| > \epsilon_2\right) = 2n \exp\left(-\frac{(C_7)^2 \log n}{4C_6}\right) \rightarrow 0.$$

Thus, $\sup_i \left\| \frac{1}{T} \sum_{t=1}^T N_{it} \right\|_2 = \mathcal{O}_{\mathbb{P}}\left(\sqrt{\frac{\log n}{T}}\right)$. This implies (32). Finally, we prove the bound (33). By Assumption (A1), it holds that $\sup_i \left\| H_i^{-1} \right\|_2 < \infty$. Moreover, we have

$$\begin{aligned}\widehat{H}_{iT}^{-1} - H_i^{-1} &= H_i^{-1}(H_i \widehat{H}_{iT}^{-1} - I) = H_i^{-1}(H_i - \widehat{H}_{iT})\widehat{H}_{iT}^{-1} \\ &= H_i^{-1}(H_i - \widehat{H}_{iT})H_i^{-1} + \mathcal{O}\left(\left\|H_i^{-1}\right\|_2^2 \left\|\widehat{H}_{iT} - H_i\right\|_2^2\right),\end{aligned}$$

where

$$\sup_i \left\| \widehat{H}_{iT} - H_i \right\|_2 = \mathcal{O}_{\mathbb{P}}\left(\sqrt{\frac{\log n}{T}}\right)$$

holds by an application of the Bernstein inequality which is similar to the one given above. This completes the proof. \square

Proof sketch of Theorem 3.4 Both parts follow by simple computations provided that we can establish the bound

$$\sup_{|\eta - \tau| \leq \varepsilon} \sup_{i \in \{1, \dots, n\}} |\hat{\alpha}_i(\eta) - \alpha_i^*(\eta)| = \mathcal{O}_{\mathbb{P}}\left(\sqrt{\frac{\log n}{T}}\right).$$

for some $\varepsilon > 0$. This can be established by following the arguments given in Step 1–Step 3 in the proof of Theorem 3.2 in Kato et al. (2012). Note that all empirical processes appearing in those steps retain the same complexity (in terms of VC dimension and envelope functions). Note also that the assumption that T grows at most polynomially in n made in their Theorem 3.2 can be dropped at the cost of replacing $\log n$ by $\log(T \vee n)$, see also

the discussion in the latter paper following Theorem 3.2. □